AD-A179 822 YAQUINA BAY OREGON TIDAL AND WAVE-INDUCED CURRENTS NEAR 1/2
THE JETTIED INLET (U) COASTAL ENGINEERING RESEARCH
CENTER VICKSBURG MS M A CIALONE DEC 86 CERC-MP-86-14
UNCLASSIFIED F/G 8/3 NL

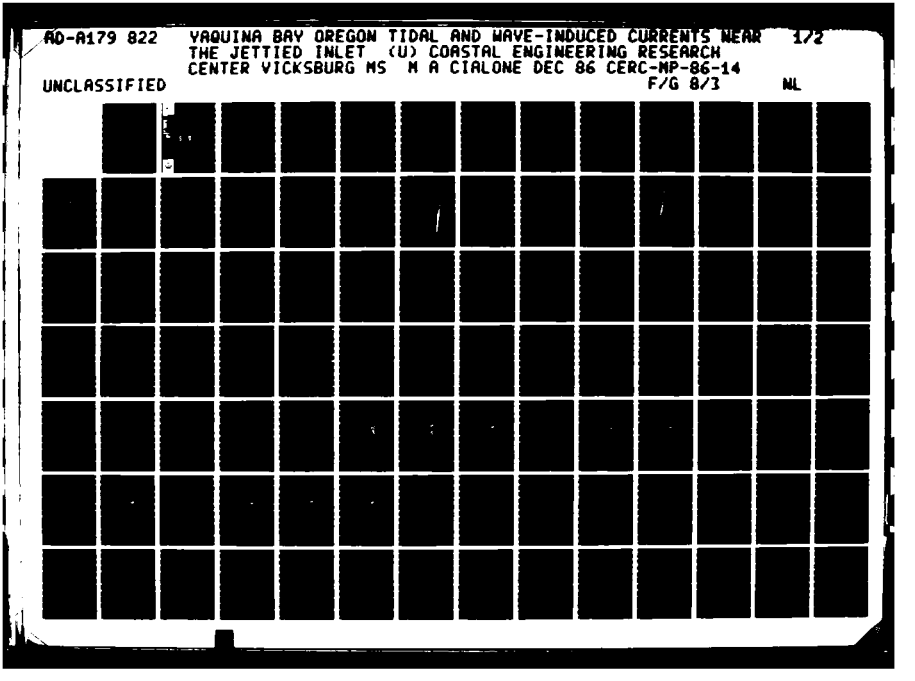

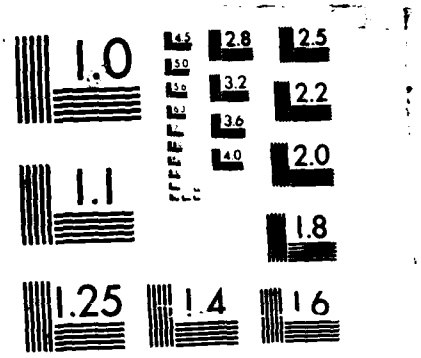

MICROCOPY RESOLUTION TEST CHART
NATIONAL BUREAU OF STANDARDS 1963 A

DTIC FILE COPY

MISCELLANEOUS PAPER CERC-86-14

YAQUINA BAY, OREGON, TIDAL AND WAVE-INDUCED CURRENTS NEAR THE JETTIED INLET

Numerical Model Investigation

by

Mary A. Cialone

Coastal Engineering Research Center

DEPARTMENT OF THE ARMY
Waterways Experiment Station, Corps of Engineers
PO Box 631, Vicksburg, Mississippi 39180-0631

DTIC
ELECTE
MAY 0 6 1987
S D
D

December 1986
Final Report

Approved For Public Release; Distribution Unlimited

Prepared for US Army Engineer District, Portland,
Portland, Oregon 97208-2946

87 5 5 032

US Army Corps of Engineers

AD-A179 822

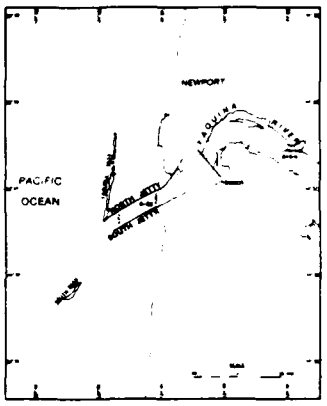

COASTAL ENGINEERING RESEARCH CENTER

Destroy this report when no longer needed. Do not return it to the originator.

The findings in this report are not to be construed as an official Department of the Army position unless so designated by other authorized documents.

The contents of this report are not to be used for advertising, publication, or promotional purposes. Citation of trade names does not constitute an official endorsement or approval of the use of such commercial products.

Unclassified
SECURITY CLASSIFICATION OF THIS PAGE

REPORT DOCUMENTATION PAGE

Form Approved
OMB No 0704 0188
Exp Date Jun 30 1986

1a REPORT SECURITY CLASSIFICATION Unclassified	1b RESTRICTIVE MARKINGS
2a SECURITY CLASSIFICATION AUTHORITY	3 DISTRIBUTION/AVAILABILITY OF REPORT Approved for public release; distribution unlimited
2b DECLASSIFICATION/DOWNGRADING SCHEDULE	
4 PERFORMING ORGANIZATION REPORT NUMBER(S) Miscellaneous Paper CERC-86-14	5 MONITORING ORGANIZATION REPORT NUMBER(S)
6a NAME OF PERFORMING ORGANIZATION USAEWES, Coastal Engineering Research Center 6b OFFICE SYMBOL (If applicable) WESCV	7a NAME OF MONITORING ORGANIZATION
6c ADDRESS (City, State, and ZIP Code) PO Box 631 Vicksburg, MS 39180-0631	7b ADDRESS (City, State, and ZIP Code)
8a NAME OF FUNDING/SPONSORING ORGANIZATION US Army Engineer District, Portland 8b OFFICE SYMBOL (If applicable)	9 PROCUREMENT INSTRUMENT IDENTIFICATION NUMBER
8c ADDRESS (City, State, and ZIP Code) Portland, OR 97208-2946	10 SOURCE OF FUNDING NUMBERS PROGRAM ELEMENT NO. / PROJECT NO. / TASK NO. / WORK UNIT ACCESSION NO

11 TITLE (Include Security Classification)
Yaquina Bay, Oregon, Tidal and Wave-Induced Currents Near the Jettied Inlet; Numerical Model Investigation

12 PERSONAL AUTHOR(S)
Cialone, Mary A.

13a TYPE OF REPORT	13b TIME COVERED	14 DATE OF REPORT (Year, Month, Day)	15 PAGE COUNT
Final report	FROM Feb 85 TO Aug 85	December 1986	104

16 SUPPLEMENTARY NOTATION
Available from National Technical Information Service, 5285 Port Royal Road, Springfield, VA 22161.

17 COSATI CODES			18 SUBJECT TERMS (Continue on reverse if necessary and identify by block number)
FIELD	GROUP	SUB-GROUP	Inlets; Tidal currents; Jetties; Yaquina Bay (Oregon); Ocean currents

19 ABSTRACT (Continue on reverse if necessary and identify by block number)

The Coastal Engineering Research Center of the US Army Engineer Waterways Experiment Station (WES) was requested by the US Army Engineer District, Portland (NPP) to model the coastal current regime in the vicinity of the Yaquina Bay entrance, with the major emphasis on tidal and wave-induced currents at the north jetty tip. This report describes the application of the WES Implicit Flooding Model (WIFM), the Regional Coastal Processes Wave Propagation Model (RCPWAVE), and the wave-induced current model (CURRENT) to the Yaquina Bay area. The purpose of the report was to provide design guidance to NPP for the rehabilitation of the collapsed, outer portion of the north jetty. Alternative plans for rehabilitation of the north jetty were modeled to determine their effectiveness in altering the current patterns near the north jetty tip.

20 DISTRIBUTION/AVAILABILITY OF ABSTRACT	21 ABSTRACT SECURITY CLASSIFICATION
☒ UNCLASSIFIED/UNLIMITED ☐ SAME AS RPT ☐ DTIC USERS	Unclassified
22a NAME OF RESPONSIBLE INDIVIDUAL	22b TELEPHONE (Include Area Code) / 22c OFFICE SYMBOL

DD FORM 1473, 84 MAR 83 APR edition may be used until exhausted
All other editions are obsolete.

SECURITY CLASSIFICATION OF THIS PAGE
Unclassified

PREFACE

This numerical model study was authorized by the US Army Engineer District, Portland (NPP), and conducted at the Coastal Engineering Research Center (CERC) of the US Army Engineer Waterways Experiment Station (WES). The study was conducted and this report was prepared during the period February-August 1985 by Mrs. Mary A. Cialone, Research Division, CERC, under the supervision of Mr. H. Lee Butler, former Chief, Coastal Processes Branch, present Chief, Research Division. General supervision at the time of the study was provided by Dr. R. W. Whalin, former Chief, CERC, Mr. C. C. Calhoun, Jr., former Acting Chief, present Assistant Chief, CERC, and Dr. J. R. Houston, former Chief, Research Division, present Chief, CERC.

The main purpose of this study was to model the coastal current regime in the vicinity of the Yaquina Bay entrance and, in so doing, determine the velocities of the tidal and wave-induced currents at the tip of the north jetty. As part of this study, the current field for five rehabilitative alternatives was modeled to provide design guidance to NPP for the rehabilitation of the north jetty at Yaquina Bay.

This report describes the application of three numerical models to the Yaquina Bay area. The numerical computations associated with this work were performed on the CYBER 865 and CYBER 205 Control Data Corporation Cyber computers at Rockville, Maryland.

Director of WES during this investigation and during the preparation and publication of this report was COL Allen F. Grum, USA. COL Dwayne G. Lee, CE, is the present Commander and Director. The Technical Director is Dr. Robert W. Whalin.

Accesion For	
NTIS CRA&I	☑
DTIC TAB	☐
Unannounced	☐
Justification	
By	
Distribution /	
Availability Codes	
Dist	Avail and / or Special
A-1	

CONTENTS

	Page
PREFACE	1
CONVERSION FACTORS, NON-SI TO SI (METRIC) UNITS OF MEASUREMENT	3
PART I: INTRODUCTION	5
The Prototype	5
The Problem	5
Model Approach	7
PART II: THE NUMERICAL TIDAL CIRCULATION MODEL	8
The Model	8
Prototype Data	12
Calibration	13
PART III: THE REGIONAL COASTAL PROCESSES WAVE PROPAGATION MODEL	14
The Model	14
Model Approach	16
PART IV: THE WAVE-INDUCED CURRENT MODEL	21
The Model	21
Initial and Boundary Conditions	22
Model Approach	24
PART V: GRID CONNECTION	26
PART VI: REHABILITATIVE ALTERNATIVES	27
PART VII: RESULTS	28
PART VIII: CONCLUSIONS	30
REFERENCES	31
PLATES 1-61	

CONVERSION FACTORS, NON-SI TO SI (METRIC)
UNITS OF MEASUREMENT

Non-SI units of measurement used in this report can be converted to SI (metric) units as follows:

Multiply	By	To Obtain
degree (angle)	0.01745329	radians
feet	0.3048	metres
miles (nautical miles)	1.852	kilometres
miles (US statute)	1.60934	kilometres

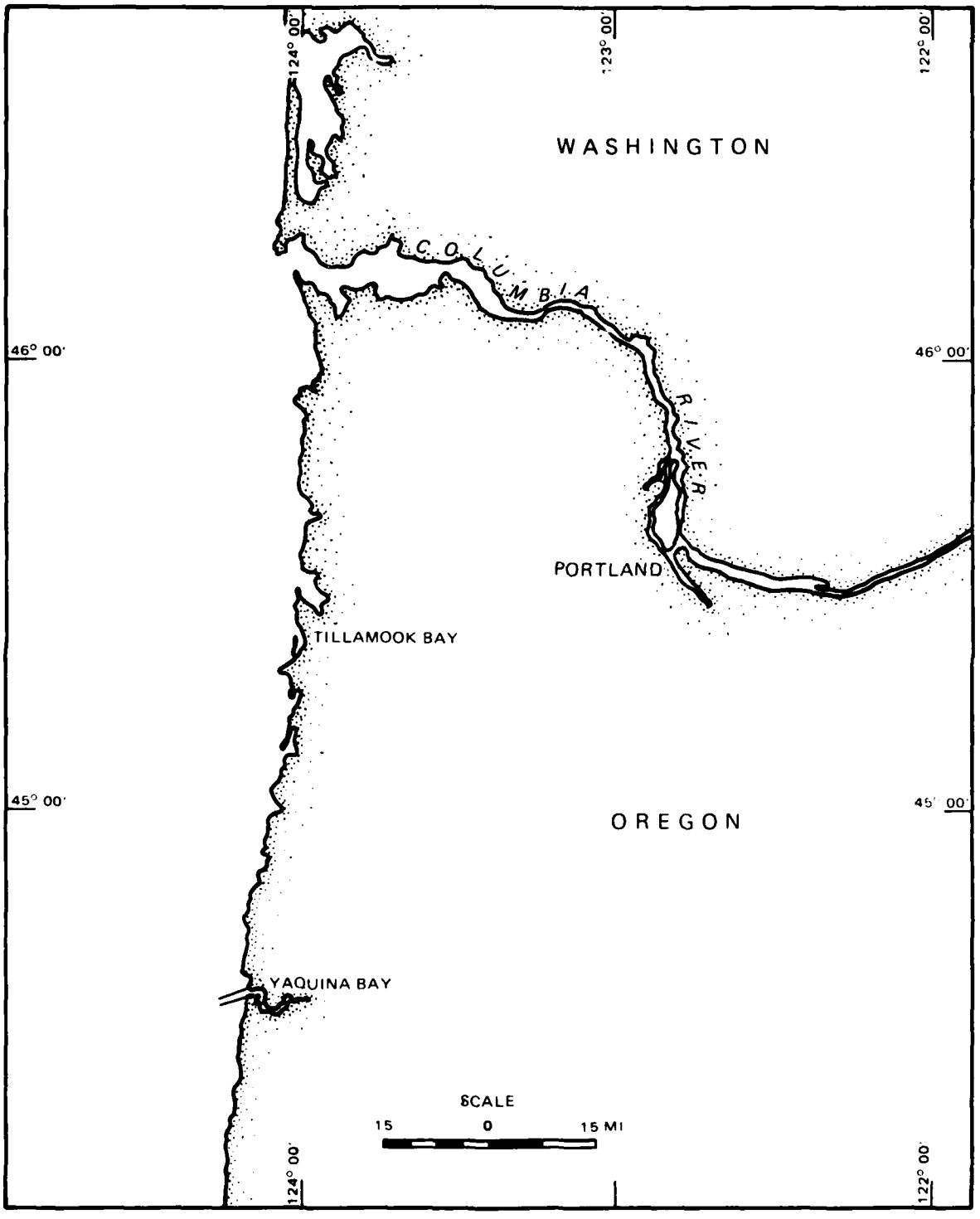

Figure 1. Location map of Yaquina Bay

YAQUINA BAY, OREGON, TIDAL AND WAVE-INDUCED CURRENTS NEAR THE JETTIED INLET

Numerical Model Investigation

PART I: INTRODUCTION

The Prototype

1. Yaquina Bay is located on the northern part of the Oregon coast about 110 miles* south of the Columbia River (Figure 1). The harbor entrance is protected by two rubble-mound jetties 1000 ft apart. The navigation channel is 400 ft wide at its outermost reach, 300 ft wide at sta 0+00 (Figure 2) and 900 to 1,200 ft wide in the turning basin. The entrance channel is dredged to 40 ft at the outermost portion, thence tapering to a depth of 30 ft at sta 0+00.

2. The entrance is flanked by Yaquina Reef to the north, approximately 4,000 ft offshore. The narrow rock reef extends to the north, approximately parallel to the coast for 6,000 ft. To the south is a less prominent feature called South Reef. The length of its shallowest part is about 1,650 ft, extending southwest.

The Problem

3. The rubble-mound jetties were originally constructed in 1918 to improve navigation into Yaquina Bay, with the entrance at a natural opening in the reef system. In 1958, construction was initiated to extend the jetties to their present length, having the north jetty nearly reaching the southern tip of Yaquina Reef. Construction was completed in 1966, but by 1970 the outer 330 ft of the north jetty had collapsed. Rehabilitation of the north jetty was completed in 1978. In 1979 60 ft had again collapsed, in 1980 250 ft had collapsed, and in 1984 360 ft had collapsed below mean lower low water (mllw). Some of the rubble material has slumped inward (or to the south) of the north jetty. The current between Yaquina Reef and the north jetty is believed to be

---

* A table of factors for converting non-SI units of measurement to SI (metric) units is presented on page 3.

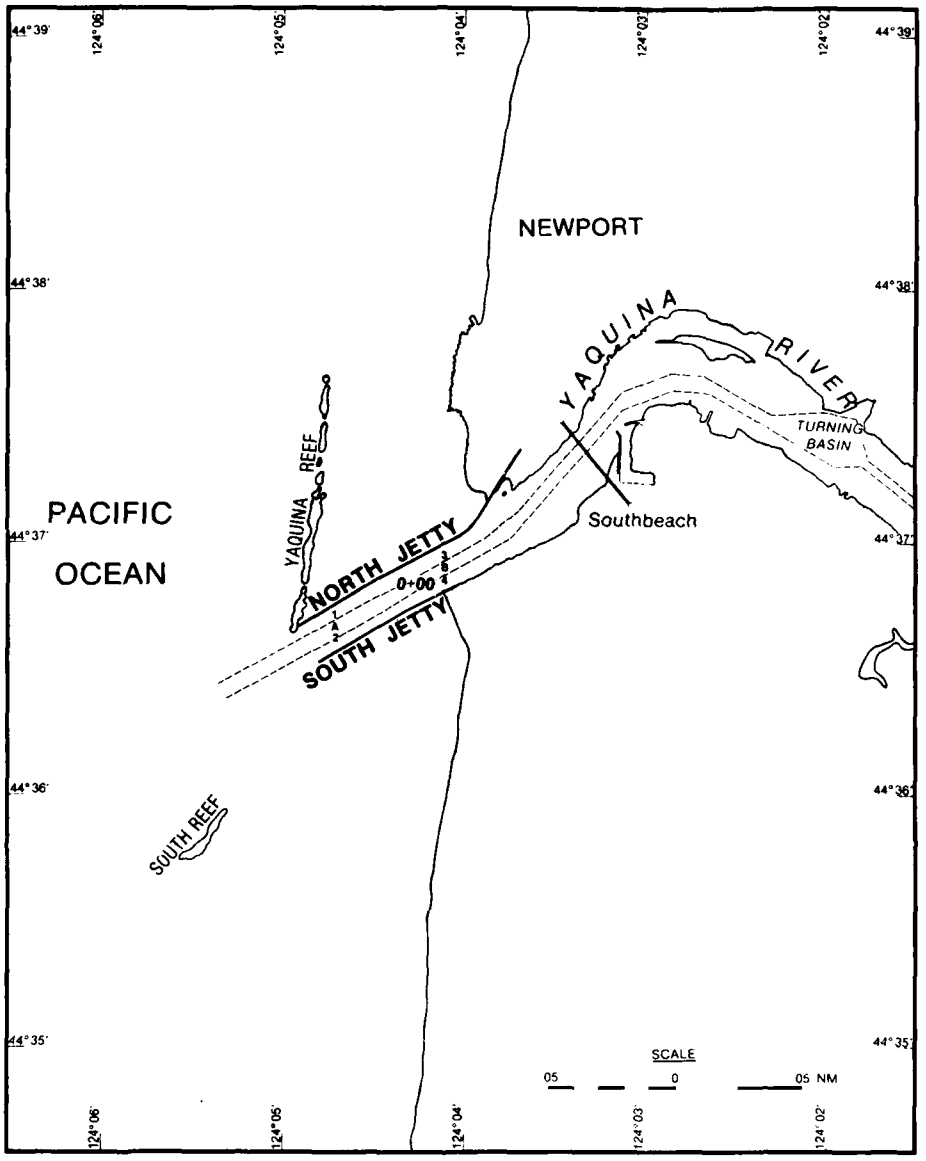

Figure 2. Location of jettied entrance to Yaquina Bay

a major contributing factor in the undermining and subsequent collapse of the jetty tip. The problem faced by the US Army Engineer District, Portland (NPP), is designing rehabilitative alternatives for the north jetty. The Coastal Engineering Research Center (CERC) was requested by NPP to provide guidance in the jetty design. Specifically, the problem faced by CERC was to define the local current regime using hydrodynamic numerical models.

Model Approach

4. The objective of this study was to describe the currents in and around the entrance to Yaquina Bay by using two hydrodynamic numerical models:

a. The numerical tidal circulation model used is the US Army Engineer Waterways Experiment Station's (WES) Implicit Flooding Model (WIFM) (Butler 1980). WIFM solves the vertically integrated Navier-Stokes equations by using an alternating direction implicit (ADI) finite difference scheme. The code uses a variably spaced finite difference grid to allow detailed modeling of areas that are important to the physical problem. Small features, such as jetties, are approximated as thin barriers between computational cells. The code allows for flooding and drying of low-lying areas as the surface elevation changes.

b. The wave-induced current model used is CURRENT. This model was developed at WES by Dr. S. Rao Vemulakonda (1984). CURRENT solves the vertically integrated Navier-Stokes equations by using an ADI finite difference scheme and the Longuet-Higgins approach to radiation stress. Mixing and advection terms are included. The code employs a variably spaced finite difference grid to allow a detailed modeling of areas that are important to the physical problem. CURRENT can approximate small features, such as jetties, as thin barriers between computational cells.

5. CURRENT requires the wave number, wave angle, and wave height at each grid cell as input. Therefore, the Regional Coastal Processes Wave Propagation Model (RCPWAVE) is run for each wave condition required for the study. RCPWAVE predicts the transformation of monochromatic waves over complex bathymetry, including refractive and diffractive effects (Ebersole, Cialone, and Prater 1985).

6. CURRENT is run until a steady-state condition is reached. Calibration and verification of the tidal model are accomplished by adjusting model parameters until computed velocities correspond to observed velocities at select locations. After verification, several rehabilitative alternatives are modeled to determine their influence on the current regime.

PART II: THE NUMERICAL TIDAL CIRCULATION MODEL

The Model

7. The numerical tidal circulation model employed is the WES Implicit Flooding Model (WIFM). The Navier-Stokes equations in a Cartesian coordinate system are used to derive the hydrodynamic equations employed by WIFM (Figure 3). The two-dimensional (2-D) equations of continuity and momentum

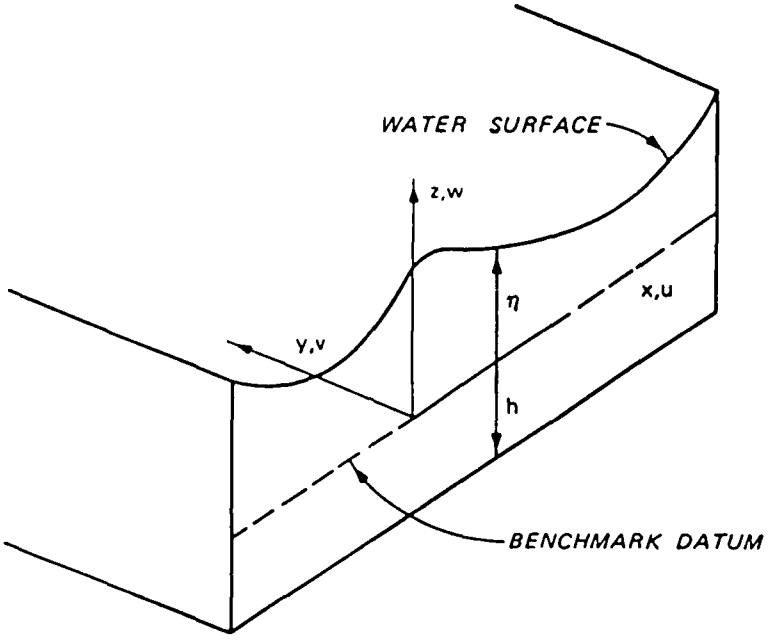

Figure 3. WIFM coordinate system

contained in WIFM are obtained by assuming vertical accelerations are small and the fluid is homogeneous:

Continuity

$$\frac{\partial \eta}{\partial t} + \frac{\partial}{\partial x}(ud) + \frac{\partial}{\partial y}(vd) = R \qquad (1)$$

Momentum

$$\frac{\partial u}{\partial t} + u\frac{\partial u}{\partial x} + v\frac{\partial u}{\partial y} - fv + g\frac{\partial}{\partial x}(\eta - \eta_a) + \frac{gu}{c^2 d}\left(u^2 + v^2\right)^{1/2}$$

$$- \varepsilon\left(\frac{\partial^2 u}{\partial x^2} + \frac{\partial^2 u}{\partial y^2}\right) + F_x = 0 \qquad (2)$$

$$\frac{\partial v}{\partial t} + u\frac{\partial v}{\partial x} + v\frac{\partial v}{\partial y} + fu + g\frac{\partial}{\partial y}(\eta - \eta_a) + \frac{gv}{c^2 d}\left(u^2 + v^2\right)^{1/2}$$

$$- \varepsilon\left(\frac{\partial^2 v}{\partial x^2} + \frac{\partial^2 v}{\partial y^2}\right) + F_y = 0 \qquad (3)$$

These equations are solved for η, u, and v, which denote the water surface elevation and the vertically averaged velocities in the x- and y-directions, respectively. The independent variables include:

t = time

$d = \eta - h$ = total water depth

h = still-water elevation

R = rate at which the water volume in the system changes through rainfall and evaporation

f = Coriolis parameter

g = acceleration due to gravity

η_a = hydrostatic water elevations due to atmospheric pressure differences

c = Chezy coefficient for bottom friction

ε = eddy viscosity coefficient

F_x, F_y = external forcing functions in the x- and y-directions, respectively (i.e., wind stress)

8. WIFM employs a variably spaced finite difference grid in its computational scheme. The grid axes are aligned such that the y-axis is approximately parallel to the shoreline, increasing in the southerly direction, and the x-axis is approximately perpendicular to the shoreline, increasing in the offshore direction at Yaquina Bay (Figure 4). The grid cells range in size from 145 to 1,460 ft in the x-direction and from 108 to 1,480 ft in the y-direction. The depth at each of the 55 by 49 grid cells is digitized from the 1982 Yaquina Bay and River Bathymetry Survey to a datum of mllw. The maximum depth of the Yaquina Bay WIFM grid is 155 ft below mllw. All data are then converted to the National Geodetic Vertical Datum (NGVD) by subtracting 4.03 ft.

9. Boundary conditions specified as input to WIFM may include open boundaries, land-water boundaries, and subgrid barriers. Open boundary

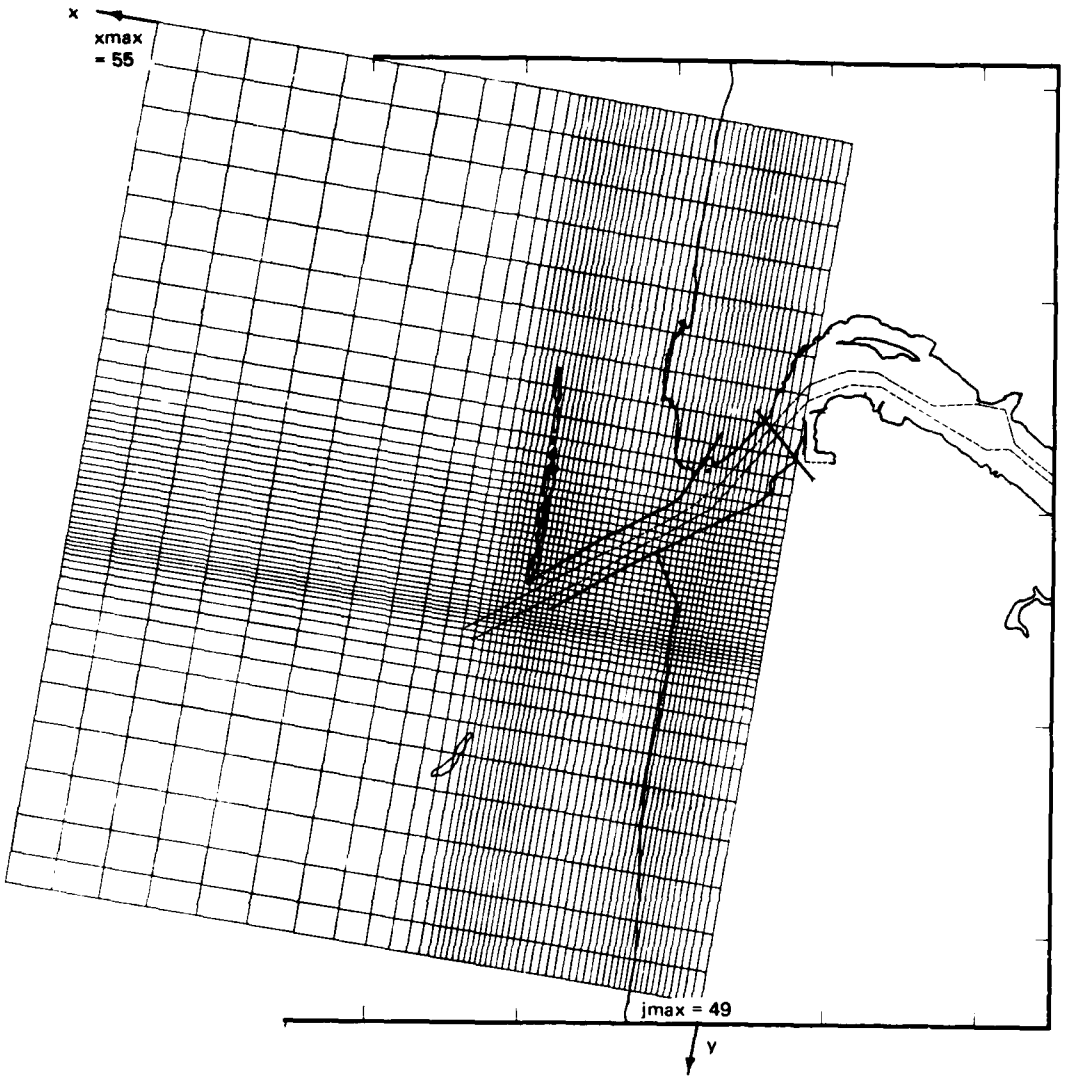

Figure 4. WIFM Grid

conditions exist when the edge of the computational grid is defined as water; in the case of a seaward boundary or when a channel lies on the edge of a computational grid, WIFM requires that the water elevation or velocity, in tabular or constituent form, be specified as forcing functions on such boundaries.

10. Land-water boundaries (i.e., the coastline) can be either fixed or variable in the WIFM code. For a fixed boundary, a no-flow condition ($u = 0$ or $v = 0$) is specified at the land-water interface. A variable land-water boundary condition allows for flooding and drying of low-lying areas. This is accomplished by comparing the water elevation in a water cell with the land elevation in an adjacent "dry" cell. When the water level exceeds the land elevation, water is moved into the dry cell by using a broad-crested weir

formula (Reid and Bodine 1968). After a specified amount of water has inundated the dry cell, it is thereafter treated as an open boundary face and computations for η, u, and v are made. The process of drying a water cell is modeled in a manner opposite to the process just described.

11. Subgrid barriers are thin walls defined along cell faces. There are three types of thin-wall barriers modeled by WIFM: exposed, submerged, and overtopping. Exposed barriers require no flow across the specified cell faces. Submerged barriers are modeled by controlling flow across a cell face by using a time-dependent friction coefficient. The third type of subgrid barrier is the overtopping barrier. These barriers are dynamic (i.e., they can become either completely exposed, completely submerged, or they can act as broad-crested weirs as model time progresses). The type of subgrid barrier used in the model is a function of its height and the water elevation in the two cells adjacent to the barrier. The WIFM grid boundaries and barriers are displayed in Figure 5.

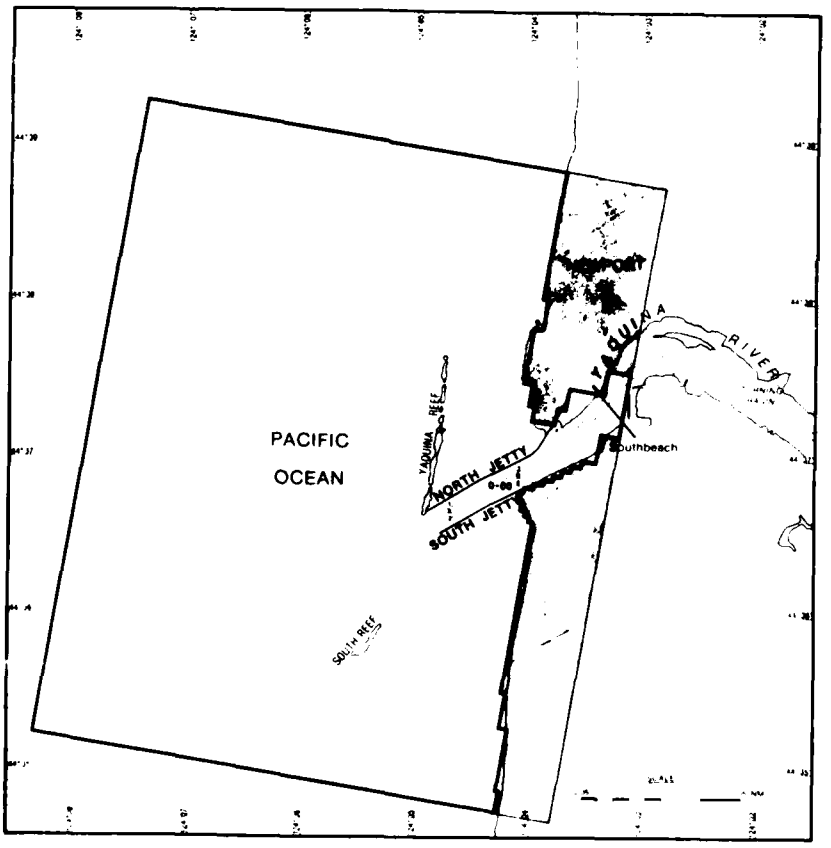

Figure 5. WIFM grid boundaries and barriers.
The shaded regions are land cells

Prototype Data

12. To calibrate and verify WIFM for tidal events, prototype tidal elevation and water current data are required. Tidal elevations are needed at the open ocean and inside the bay entrance as boundary conditions for WIFM.

13. Oregon State University (OSU) supplied the established tidal datums at South Beach, Oreg., inside the bay entrance, and hourly water elevations during the month of September 1984 at the same location.

14. CERC placed a Temperature-Depth Recorder (TDR) near the 70-ft sea buoy located at 44°36' N latitude, 124°06' W longitude from 24-26 September 1984 for 48 hr. The tidal elevations were recorded relative to an arbitrary datum every 7.5 min. The OSU-established datums and short-term data were used to correlate the CERC data to the NGVD for use as an open-ocean boundary condition in the tidal model.

15. The US Department of Commerce 1984 provided tabulated tidal constituents at South Beach (44°38' N latitude, 124°03' W longitude) that could be used by WIFM as a channel-boundary condition. The eight constituents used for the tide at South Beach (M2, K1, O1, S2, N2, P1, K2, and Q1) form 90 percent of the total tide. Table 1 provides the amplitudes and epochs for the eight constituents aforementioned.

Table 1

Tidal Constituents at South Beach, Oreg.

Constituent	Height, ft	Kelvin, deg
M2	2.884	342.97
K1	1.431	113.83
O1	0.878	96.74
S2	0.782	10.52
N2	0.595	319.96
P1	0.439	111.83
K2	0.230	12.90
Q1	0.161	88.95

16. Current data were taken in the inlet along two ranges (six gage locations) using an Endeco Model 110 current meter (Figure 2). Hourly readings were recorded by CERC during an 11-hr period on 25 September 1984. A second day's field data collection effort on 26 September 1984, at the six gage locations, proved to be unsuccessful. Therefore, a limited amount of data were available for calibration of the tidal model.

Calibration

17. Calibration of WIFM begins with the selection of boundary conditions for all open-water cells at the edges of the computational grid. In this study, tidal elevations were used as forcing functions on the seaward boundaries and the inlet boundary. WIFM is calibrated by adjusting the boundary conditions, the Chezy frictional coefficients in each cell, and/or the bathymetry until the model computes the correct tidal signals or velocities for locations inside the grid. The model was required to reproduce the velocities at six gages in the inlet during an 11-hr period on 25 September 1984 for this study. Since the field data collection effort was not extensive, this single day of data was used for calibration and verification of WIFM.

18. The calibration procedure started by using the TDR prototype tidal elevations on the open-ocean boundaries and modified TDR prototype tidal elevations at the inlet boundary. The inlet boundary condition was modified because its tidal signal is expected to lag that of the seaward boundary. The frictional values in the inlet were adjusted to account for shoals and the jetty material which slumped into the inlet. With these adjustments, the numerical model tidal velocity predictions adequately matched the prototype tidal velocities (Plates 1-3).

19. Discrepancies occurring at sta A and sta 2 may be caused by the lack of data concerning the amount of slumping near the north jetty. Another factor which may have contributed to the discrepancy is the cell size in this region. Although fine cells (150 ft) were used in the north jetty region, the grid may not have been fine enough to resolve the velocities accurately. Running WIFM with smaller grid cells was economically impractical due to the small time-step the grid would require.

PART III: THE REGIONAL COASTAL PROCESSES WAVE PROPAGATION MODEL

The Model

20. The RCPWAVE model predicts the transformation of monochromatic waves over complex bathymetry, including refractive and diffractive effects. The wave propagation model computes the wave height, direction, and number throughout a finite difference grid. These wave parameters are then used as forcing functions to drive CURRENT.

21. Berkhoff (1972) derived an elliptical equation to approximate the wave transformation of linear waves over an arbitrary bathymetry with mild bottom slope. The governing equation is given by

$$\frac{\partial}{\partial x}\left(cc_g \frac{\partial \phi}{\partial x}\right) + \frac{\partial}{\partial y}\left(cc_g \frac{\partial \phi}{\partial y}\right) + \sigma^2 \frac{c_g}{c} \phi = 0 \qquad (4)$$

where

$c(x,y)$ = wave celerity

$c_g(x,y)$ = group velocity

$\phi(x,y)$ = the complex velocity potential = ae^{is}

$a(x,y)$ = a wave amplitude function

e = 2.71828

$i = \sqrt{-1}$

$s(x,y)$ = wave phase function

σ = angular wave frequency

The wave number is found from the dispersion relation

$$\sigma^2 = gk \tanh (kh)$$

where

g = acceleration due to gravity

$k(x,y)$ = wave number

$h(x,y)$ = still-water depth

By substituting the expression for the velocity potential into Equation 4 and solving for the real and imaginary parts, two equations can be derived:

$$\frac{1}{a}\left\{\frac{\partial^2 a}{\partial x^2}+\frac{\partial^2 a}{\partial y^2}+\frac{1}{cc_g}\left[\nabla a \times \nabla(cc_g)\right]\right\}+k^2-\left|\nabla s^2\right|=0 \tag{5}$$

and

$$\nabla\left(a^2 cc_g \nabla s\right)=0 \tag{6}$$

These equations, along with the dispersion relation and the irrotationality condition, describe the combined refraction and diffraction process.

22. The RCPWAVE model has the capability of computing solutions on rectilinear grid systems having uniform or variably sized grid cells. The coordinate system and grid cell convention used in the model are given in Figure 6. Lateral boundary conditions are such that the value at cells $J = N$ and $J = 1$ are set equal to the value at cells $J = N - 1$ and $J = 2$, respectively. Boundary conditions along the seaward length of the grid are computed from deepwater wave conditions and are used to initiate the shoreward marching scheme of the model, assuming Snell's law is valid from deepwater to the outer boundary of the grid.

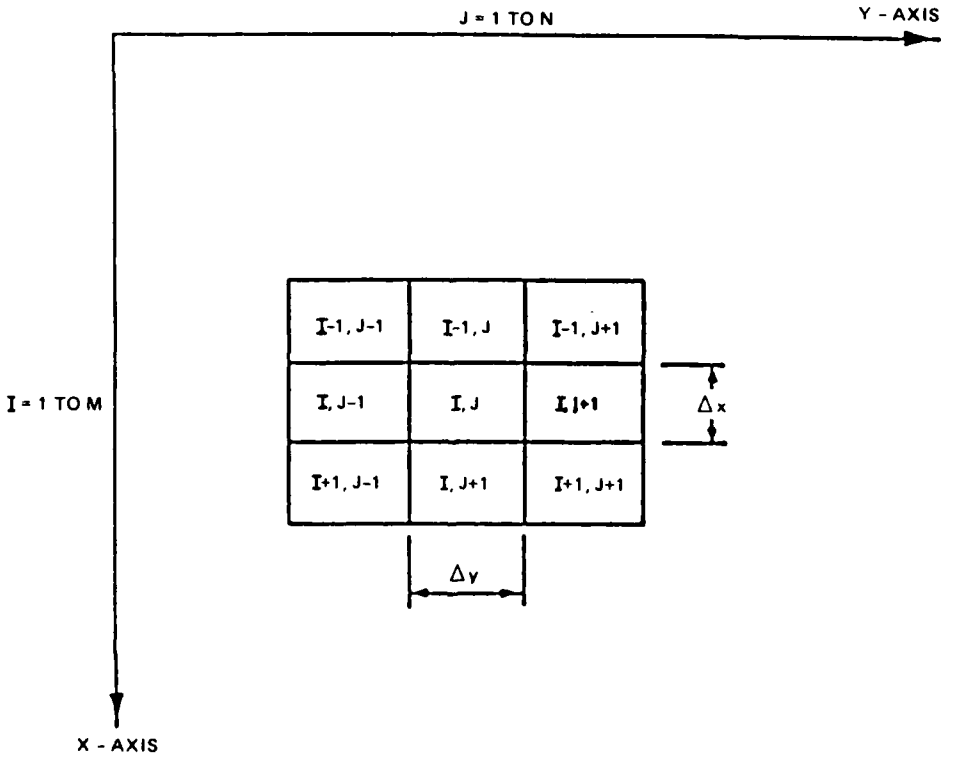

Figure 6. Definition of coordinate system and grid cell conventions used in the model

Model Approach

23. The RCPWAVE model is run on two separate grids. The larger (93 by 83), variably spaced, rectangular grid used for this model is shown in Figure 7. This grid was developed for the wave propagation analysis performed by CERC as part of the Yaquina Bay North Jetty Rehabilitation Study. Grid dimensions are 20.1 nautical miles (n.m.) in the longshore (y) direction and 18.6 n.m. in the offshore (x) direction, with the y-axis 6.5 deg east of true north (Figure 8). Water depths are digitized from the NOS nautical charts, except near the jetties where NPP provided survey data. Depths relative to

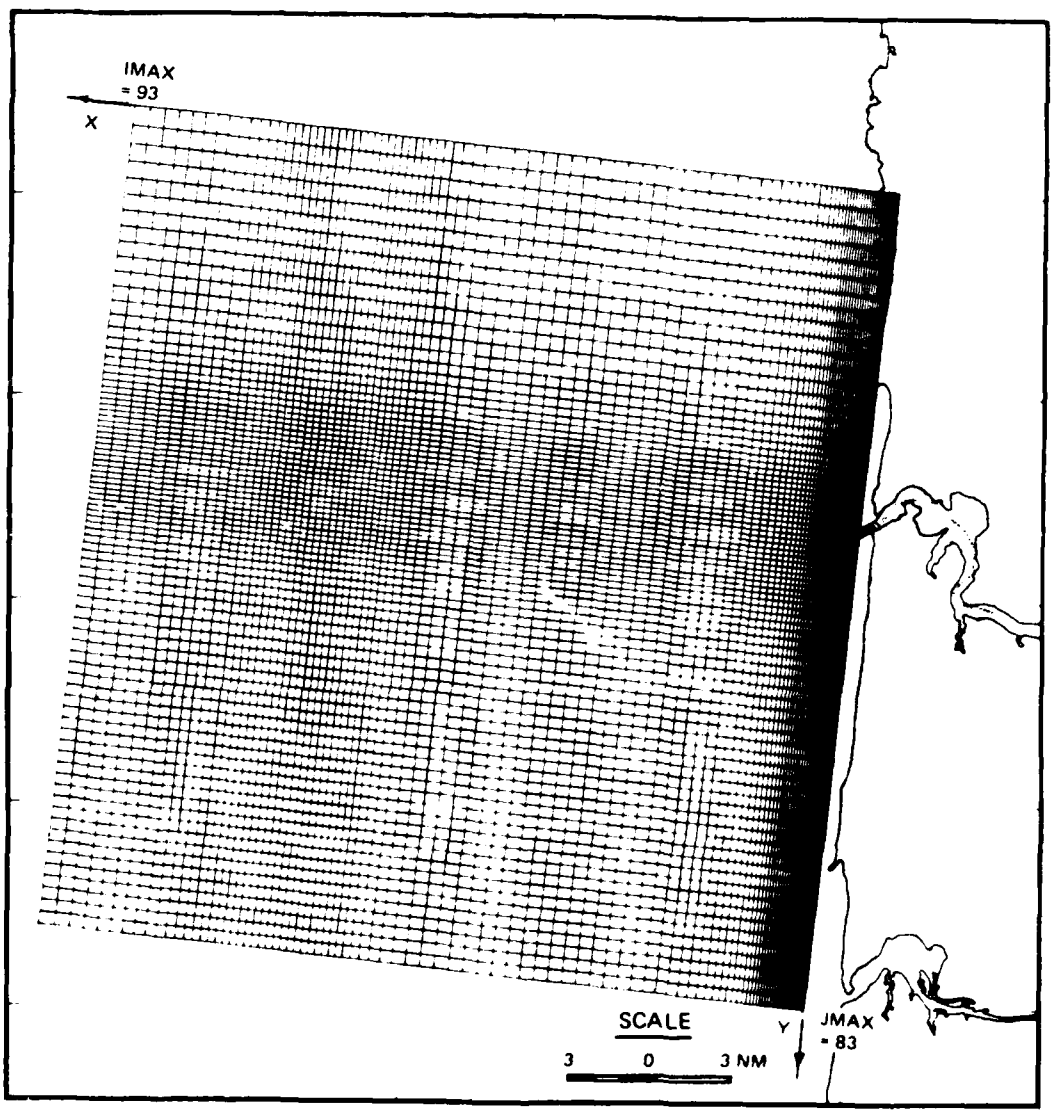

Figure 7. RCPWAVE 93 by 83 grid

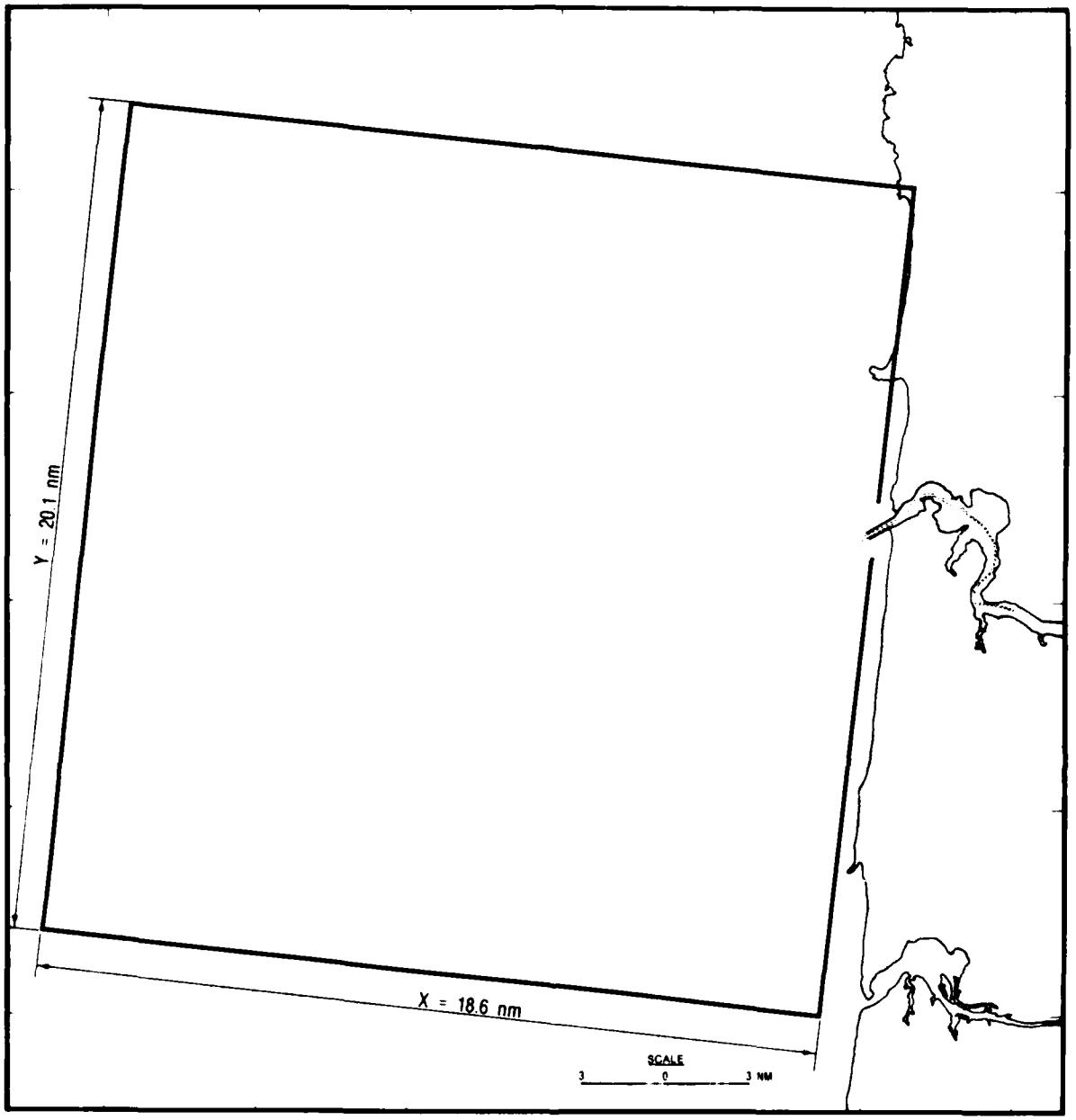

Figure 8. RCPWAVE 93 by 83 grid boundaries

mllw range from approximately -12.0 to -40.0 ft along the y-axis (I = 1) and -300.0 to -500.0 ft along the seaward boundary (I = 93). Deepwater wave information is required as input to the model, specifically height, period, and direction. Table 2 displays the wave conditions selected. The model is run on the larger grid to propagate waves from far offshore into the jetty area. For each of the 24 runs, the wave height and angle at each grid cell are stored permanently.

Table 2

RCPWAVE Model Wave Conditions

Deepwater Wave Height, ft	Period, sec	Direction, deg
14	8.0	West-northwest (-16.0)*
	11.0	
	14.0	
	16.0	
14	8.0	West (6.5)
	11.0	
	14.0	
	16.0	
14	8.0	West-southwest (29.0)
	11.0	
	14.0	
	16.0	
10	8.0	West-northwest (-16.0)
	11.0	
	14.0	
	16.0	
10	8.0	West (6.5)
	11.0	
	14.0	
	16.0	
10	8.0	West-southwest (0.0)
	11.0	
	14.0	
	16.0	

* The grid is rotated 6.5 deg east of north; therefore, 22.5 deg becomes 16.0 deg, etc.

24. The stored values of wave height and angle are then interpolated onto a finer, smaller grid (Figure 9). The interpolation program uses a fairly simple scheme to determine values of wave height and angle at each grid cell in the smaller, "new" grid. For every new grid cell, a search is done in each 90-deg quadrant for the nearest value of wave height from the larger "old" grid. A weighted average of these four values is used to compute a new wave height. The weighting functions are based on relative distances from the new grid centers to the cell centers defining the positions of the four closest, old wave height values. The procedure is repeated to determine values of the wave angle throughout the new grid.

25. The RCPWAVE model is run on the smaller, finer grid. The initial guess of wave heights and wave angles over the entire grid is the interpolated results from the larger grid rather than the results from using Snell's law. The smaller (61 by 80), variably spaced, rectangular grid used by the model is shown in Figure 9. Grid dimensions are 4.58 n.m. in the longshore (y) direction and 2.05 n.m. in the offshore (x) direction, with the y-axis 9.5 deg east of true north. Water depths are digitized from the 1982 Yaquina Bay and River Bathymetry Survey except in the entrance channel where NPP provided a more detailed bathymetric chart. Depths relative to mllw range from approximately -1.0 to -96.0 ft. Since the RCPWAVE model does not model structures, a routine was developed to use with the RCPWAVE model to model the diffractive effect of the jetties. The wave model is run on the smaller grid to provide the wave height, angle, and number at each grid cell as input to CURRENT. CURRENT also uses the 61 by 80 cell grid; therefore, no interpolation is required.

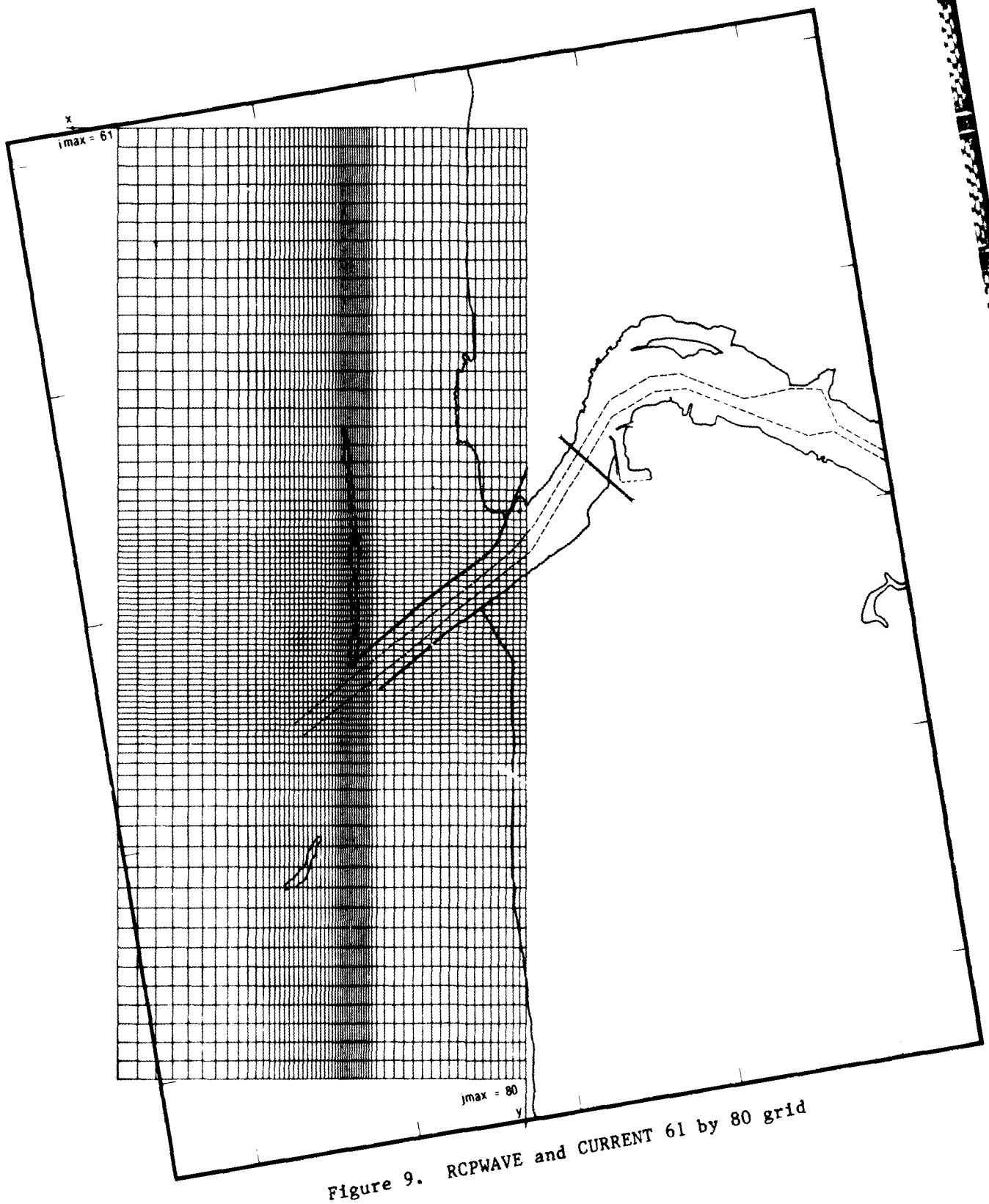

Figure 9. RCPWAVE and CURRENT 61 by 80 grid

PART IV: THE WAVE-INDUCED CURRENT MODEL

The Model

26. CURRENT is used to predict the currents induced by breaking waves at Yaquina Bay. The model takes the radiation stress approach of Longuet-Higgins and solves the vertically integrated equations of continuity and momentum by using an ADI scheme. Mixing and advection terms are included. The hydrodynamic equations used in the model are derived from the Navier-Stokes equations, assuming the fluid is homogeneous and incompressible and the vertical accelerations are negligible. The 2-D, depth-averaged forms of the equations are obtained by vertically integrating the three-dimensional form of the equations with the appropriate boundary conditions applied. The 2-D equations are time-averaged over one wave period to give

$$\frac{\partial u}{\partial t} + u\frac{\partial u}{\partial y} + v\frac{\partial u}{\partial y} + g\frac{\partial \bar{\eta}}{\partial x} + \frac{1}{\rho d}\tau_{bx} + \frac{1}{\rho d}\left(\frac{\partial S_{xx}}{\partial x} + \frac{\partial S_{xy}}{\partial y}\right) - \frac{1}{\rho}\frac{\partial \tau_{xy}}{\partial y} = 0 \qquad (7)$$

$$\frac{\partial v}{\partial t} + u\frac{\partial v}{\partial x} + v\frac{\partial v}{\partial y} + g\frac{\partial \bar{\eta}}{\partial y} + \frac{1}{\rho d}\tau_{by} + \frac{1}{\rho d}\left(\frac{\partial S_{xy}}{\partial x} + \frac{\partial S_{yy}}{\partial y}\right) - \frac{1}{\rho}\frac{\partial t_{xy}}{\partial x} = 0 \qquad (8)$$

$$\frac{\partial \bar{\eta}}{\partial t} + \frac{\partial}{\partial x}(ud) + \frac{\partial}{\partial y}(vd) = 0 \qquad (9)$$

where

u and v = depth-averaged horizontal velocity components at time t in the x- and y-directions, respectively

g = acceleration due to gravity

$\bar{\eta}$ = displacement of the mean-free surface with respect to the still-water level

ρ = mass density of seawater

$d = \bar{\eta} - h$ = total water depth (Figure 10)

h = bed elevation with respect to the still-water level ((+) land, (-) water)

τ_{bx} and τ_{by} = bottom friction stresses in the x- and y-directions, respectively

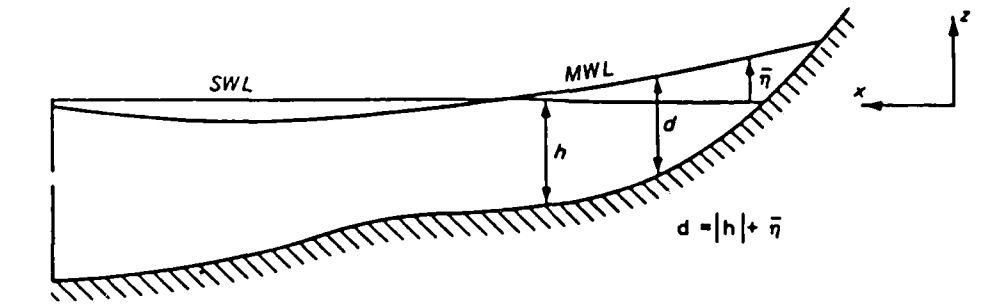

a. CROSS SECTION A-A

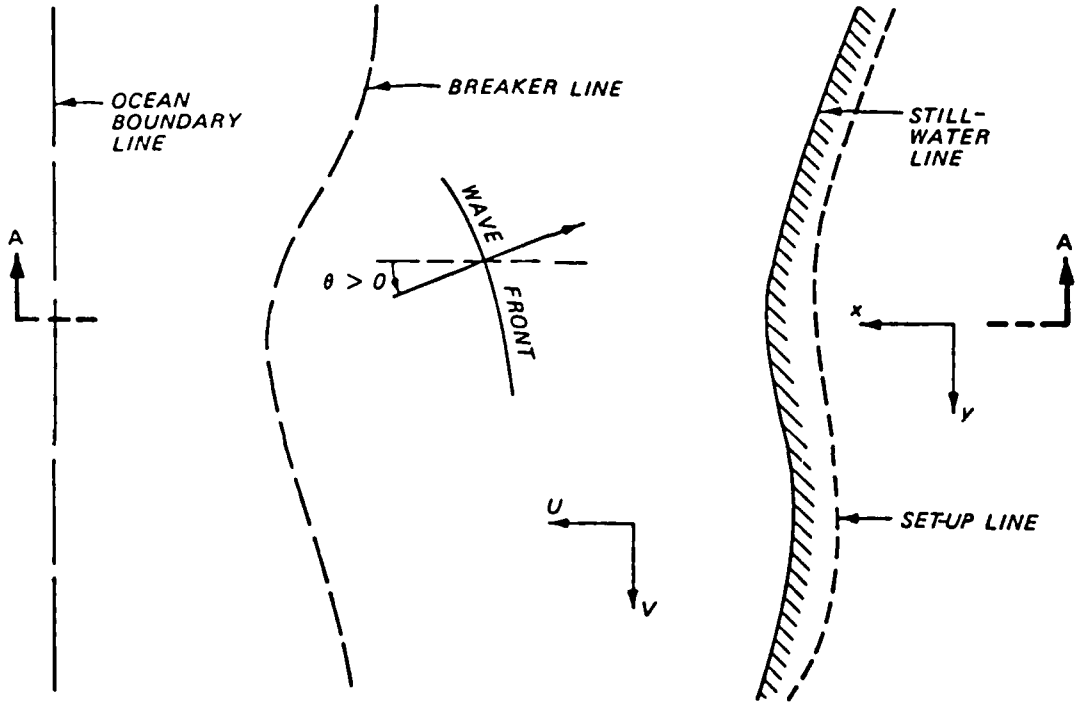

b. PLAN

Figure 10. Definition sketch for an irregular beach (swl = still water level, mwl = mean water level)

S_{xx}, S_{xy}, and S_{yy} = radiation stresses which arise because of the excess momentum flux due to waves

τ_{xy} = lateral shear stress due to turbulent mixing

Initial and Boundary Conditions

27. To run CURRENT, appropriate initial and boundary conditions must be specified. At Yaquina Bay, the model calculations are started from rest, setting η, u, and v to zero. Model boundaries are shown in Figure 11.

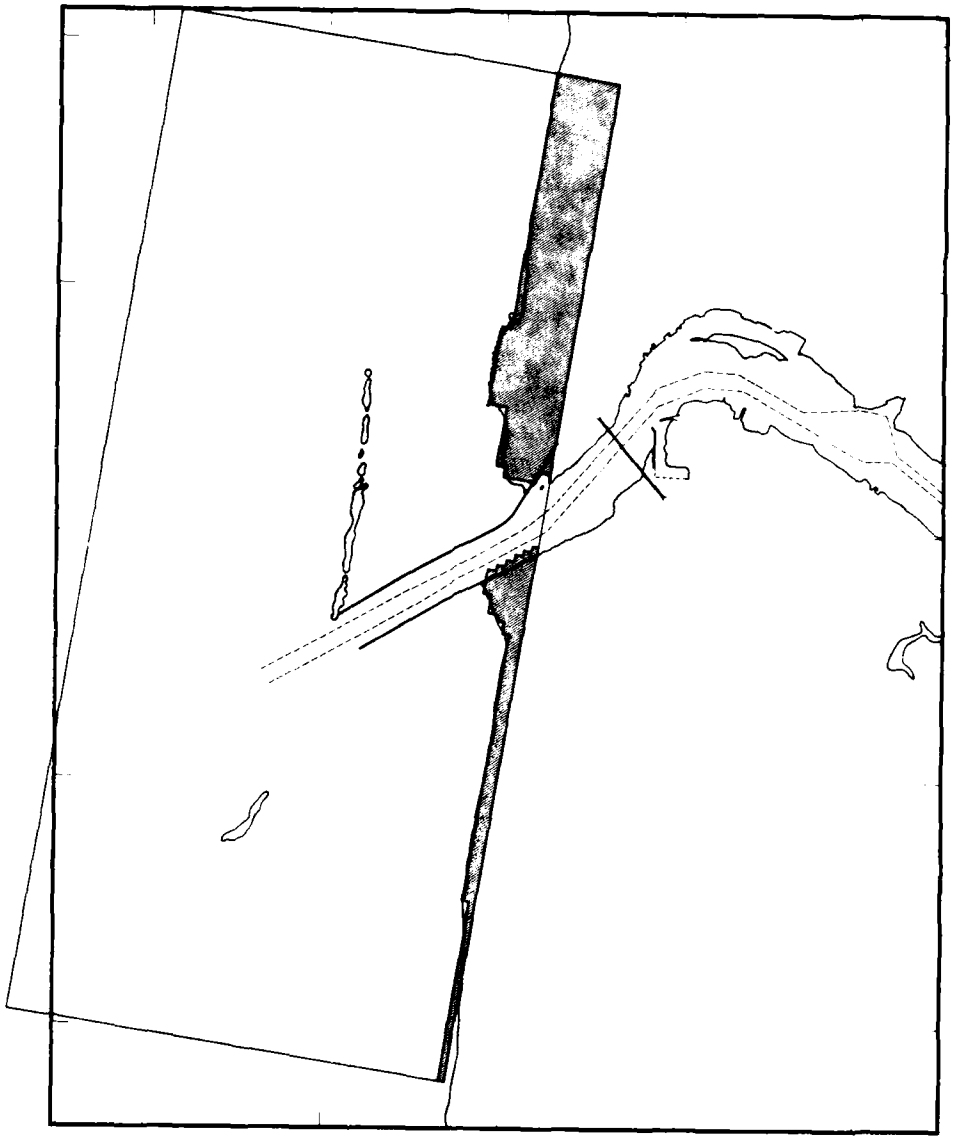

Figure 11. CURRENT and RCPWAVE grid boundaries

The radiation stress gradients are gradually applied to avoid unwanted transients in the solution. This is accomplished by gradually building up to the full radiation stress values over a number of time-steps. The numerical computations continue until a steady-state condition is reached.

28. CURRENT permits the following boundary conditions:

a. "No flow" (wall). This boundary condition is used at closed boundaries (i.e., land-water boundaries and at impermeable structures). Land-water boundaries are closed because CURRENT does not permit flooding and drying. The jetties at Yaquina Bay are treated as impermeable, nonovertopping structures, and

the no-flow boundary condition is applied. The velocity perpendicular to closed boundaries is set to zero.

b. Elevation (tide). This condition may be used at the offshore boundary since the setup is an unknown quantity. It should be noted, however, that a radiation stress boundary condition is preferred at the offshore boundary.

c. Uniform flux. The uniform flux boundary condition is used for lateral boundaries. The flux at a boundary cell is set equal to its adjacent interior cell. Thus, the condition assumes $\partial(ud)/\partial x = 0$ or $\partial(vd)/\partial y = 0$ at the boundary.

d. Radiation. The radiation boundary condition requires that any transients initially developing within the numerical grid propagate out of the grid as gravity waves. The radiation condition takes the following form:

$$\frac{\partial \eta}{\partial t} + c \frac{\partial \eta}{\partial x} = 0$$

where

$\eta(t,x)$ = surface disturbance

c = phase speed of η

CURRENT uses this boundary condition at the offshore boundary rather than boundary condition of elevation and no flow, due to the reflective nature of the elevation and no-flow boundary conditions. The elevation and no-flow boundary conditions tend to trap transients between the offshore and nearshore boundaries, and damping of transients would take place at a slow rate. The radiation boundary condition allows the transients to propagate out of the grid, producing an appropriate η value at the offshore boundary. Figure 12 displays the boundary conditions used for the Yaquina Bay CURRENT runs.

Model Approach

29. CURRENT is run at Yaquina Bay to predict the currents caused by breaking waves. The model requires the wave heights, angles, and numbers throughout a gridded region as input conditions. This information is provided by the RCPWAVE model. The 24 deepwater wave conditions used to run RCPWAVE and then CURRENT are shown in Table 2.

30. CURRENT employs a variably spaced finite difference grid in the computational scheme. The grid axes are aligned such that the y-axis is approximately parallel to the shoreline, increasing in the southerly direction

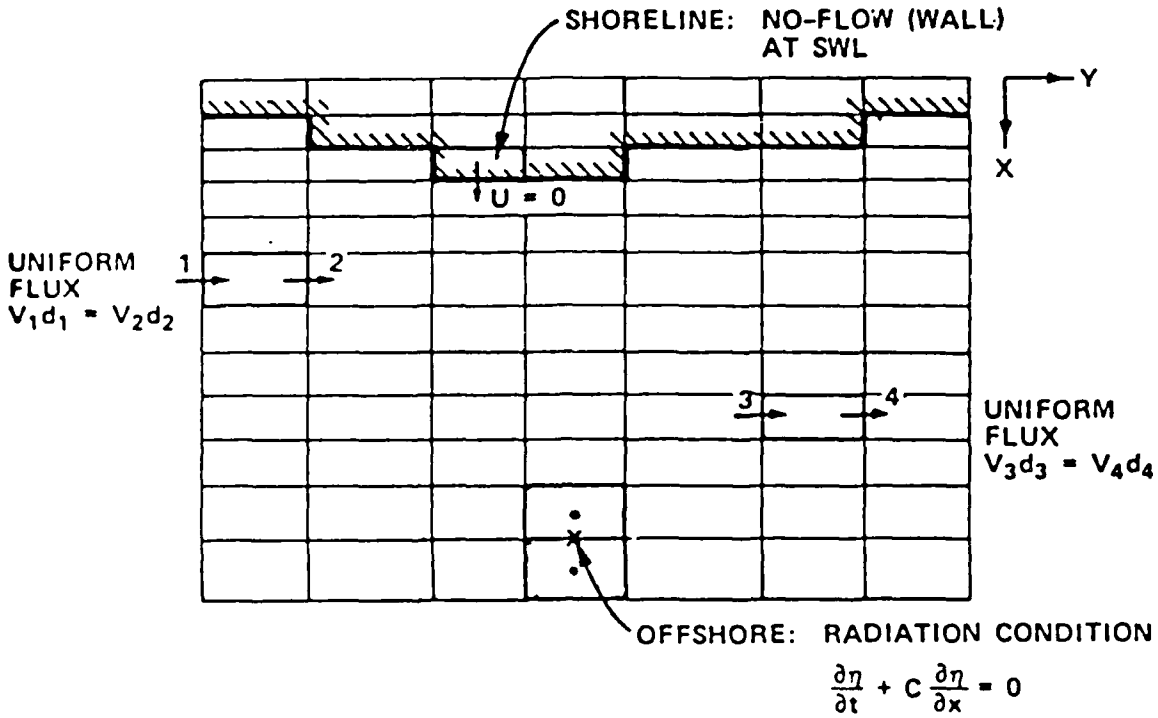

Figure 12. CURRENT model boundary conditions

and the x-axis is approximately perpendicular to the shoreline, increasing in the offshore direction at Yaquina Bay (Figure 9). The RCPWAVE model was also run on this grid. The grid cells range in size from 60 to 545 ft in the x-direction and from 150 to 511 ft in the y-direction. The depth at each of the 61 by 80 grid cells is digitized from the 1982 Yaquina Bay and River Bathymetry Survey to a datum of mllw. The maximum depth of the Yaquina Bay CURRENT grid is 96 ft below mllw. All data are then converted to NGVD by subtracting 4.03 ft. At this point, CURRENT is run until a steady-state condition is reached.

PART V: GRID CONNECTION

31. The purpose of this study is to model the velocities of the tidal and wave-induced currents in the vicinity of the Yaquina Bay entrance and, in so doing, determine the current regime at the tip of the north jetty. This is accomplished by superimposing the tidal and wave-induced currents predicted by the hydrodynamic, numerical models, WIFM and CURRENT. Since WIFM is run on a grid of 49 by 55 cells and CURRENT is run on a grid of 61 by 80 cells, interpolation is required before superposition can be performed. The 49 by 55 WIFM grid velocities are interpolated to the finer CURRENT grid by using the following method:

a. For every (I, J) cell in the CURRENT grid, a search is executed for the nearest WIFM u-velocity component in each 90-deg quadrant of the WIFM grid.

b. A weighted average of the four closest WIFM u-values is used to compute a WIFM u-value for the CURRENT (I, J) grid cell. The weighting functions are based on the relative distances from the CURRENT (I, J) grid cell to the cell centers defining the positions of the four closest WIFM values.

c. The procedure is repeated to determine the WIFM v-velocity component throughout the CURRENT grid.

32. The WIFM values of u interpolated onto the CURRENT grid are superimposed on the CURRENT u-values , providing the total u-velocity component at each grid cell. The v-velocity is dealt with in the same manner. Vectorially summing u and v , the total current regime at Yaquina Bay is determined.

PART VI: REHABILITATIVE ALTERNATIVES

33. Five rehabilitative alternatives were modeled to provide the current field throughout the gridded region. The following structural alternatives were included:

a. Extending the north jetty to its original length.

b. Adding a spur near the end of the north jetty, approximately perpendicular to Yaquina Reef.

c. Adding a spur near the end of the north jetty, approximately perpendicular to the jetty.

d. Extending the north jetty to its original length and adding a spur near the end of the north jetty, approximately perpendicular to Yaquina Reef.

e. Adding an L-shaped barrier near the end of the north jetty.

34. The tidal model was run for the five rehabilitative alternatives. Structural alternatives a, b, d, and e were effective in altering the water current pattern. Alternatives b and e were selected to use with CURRENT because those structural alternatives produced beneficial effects on the wave-induced current pattern near the north jetty tip.

PART VII: RESULTS

35. After calibration and verification, the tidal model was run with five rehabilitative alternatives to test their effects on the tidal current patterns near the inlet. The structural alternatives were modeled as thin-wall barriers in the tidal model. Plates 4 and 5 show the tidal current patterns at peak flood and ebb for the existing conditions at Yaquina Bay. The tidal current patterns at peak flood and ebb for the five rehabilitative alternatives are displayed in Plates 6-15. Plates 16-25 show (vectorially) the difference between the existing tidal current patterns and the tidal current patterns produced by the five rehabilitative alternatives at peak flood and ebb. Structural alternatives a, b, d, and e (Part VI) alter the tidal current pattern near the tip of the north jetty.

36. CURRENT was used to predict the existing wave-induced currents at the entrance to Yaquina Bay for 24 wave conditions (Table 2). Plates 26 through 31* show the steady-state, wave-induced current patterns produced by CURRENT for 6 of the 24 wave conditions. Wave period did not appear to have a strong effect on the wave-induced current patterns, whereas the wave height and angle influenced the current patterns significantly. (Plates are shown only for the various wave heights and angles.) Plates 32-37 and 38-43 show the superposition of tidal and wave-induced currents at peak flood and peak ebb, respectively. The consistent circulation pattern to the south of the south jetty is related to the acute angle that the structure makes with the shoreline. Coast Guard personnel verified the existence of the circulation pattern.** The wave-induced currents are significantly stronger than the tidal currents at the tip of the north jetty.

37. Testing the five rehabilitative alternatives for 24 wave conditions was economically infeasible. Alternatives b and e were selected from the five rehabilitative alternatives to use with CURRENT. The selection was based on the knowledge of the wave-induced current patterns produced by the initial 24 CURRENT runs for existing jetty conditions and the performance of the

---

* In the plates, H_o = deepwater wave height, T = period, θ = wave direction.

** Personal Communication, December 3, 1985, David Edwards, Boatswains Mate First Class, US Coast Guard.

five rehabilitative alternatives in varying the tidal current patterns. Three wave conditions were selected for testing with the rehabilitative alternatives:

Height ft	Period sec	Direction deg
14	11	West-northwest
14	14	West
14	11	West-southwest

The three wave conditions were selected to represent waves arriving from the three directions and occurrences of strong currents near the north jetty. Using a wave height of 14 ft best produced the specified conditions. Plates 44-61 display the wave-induced current patterns and the superposition of tidal and wave-induced currents at peak flood and peak ebb for alternatives b and e.

38. In comparing Plates 32-34 with Plates 47-49 and 56-58, it is evident that structural alternatives b and e diminish the intensity of the currents north of the north jetty for flood tidal flow. At ebb tide, a comparison of Plates 38-40 with Plates 50-52 and 59-61 shows a similar trend in reducing current intensity when structural alternatives b and e are in place. Currents at the north jetty are reduced because the structures redirect the flow outside the north jetty tip. Flows north of the inlet are generally north to south and parallel to the Yaquina Reef, regardless of the deepwater wave direction. The current appears to be channelized by the reef and structural alternatives b and e redirect the channelized current.

PART VIII: CONCLUSIONS

39. WIFM provided the tidal current field near the entrance to Yaquina Bay for existing conditions and for the following five rehabilitative alternatives:

a. Extend the north jetty to its original length.

b. Add a spur to the north jetty, approximately perpendicular to Yaquina Reef.

c. Add a spur to the north jetty, approximately perpendicular to the north jetty.

d. Extend the north jetty to its original length and add a spur to the north jetty, approximately perpendicular to Yaquina Reef.

e. Add an L-shaped barrier to the north jetty.

The results of this model investigation indicate that rehabilitative alternatives a, b, d, and e are effective in altering the tidal current pattern near the tip of the north jetty.

40. CURRENT provided the wave-induced current field near the entrance to Yaquina Bay for 24 wave conditions. For each wave condition, the wave-induced current field was superimposed onto the existing tidal current field at peak flood and peak ebb, providing the total current field at Yaquina Bay. CURRENT was then run for three selected wave conditions with rehabilitative alternatives b and e. For the selected alternatives b and e, the wave-induced current field was superimposed onto the tidal current field. The resulting current patterns demonstrate that structural alternatives b and e are effective in altering the current field at the tip of the north jetty.

REFERENCES

Berkhoff, J. C. W. 1972. "Computation of Combined Refraction - Diffraction," Proceedings of the 13th International Conference on Coastal Engineering, American Society of Civil Engineers, Vol 1, pp 471-490.

Butler, H. L. 1980. "Evolution of a Numerical Model for Simulating Long Period Wave Behavior in Ocean-Estuarine Systems," Estuarine and Wetlands Processes with Emphasis on Modeling, Marine Science Series, Vol II, Plenum Press, New York.

Ebersole, B. A. 1985 (Nov). "Refraction-Diffraction Model for Linear Water Waves," Journal of Waterways, Ports and Harbors, Vol 111, No. 6, pp 939-953.

Ebersole, B. A., Cialone, M. A., and Prater, M. D. 1985. "Regional Coastal Processes Numerical Modeling System; Report 1, RCPWAVE - A Linear Wave Propagation Model for Engineering Use," US Army Engineer Waterways Experiment Station, Coastal Engineering Research Center, Vicksburg, Miss.

Reid and Bodine. 1968. "Numerical Model for Storm Surges in Galveston Bay," Journal of Waterways and Harbors Division, American Society of Civil Engineers, Vol 94, No. WW1, pp 33-57.

US Department of Commerce. 1984. "Tide Tables--1984," National Ocean Survey, Washington, DC.

Vemulakonda, S. R. 1984. "Erosion Control of Scour During Construction; Report 7, CURRENT - A Wave-Induced Current Model," US Army Engineer Waterways Experiment Station, Coastal Engineering Research Center, Vicksburg, Miss.

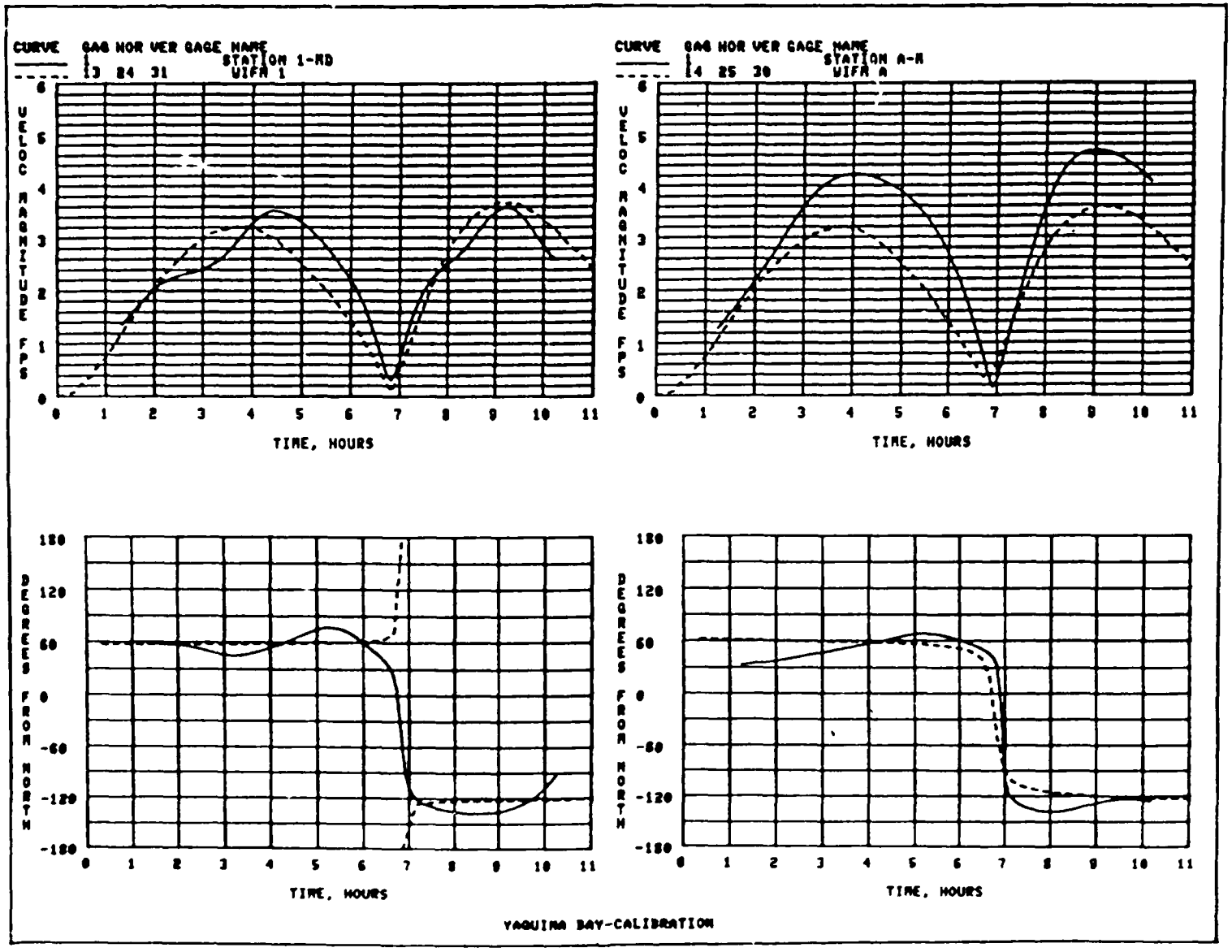

Plate 1. WIFM calibration: sta 1 and sta A

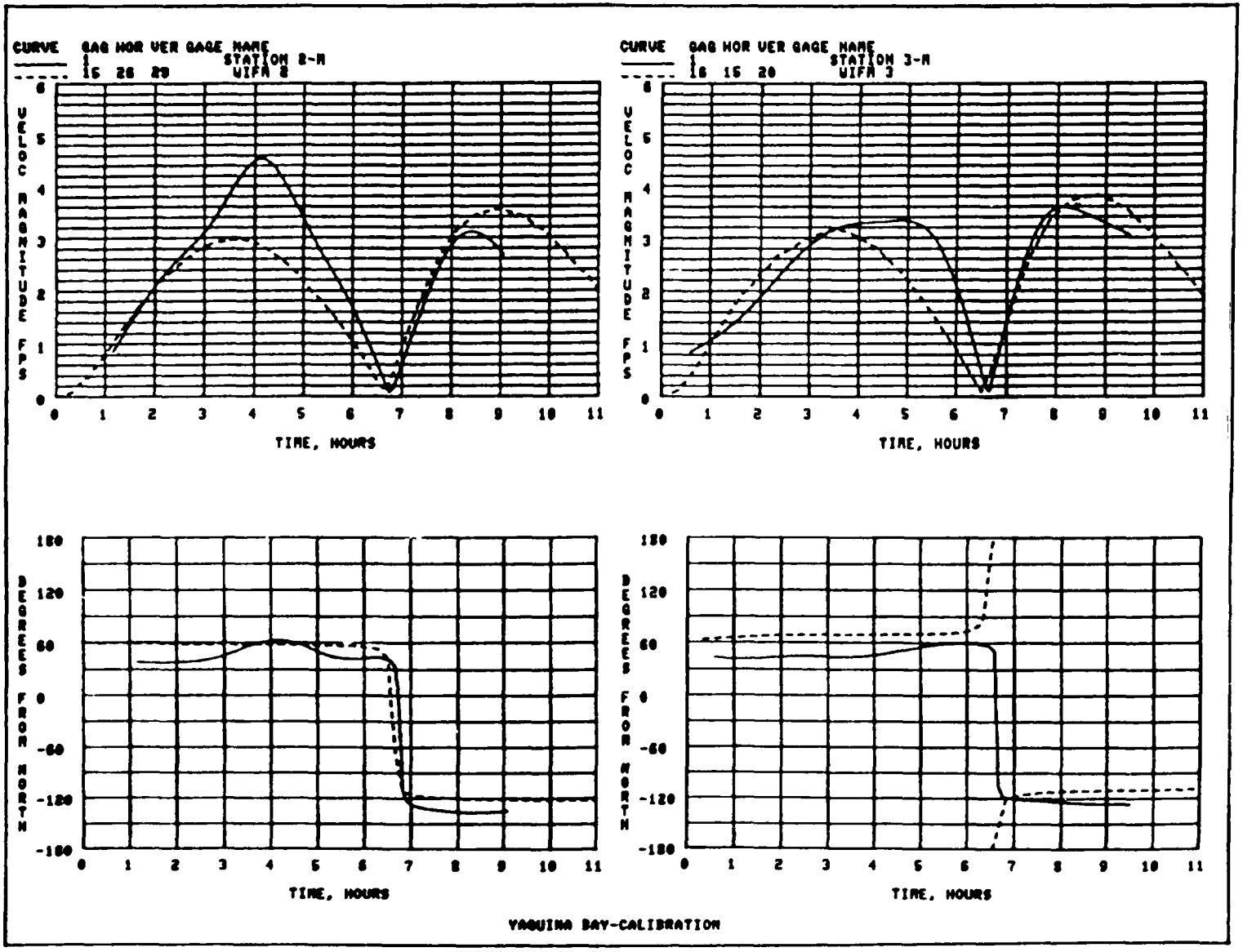

Plate 2. WIFM calibration: sta 2 and sta 3

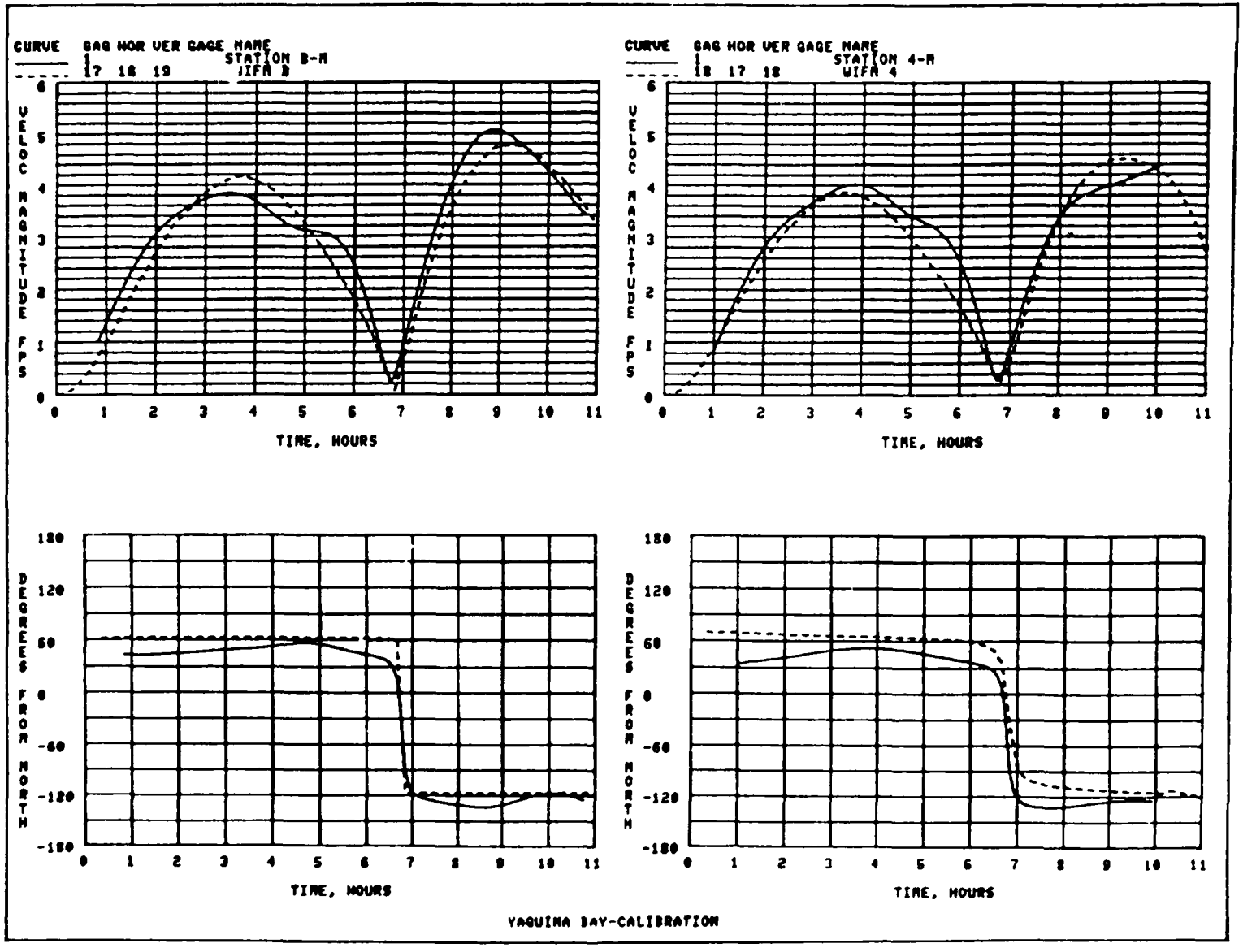

Plate 3. WIFM calibration: sta B and sta 4

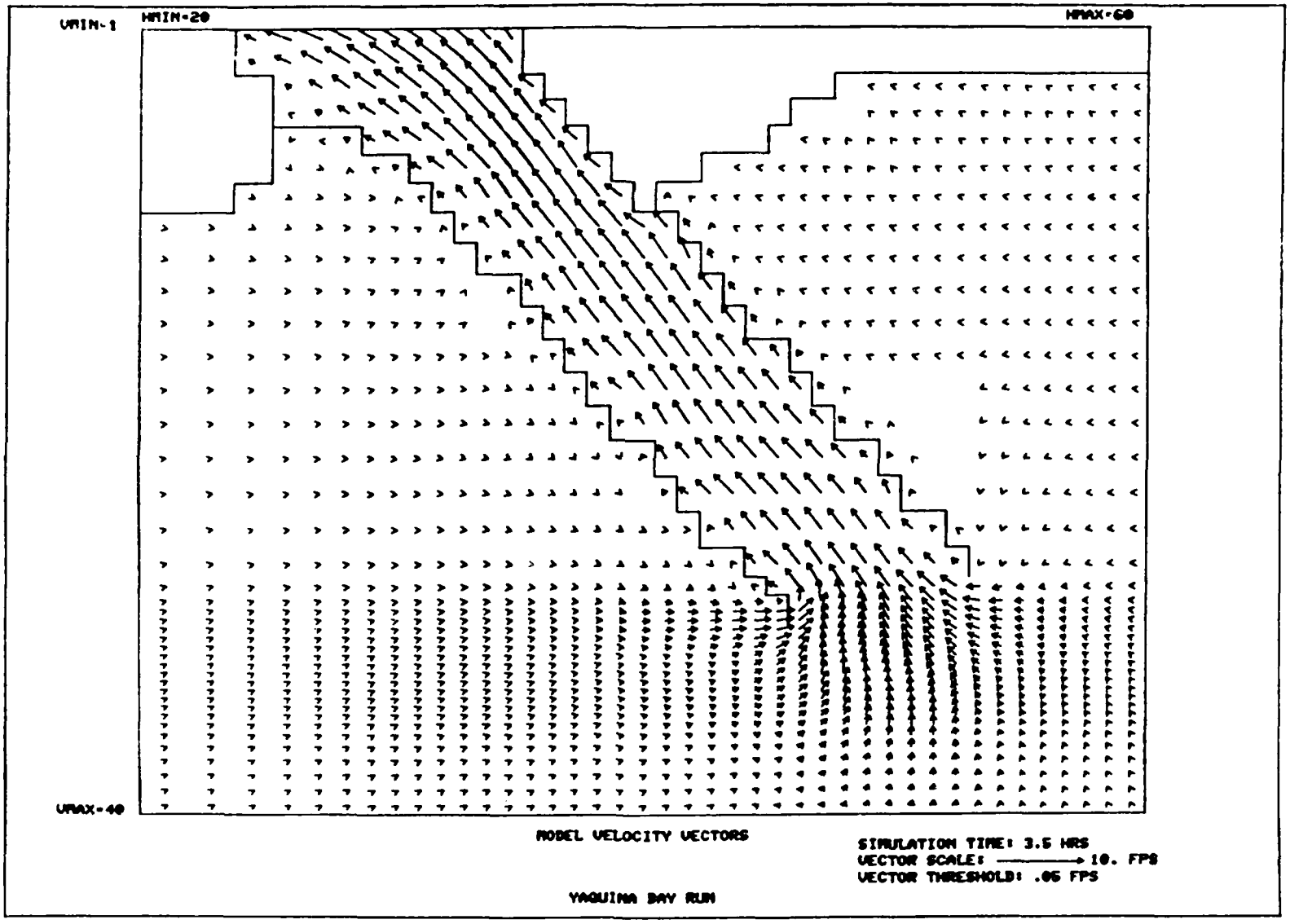

Plate 4. Tidal current pattern: existing conditions; peak flood

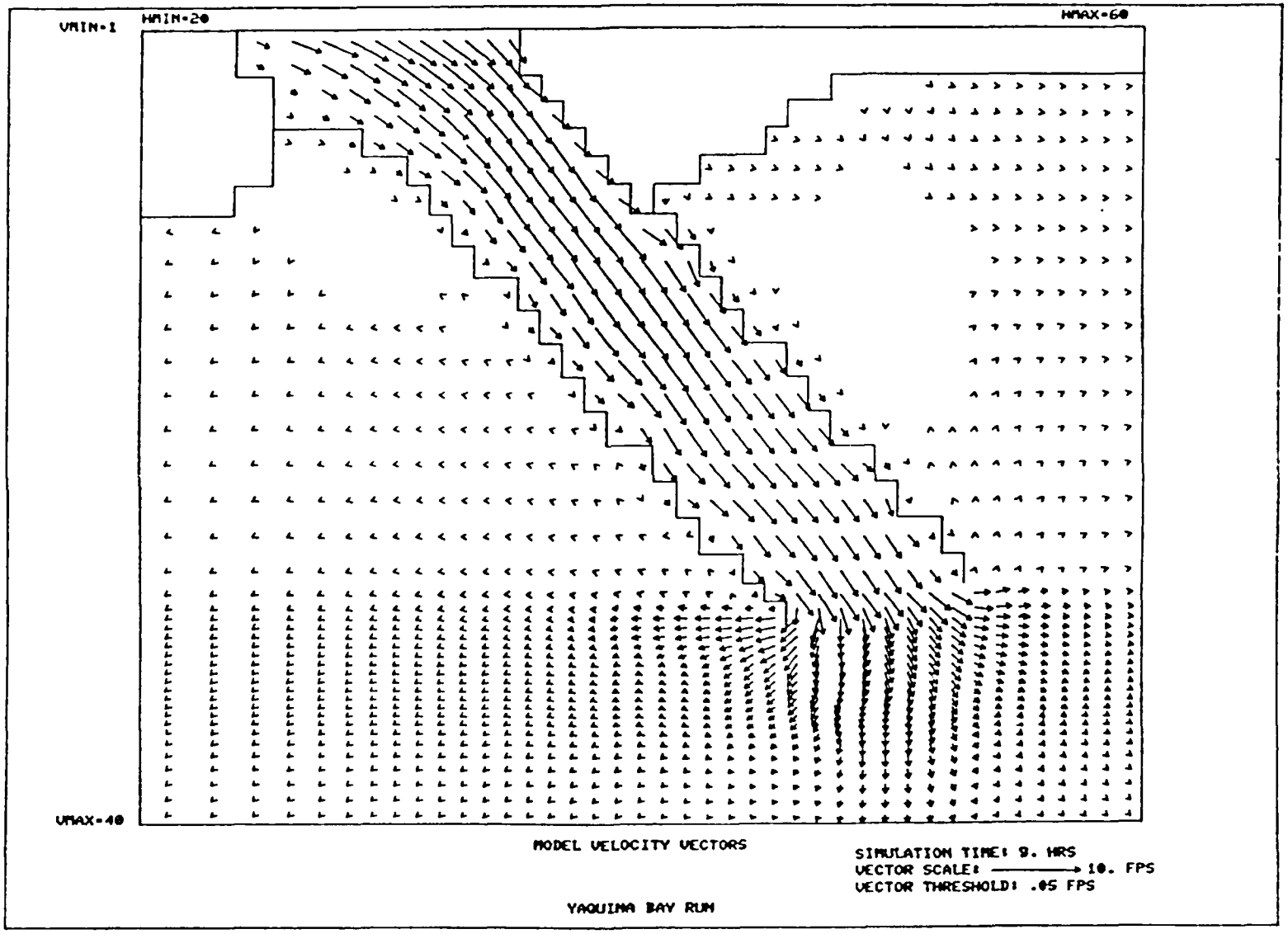

Plate 5. Tidal current pattern: existing conditions; peak ebb

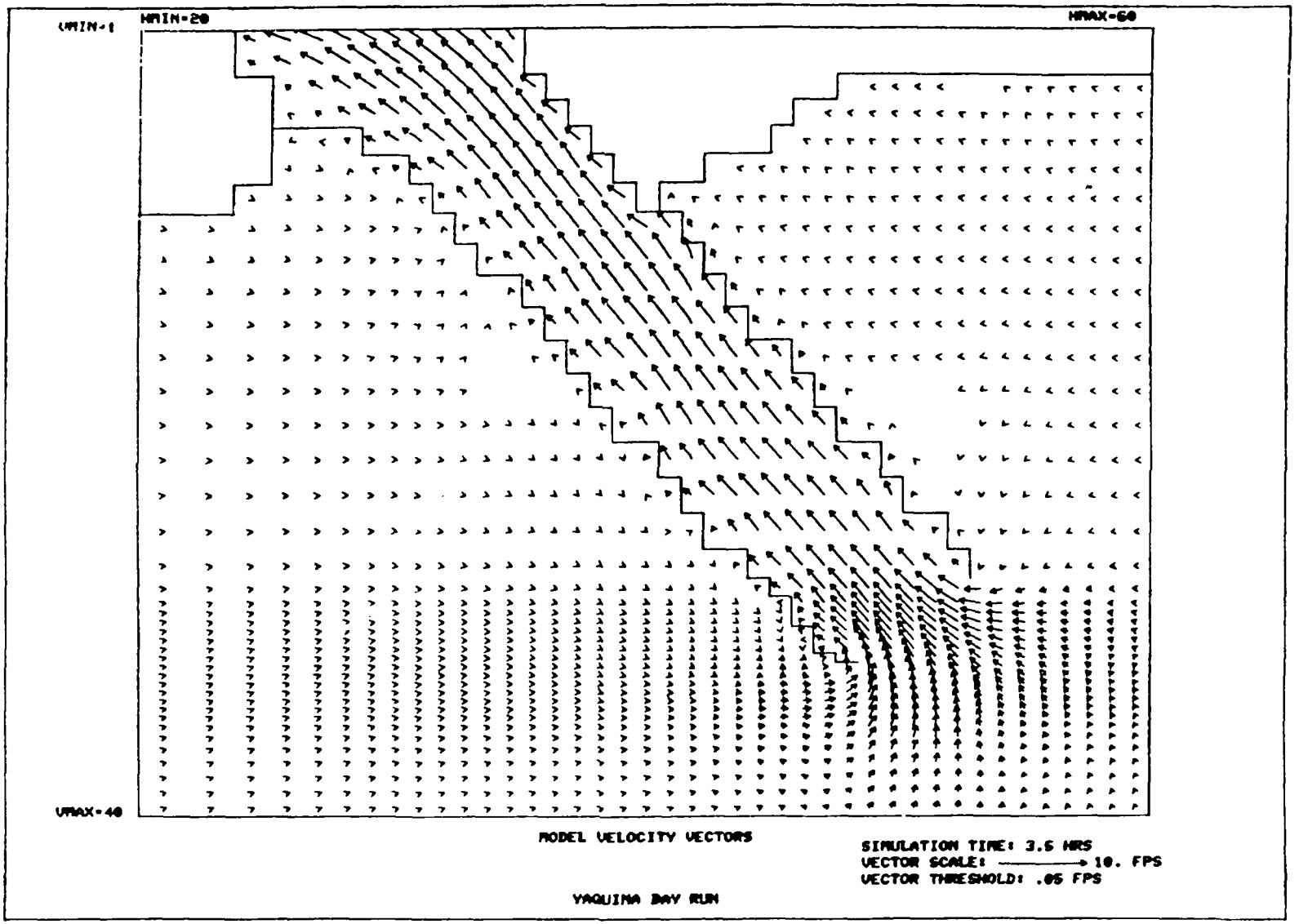

Plate 6. Tidal current pattern: alternative a Part VI; peak flood

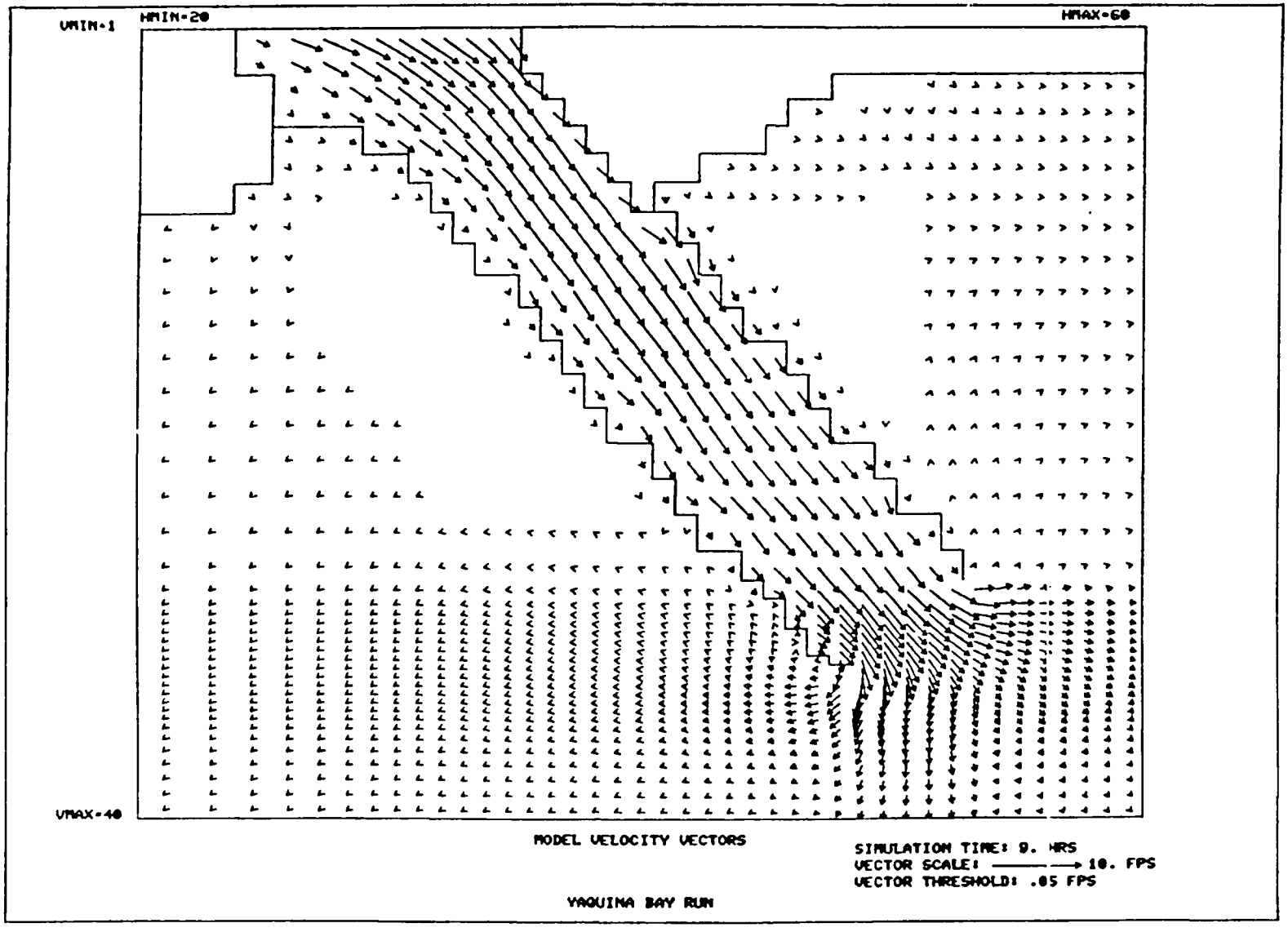

Plate 7. Tidal current pattern: alternative a; peak ebb

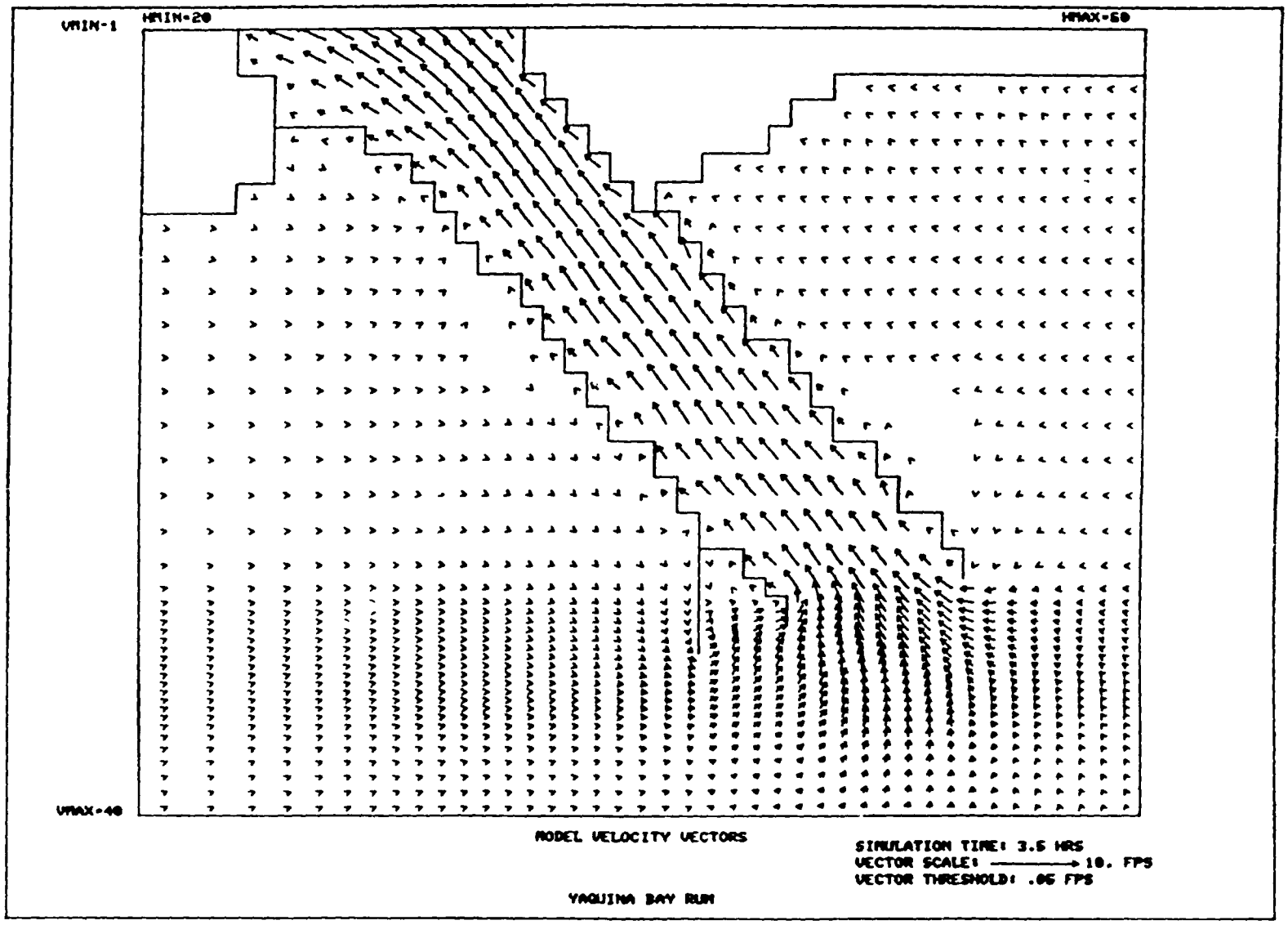

Plate 8. Tidal current pattern: alternative b; peak flood

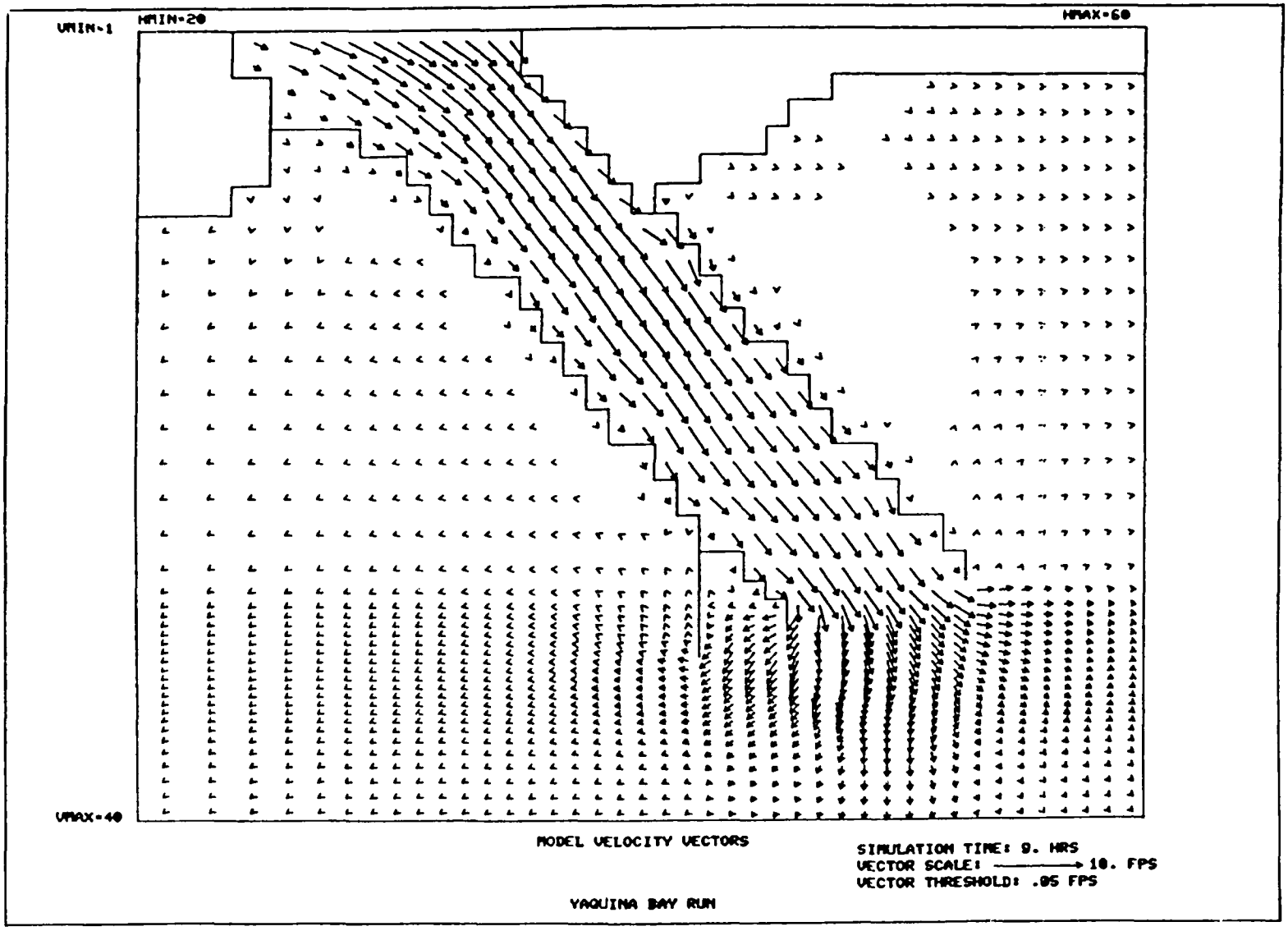

Plate 9. Tidal current pattern: alternative b; peak ebb

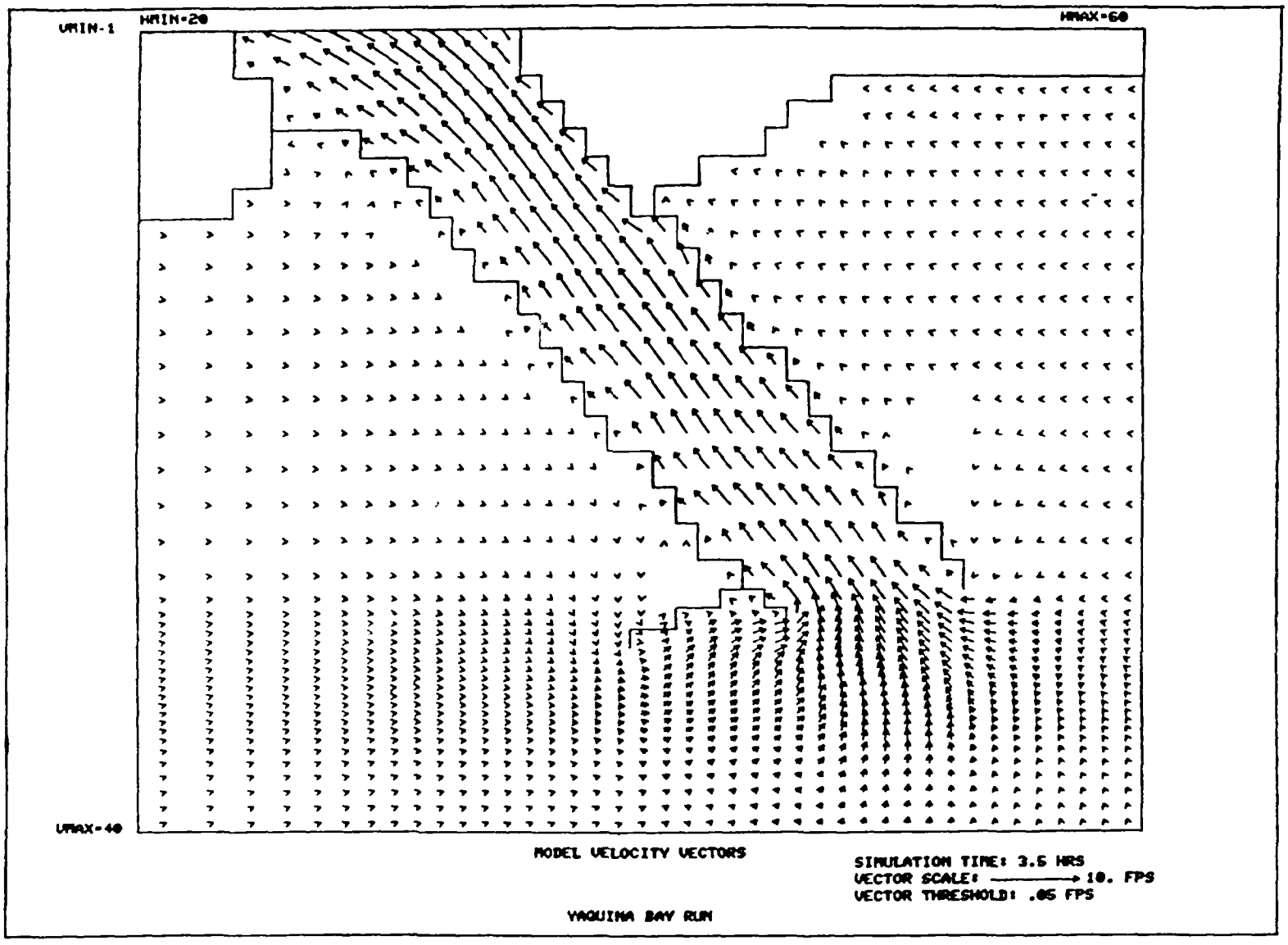

Plate 10. Tidal current pattern: alternative c; peak flood

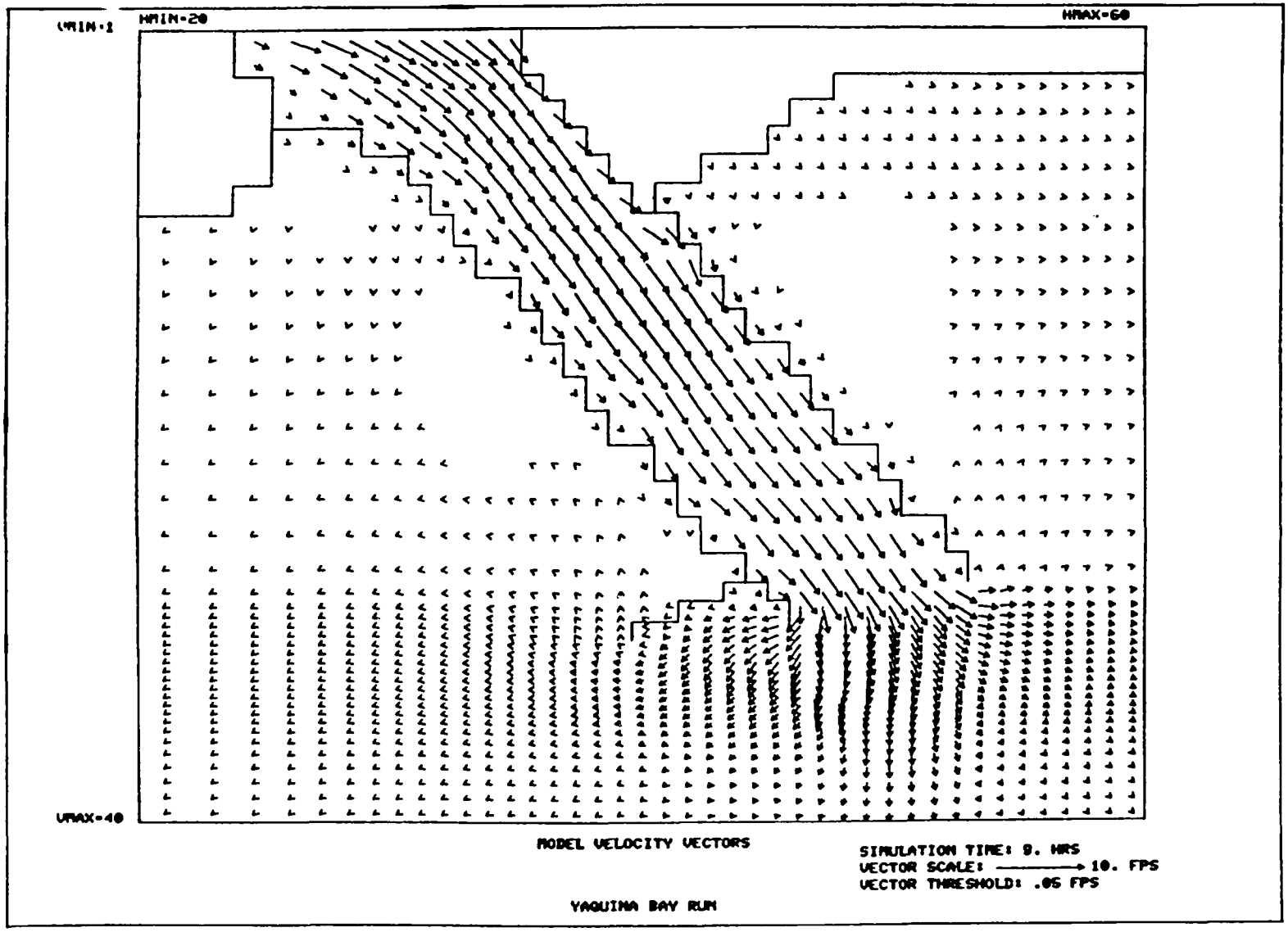

Plate 11. Tidal current pattern: alternative c; peak ebb

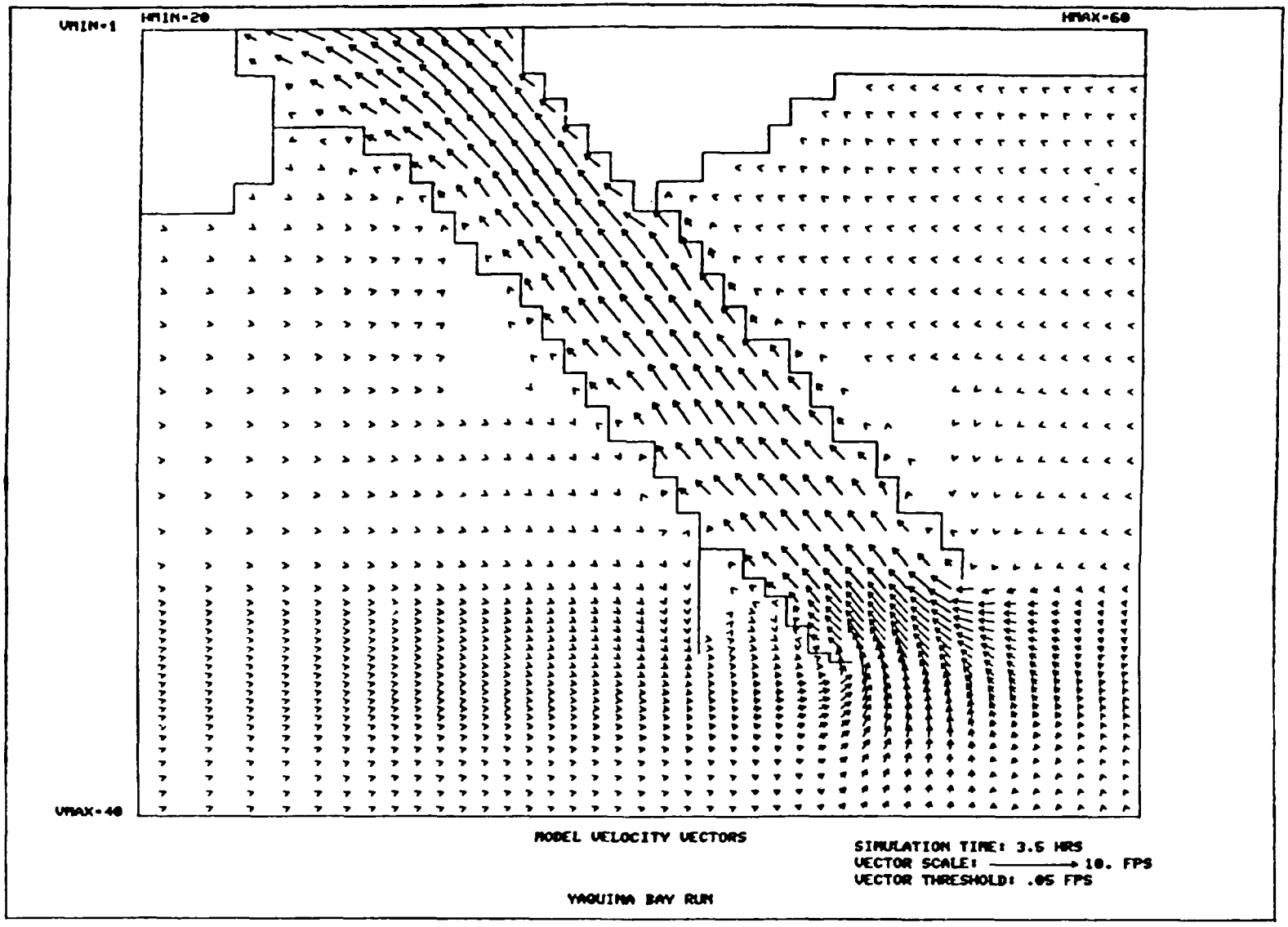

Plate 12. Tidal current pattern: alternative d; peak flood

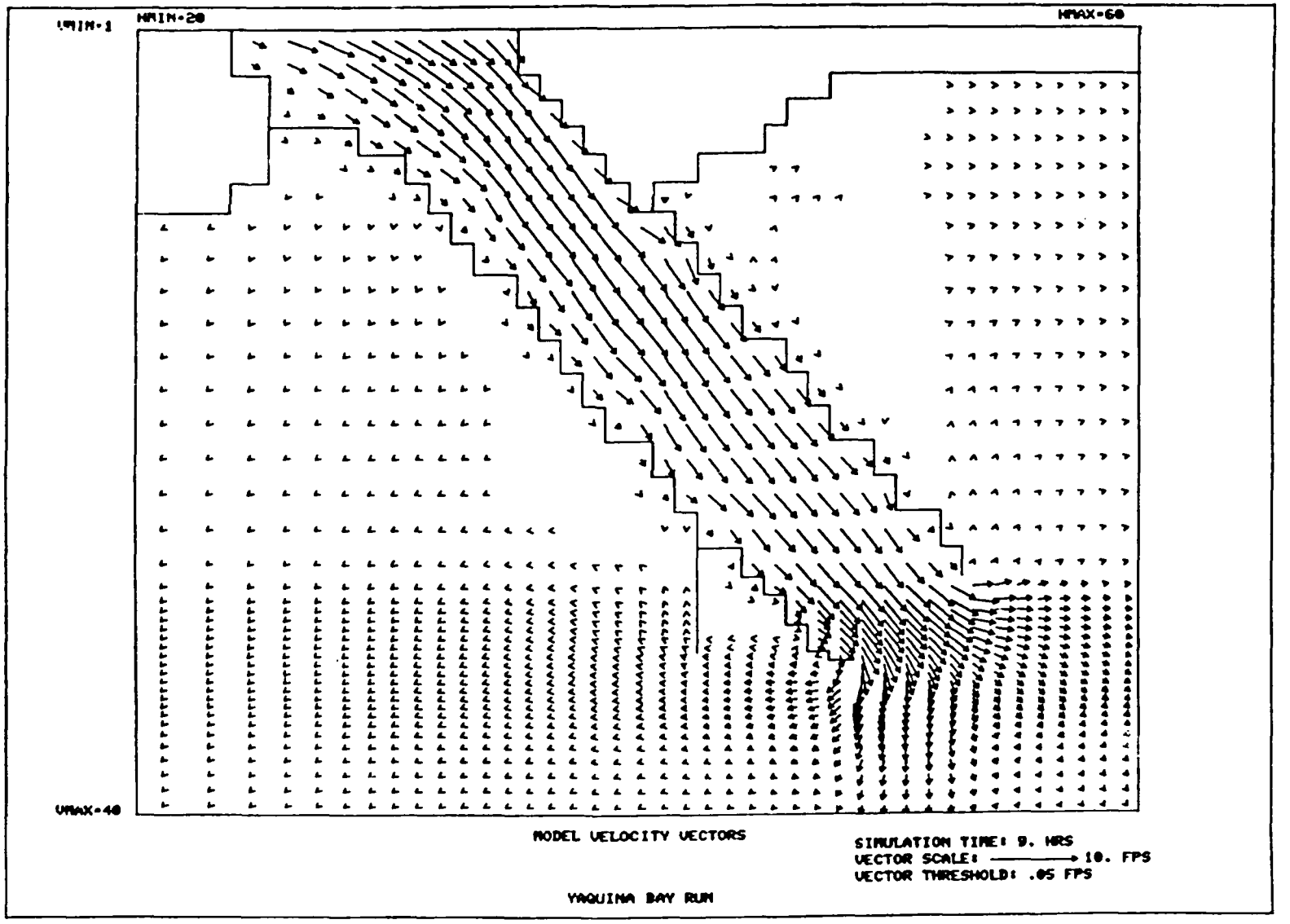

Plate 13. Tidal current pattern: alternative d; peak ebb

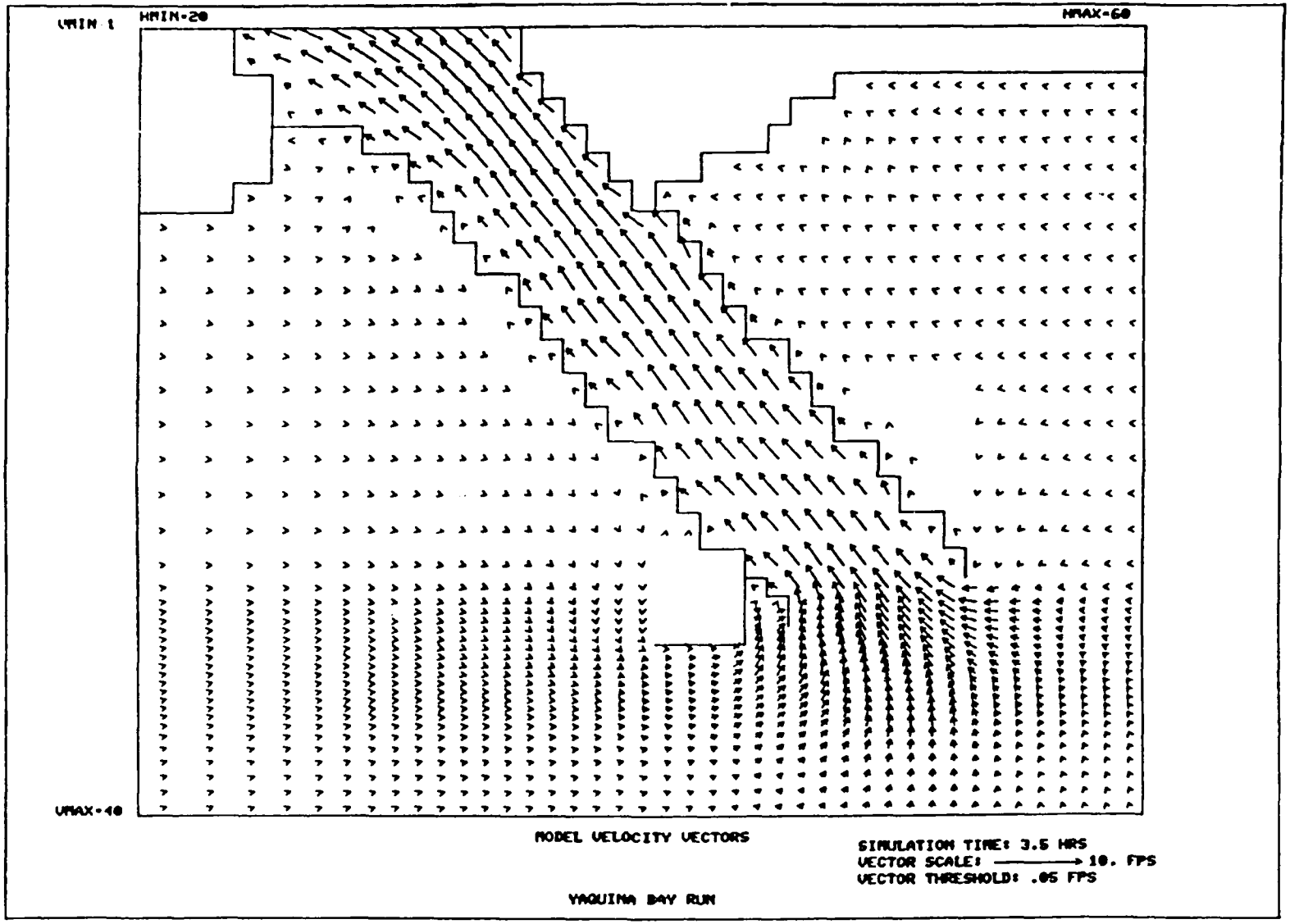

Plate 14. Tidal current pattern: alternative e; peak flood

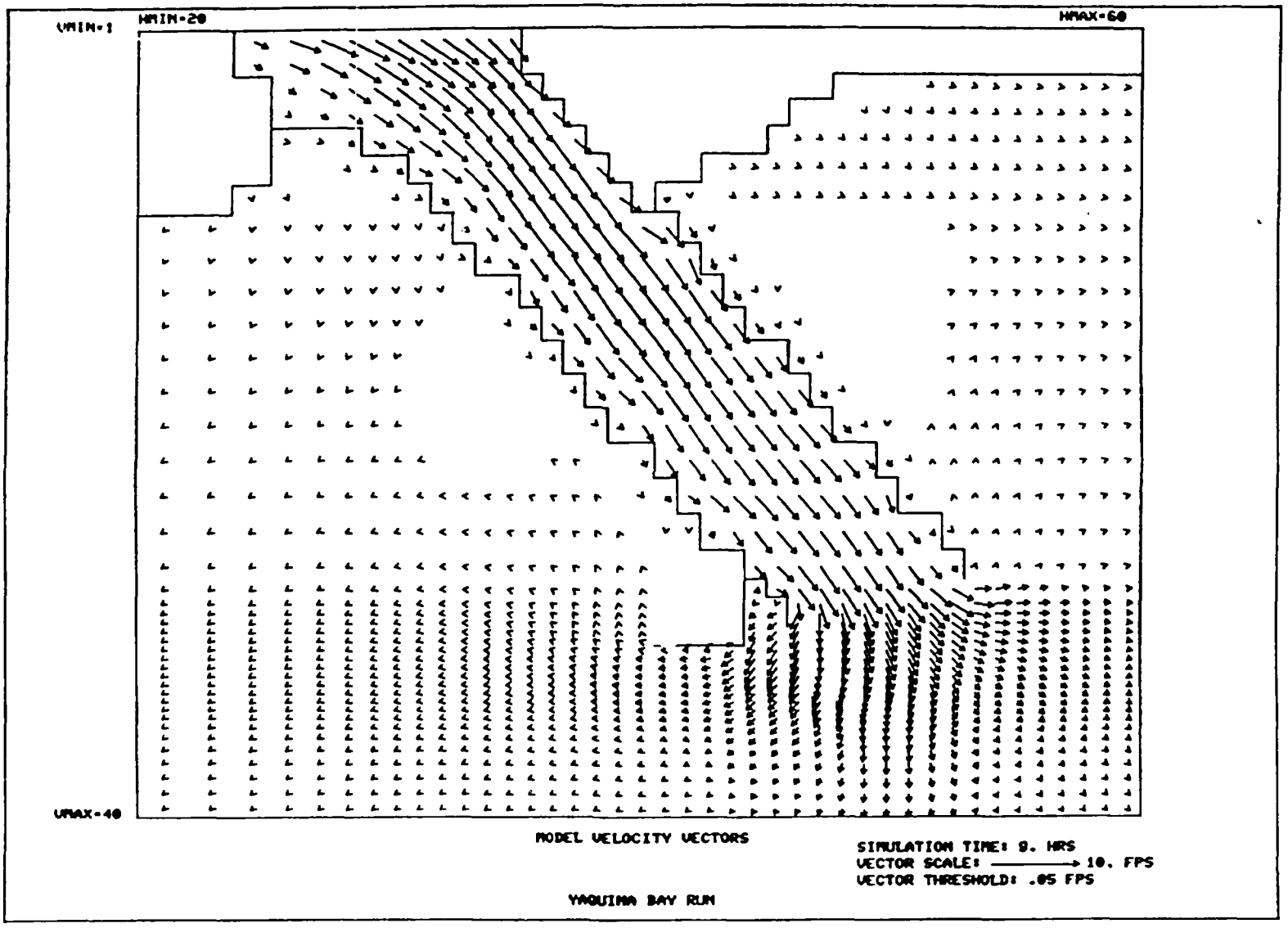

Plate 15. Tidal current pattern: alternative e; peak ebb

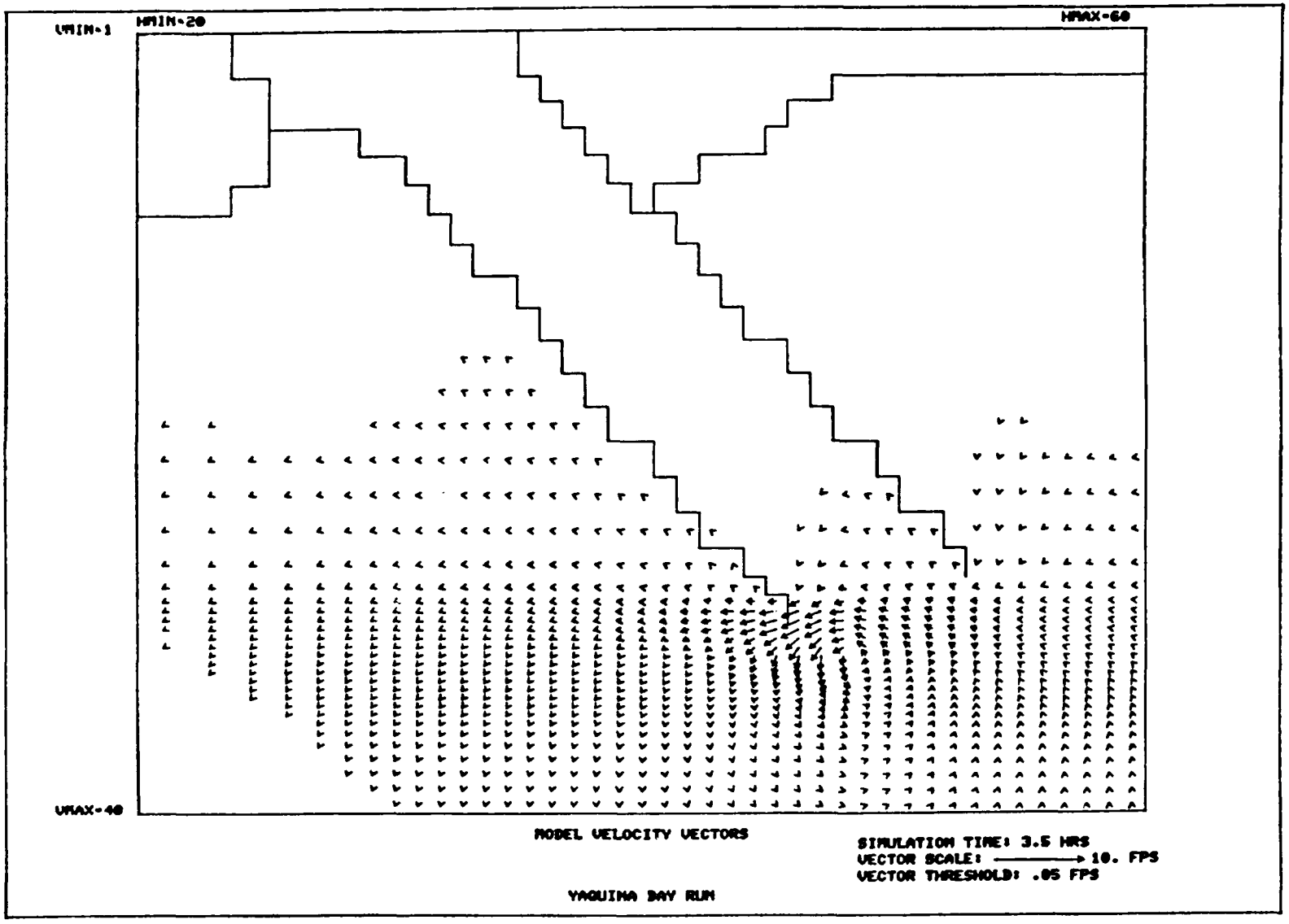

Plate 16. Difference between existing conditions and alternative a; peak flood

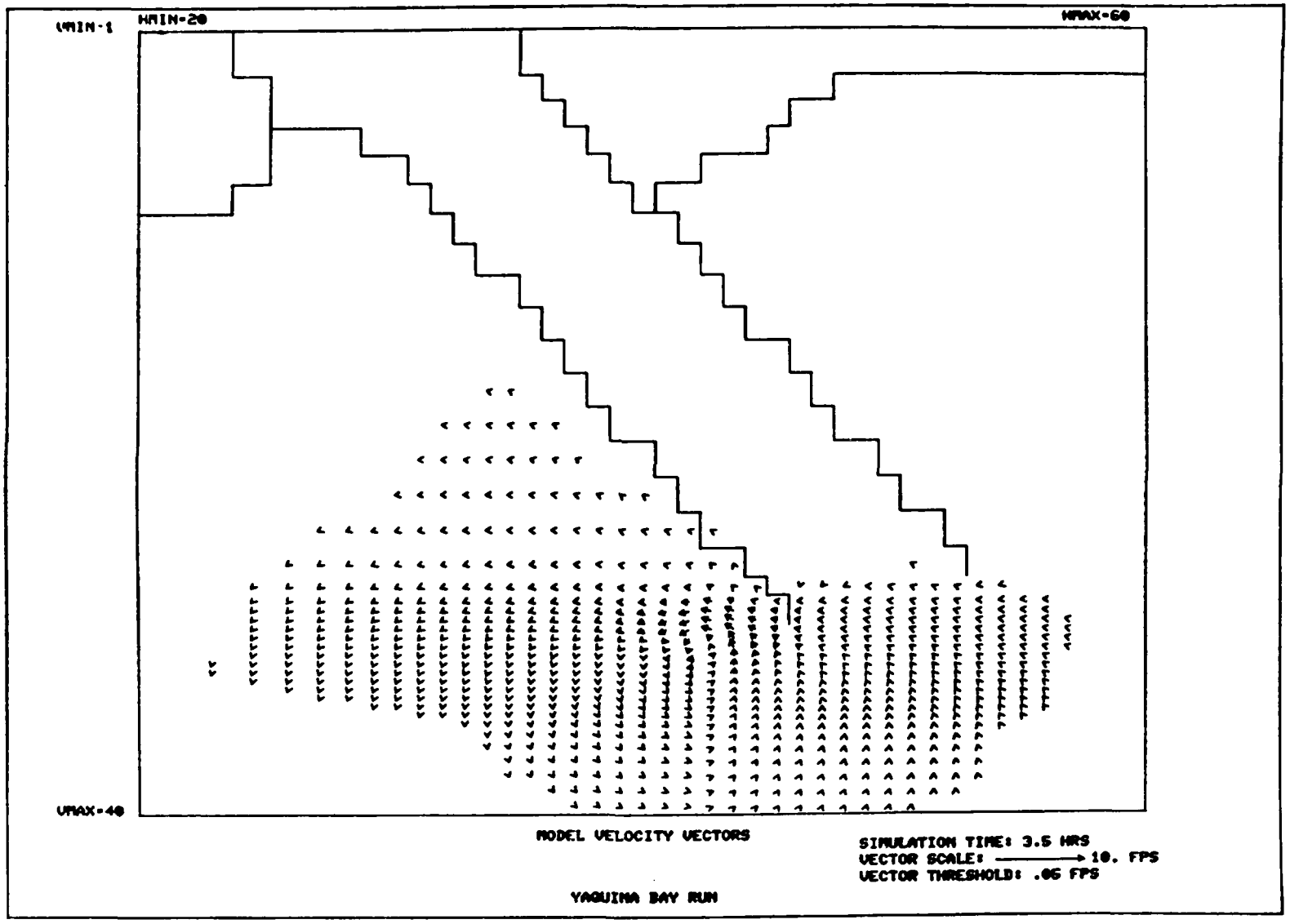

Plate 17. Difference between existing conditions and alternative a; peak ebb

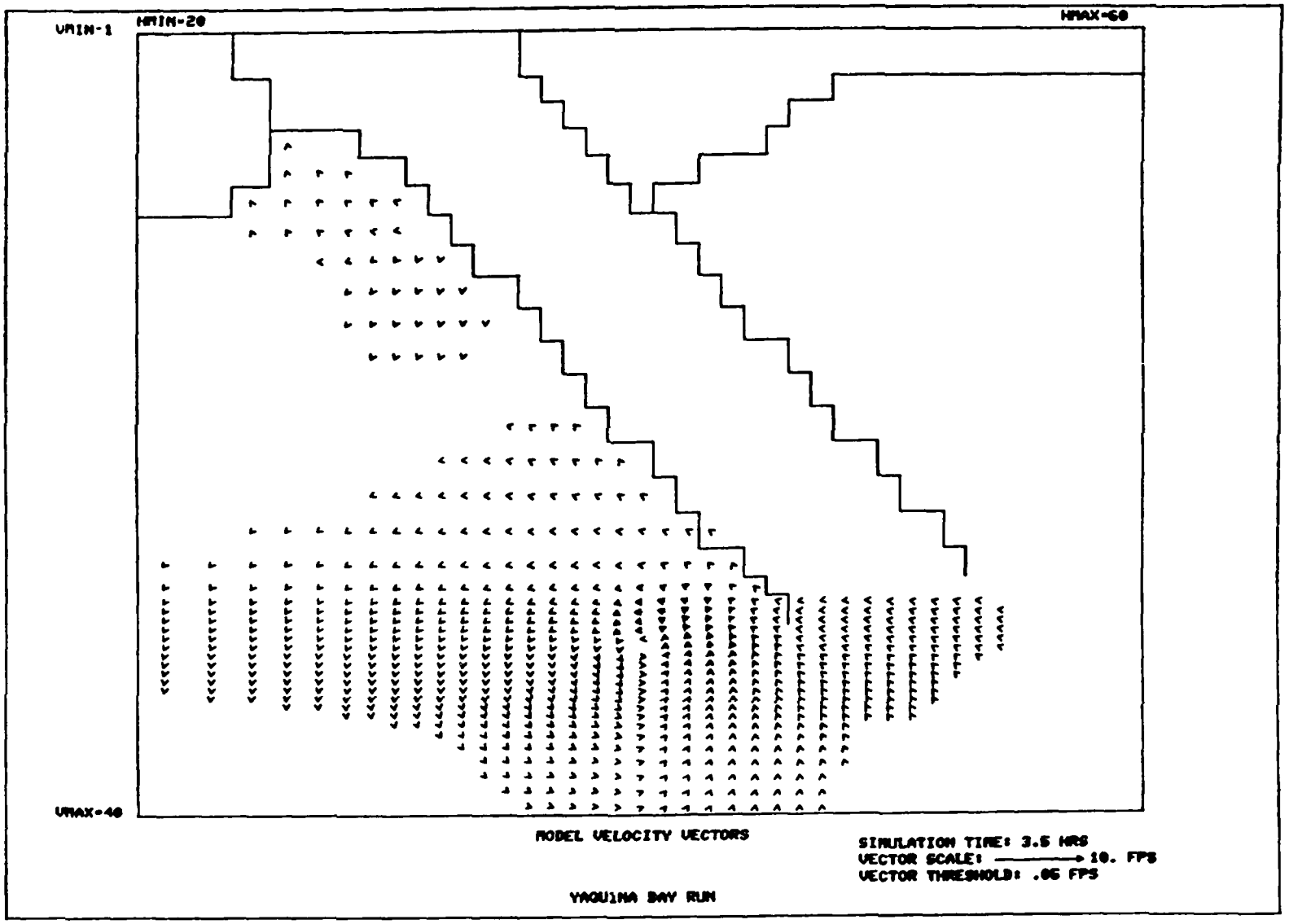

Plate 18. Difference between existing conditions and alternative b; peak flood

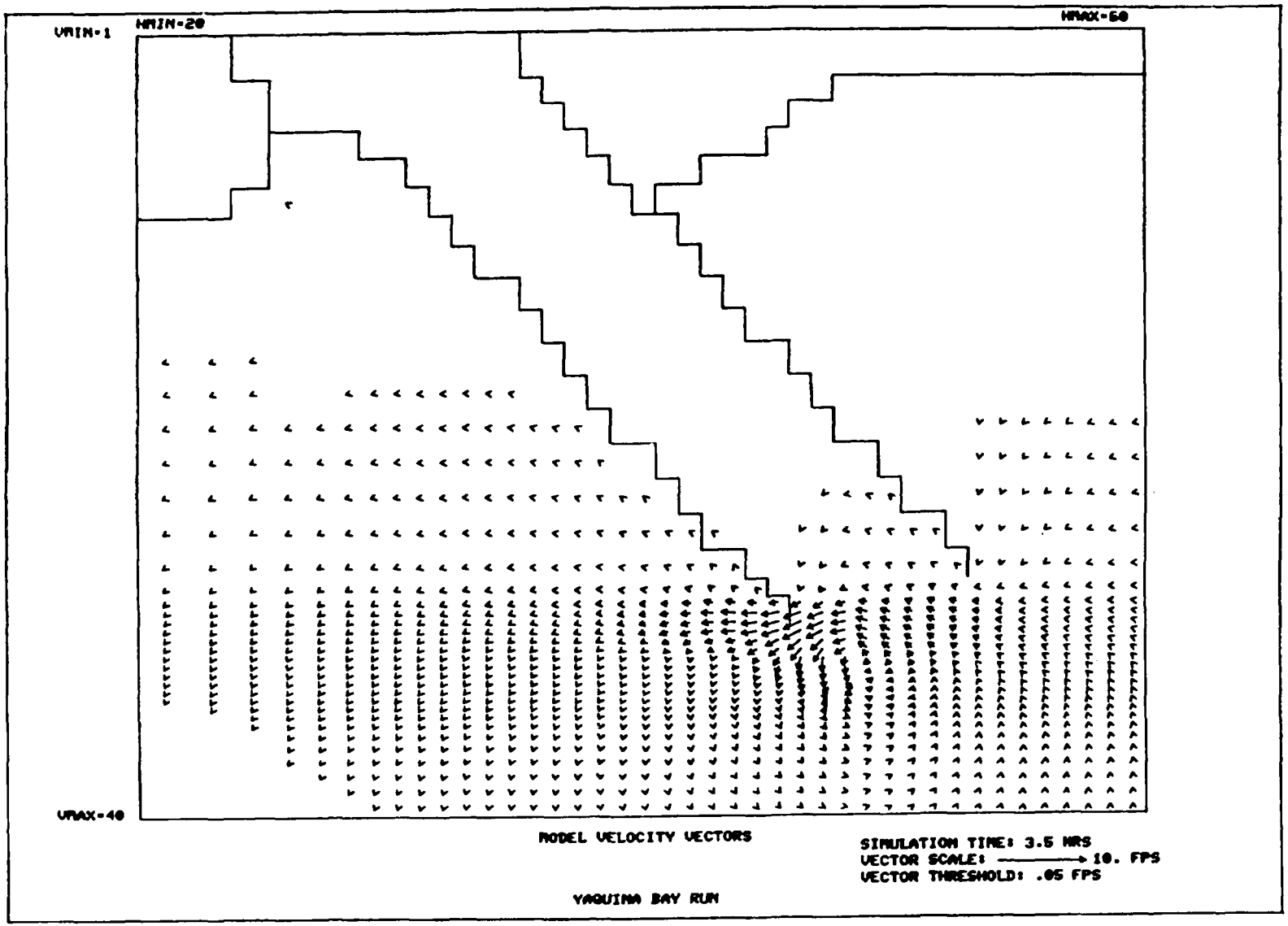

Plate 19. Difference between existing conditions and alternative b; peak ebb

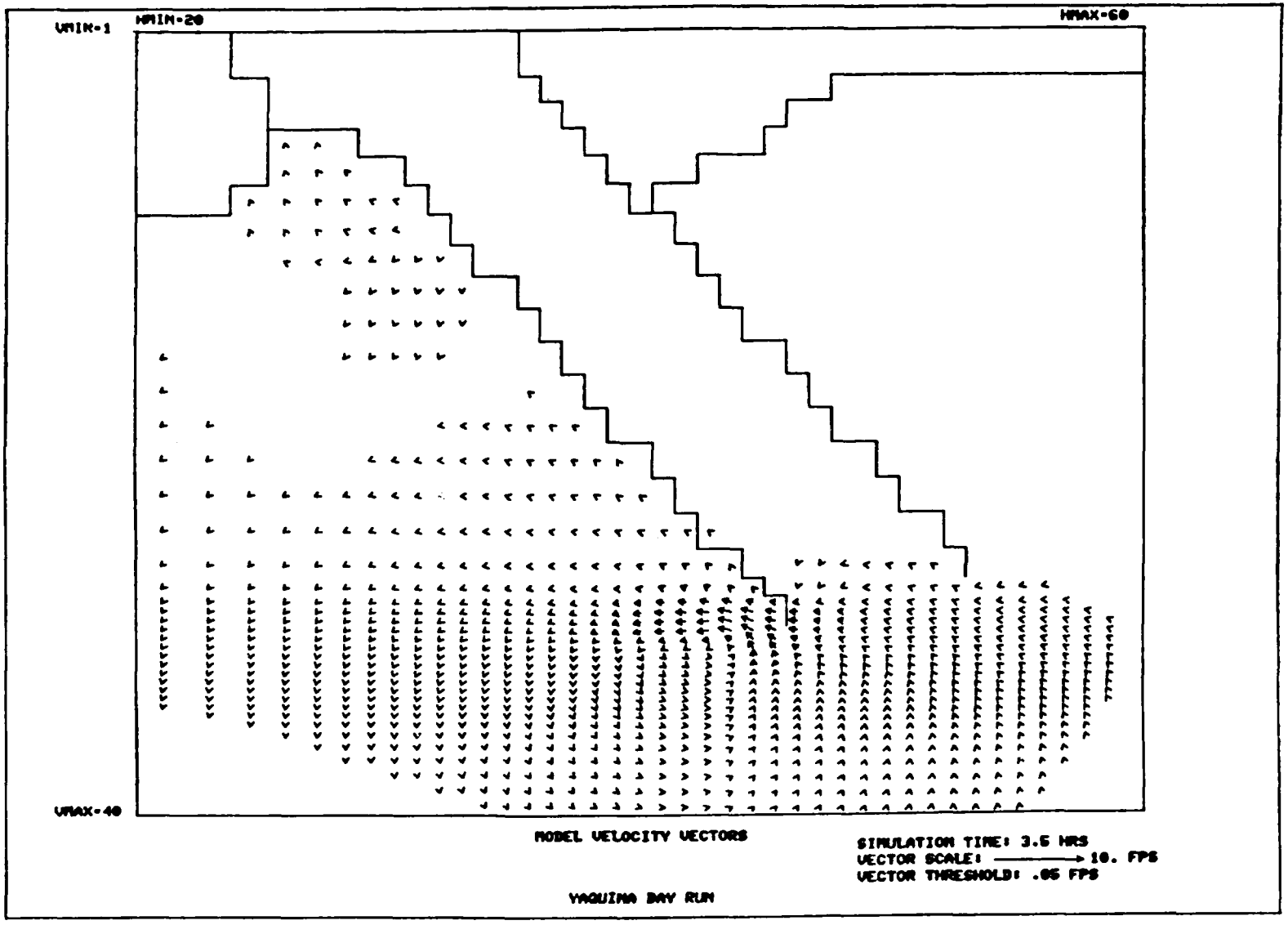

Plate 20. Difference between existing conditions and alternative c; peak flood

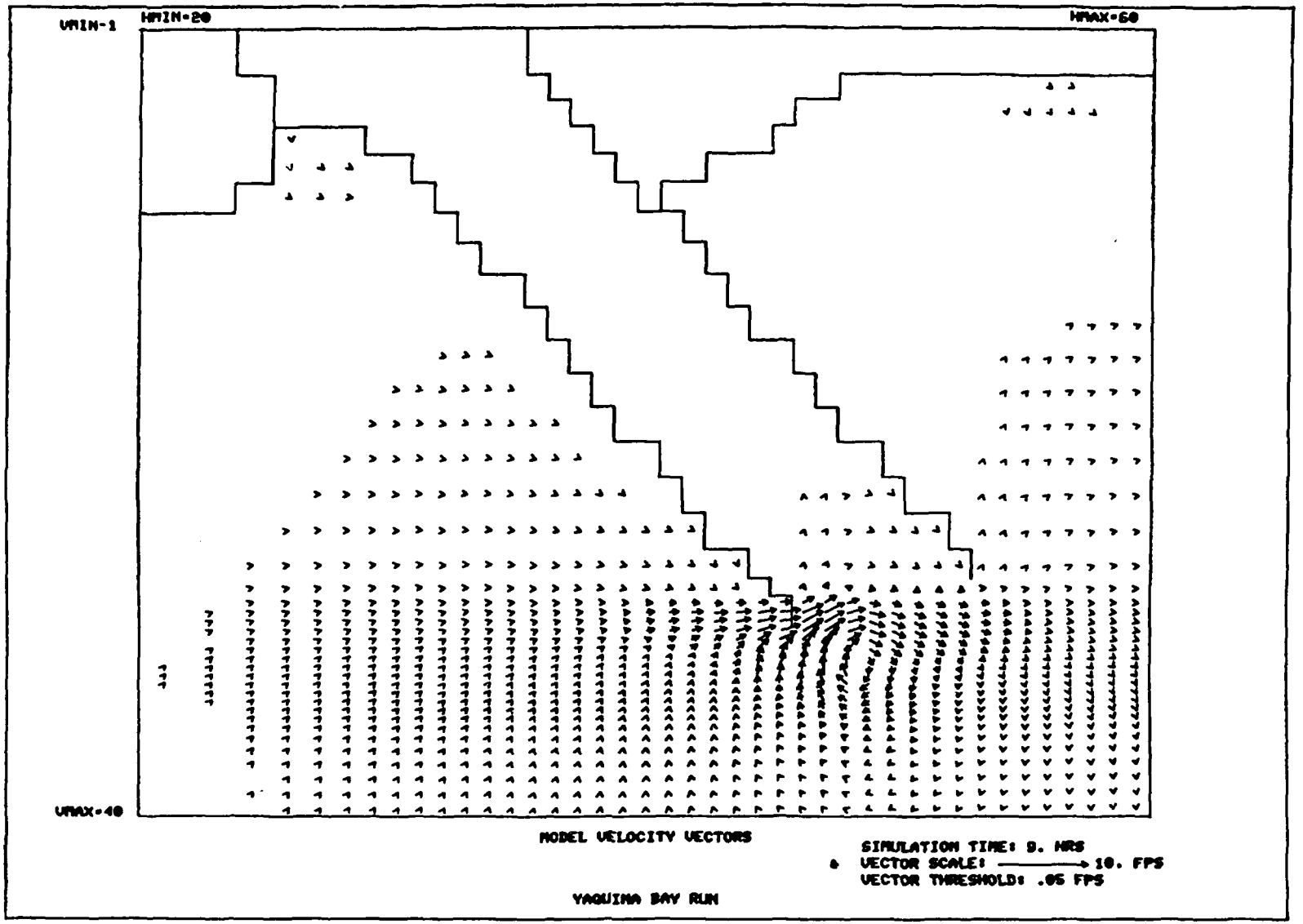

Plate 21. Difference between existing conditions and alternative c; peak ebb

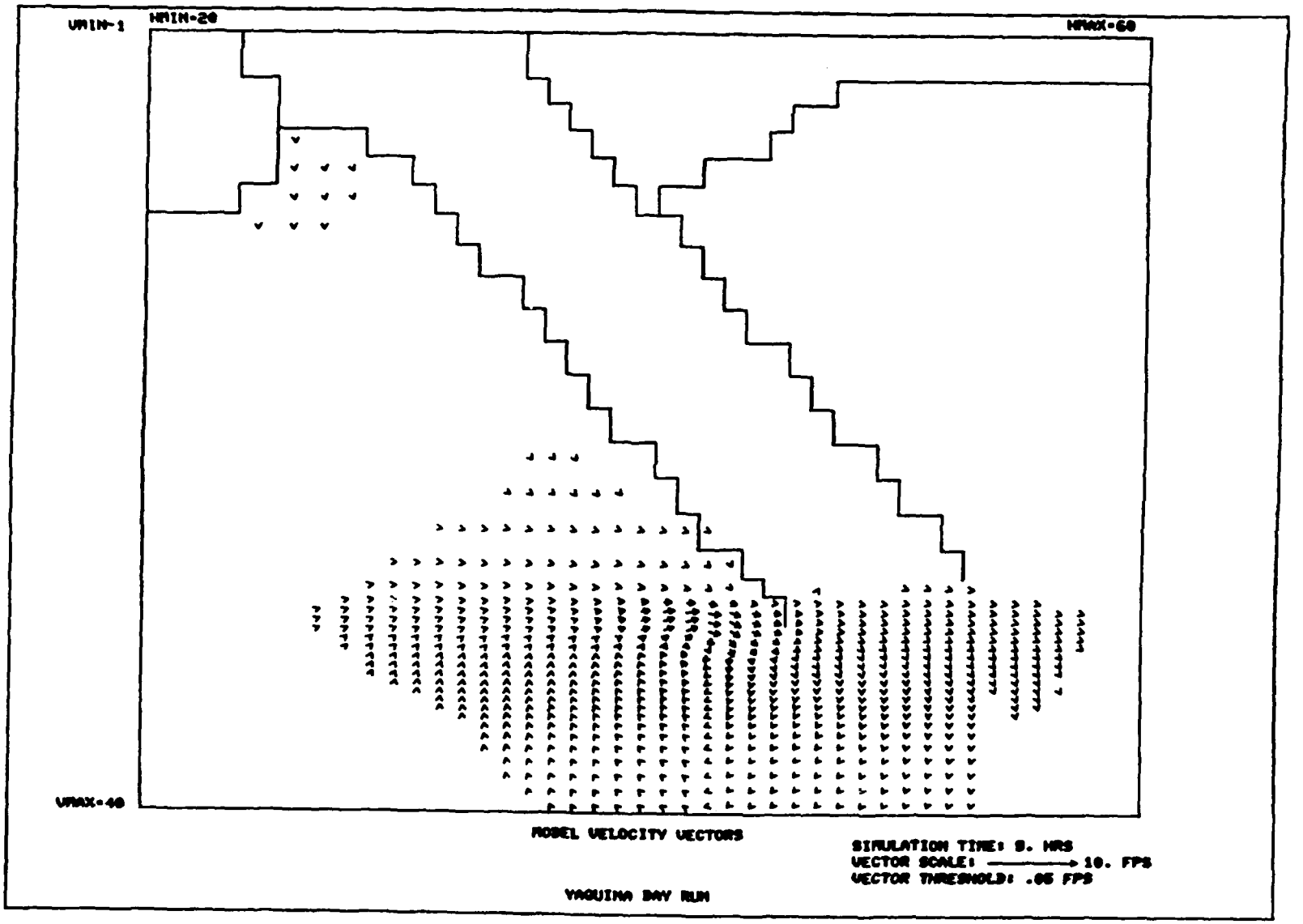

Plate 22. Difference between existing conditions and alternative d; peak flood

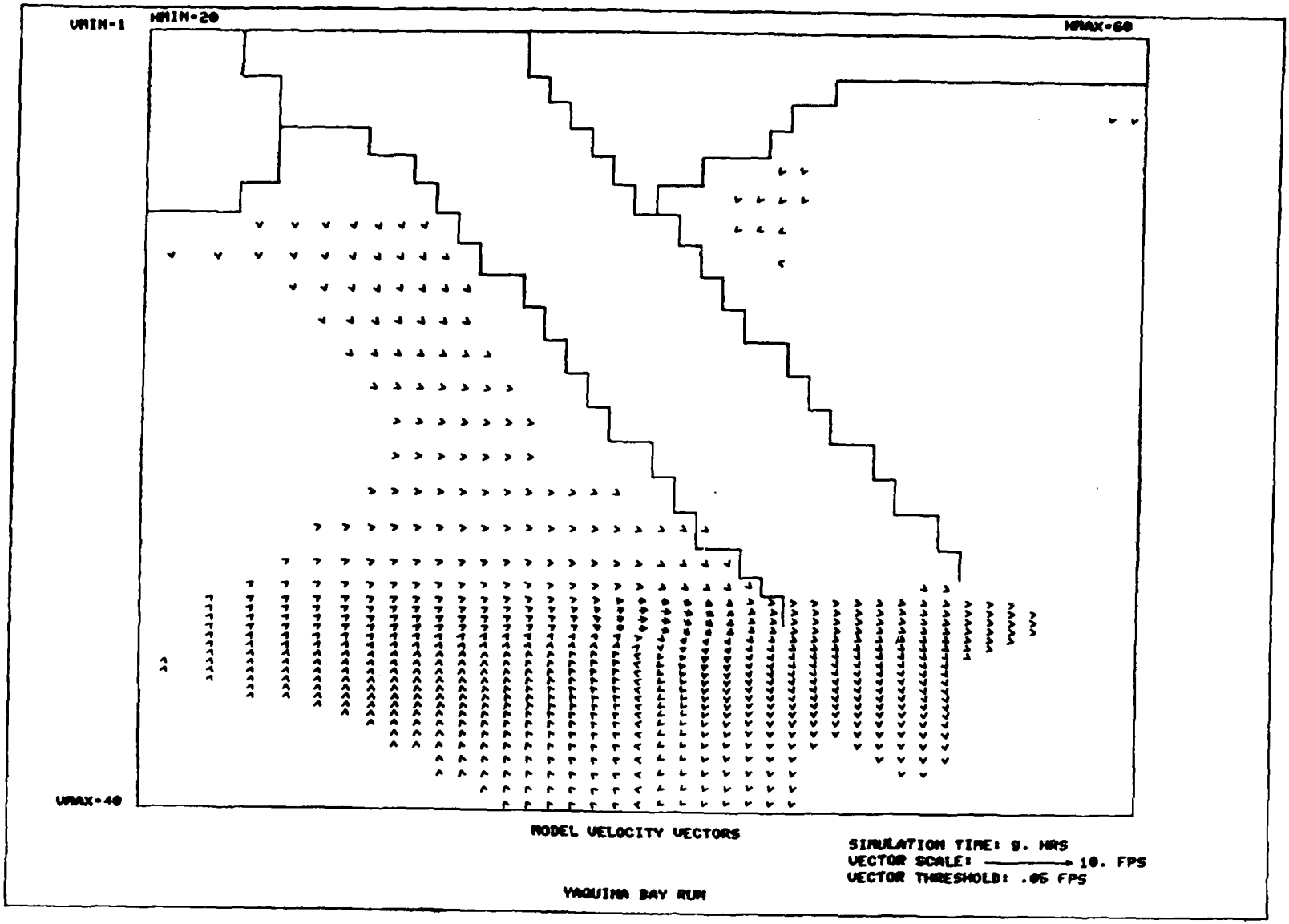

Plate 23. Difference between existing conditions and alternative d; peak ebb

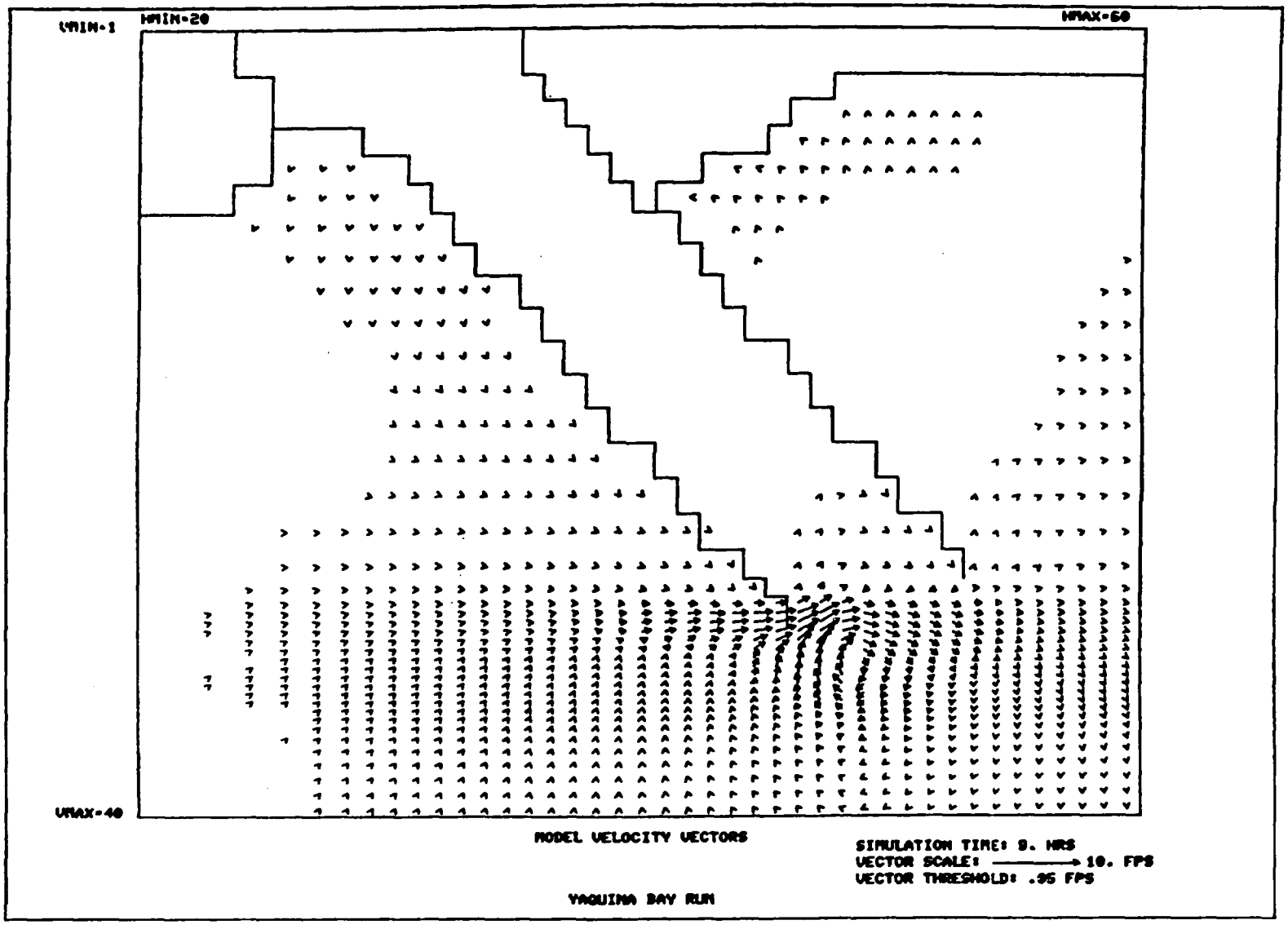

Plate 24. Difference between existing conditions and alternative e; peak flood

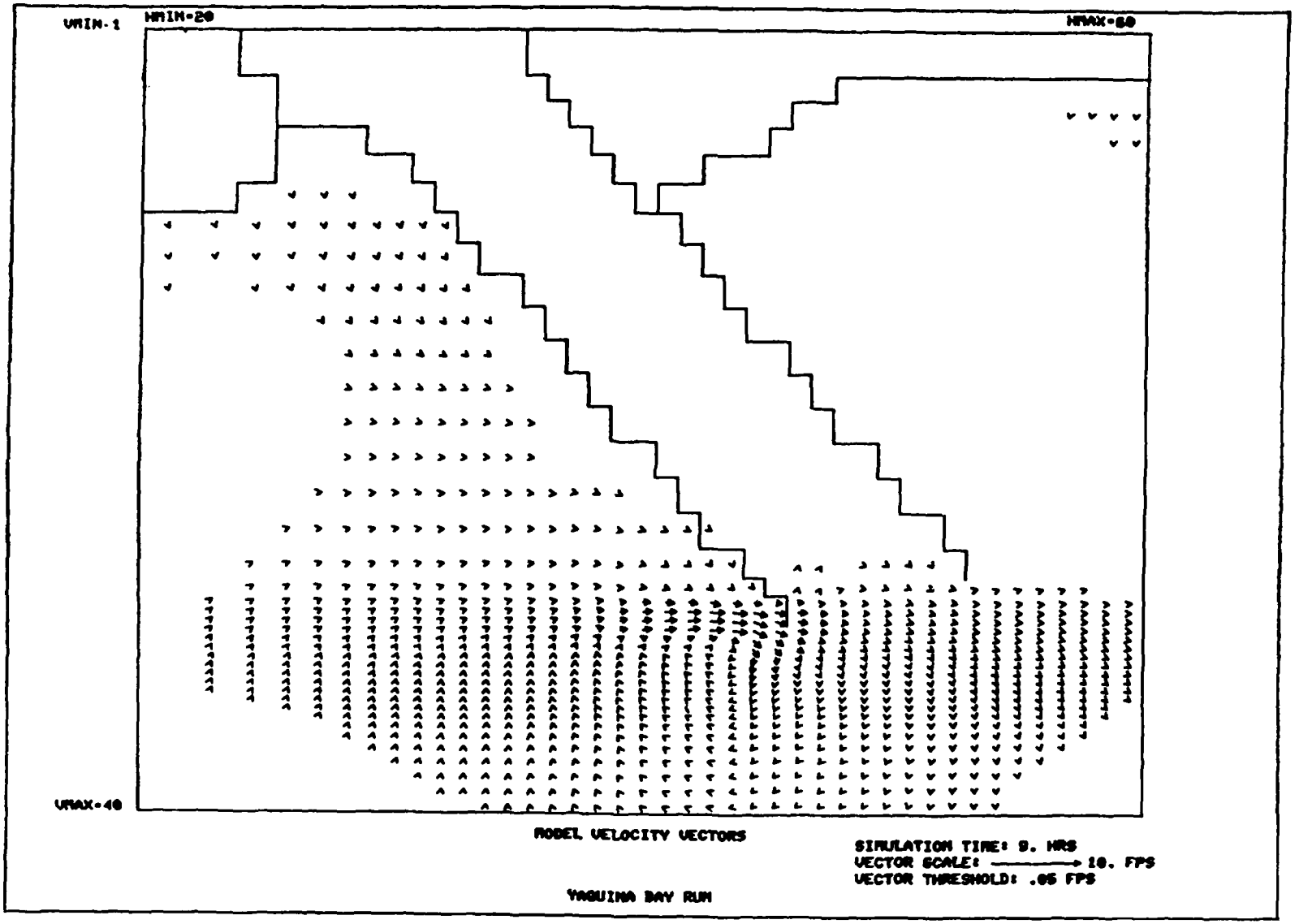

Plate 25. Difference between existing conditions and alternative e; peak ebb

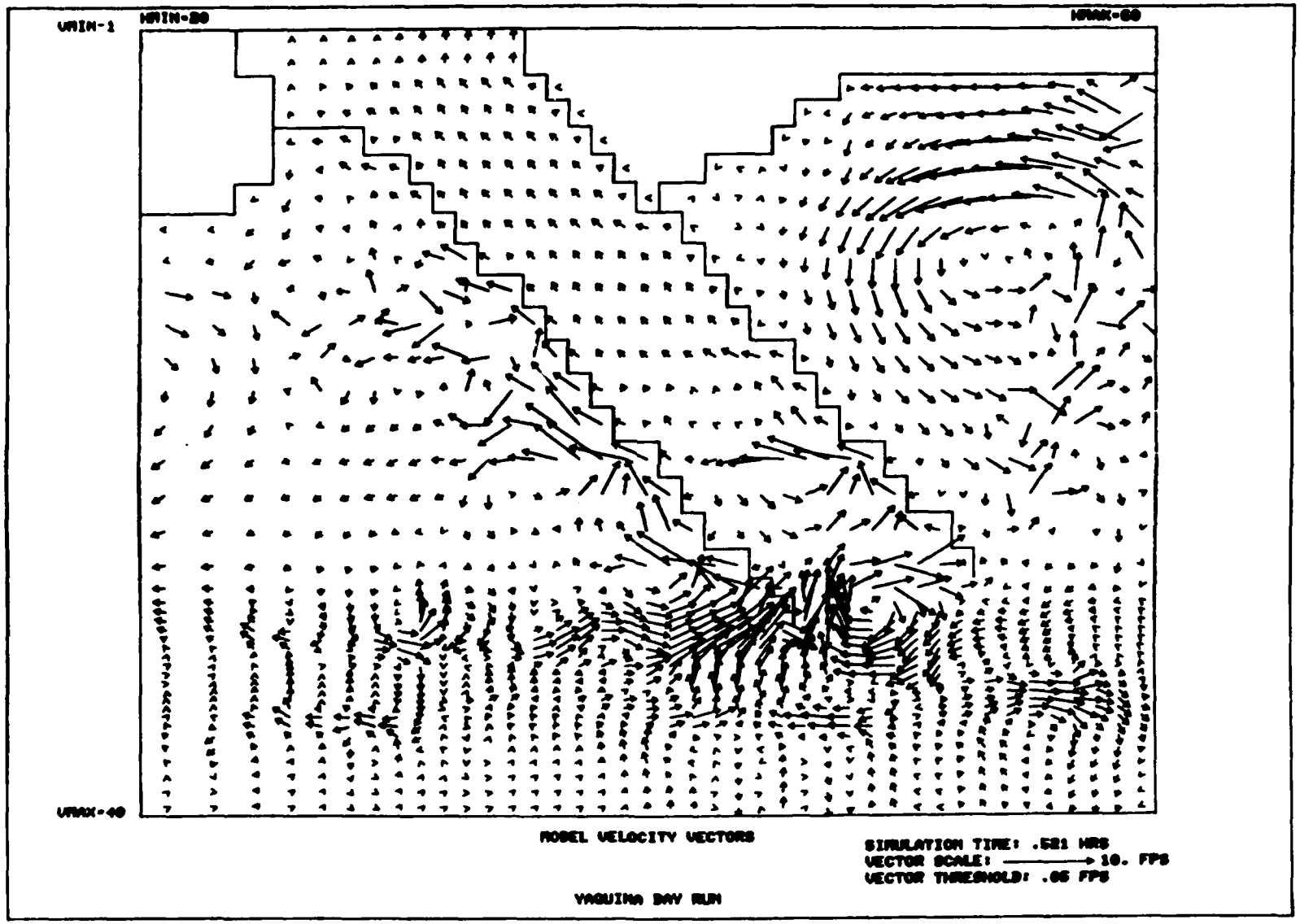

Plate 26. Wave-induced current pattern: H_o = 14 ft, T = 11 sec, θ_o = WNW

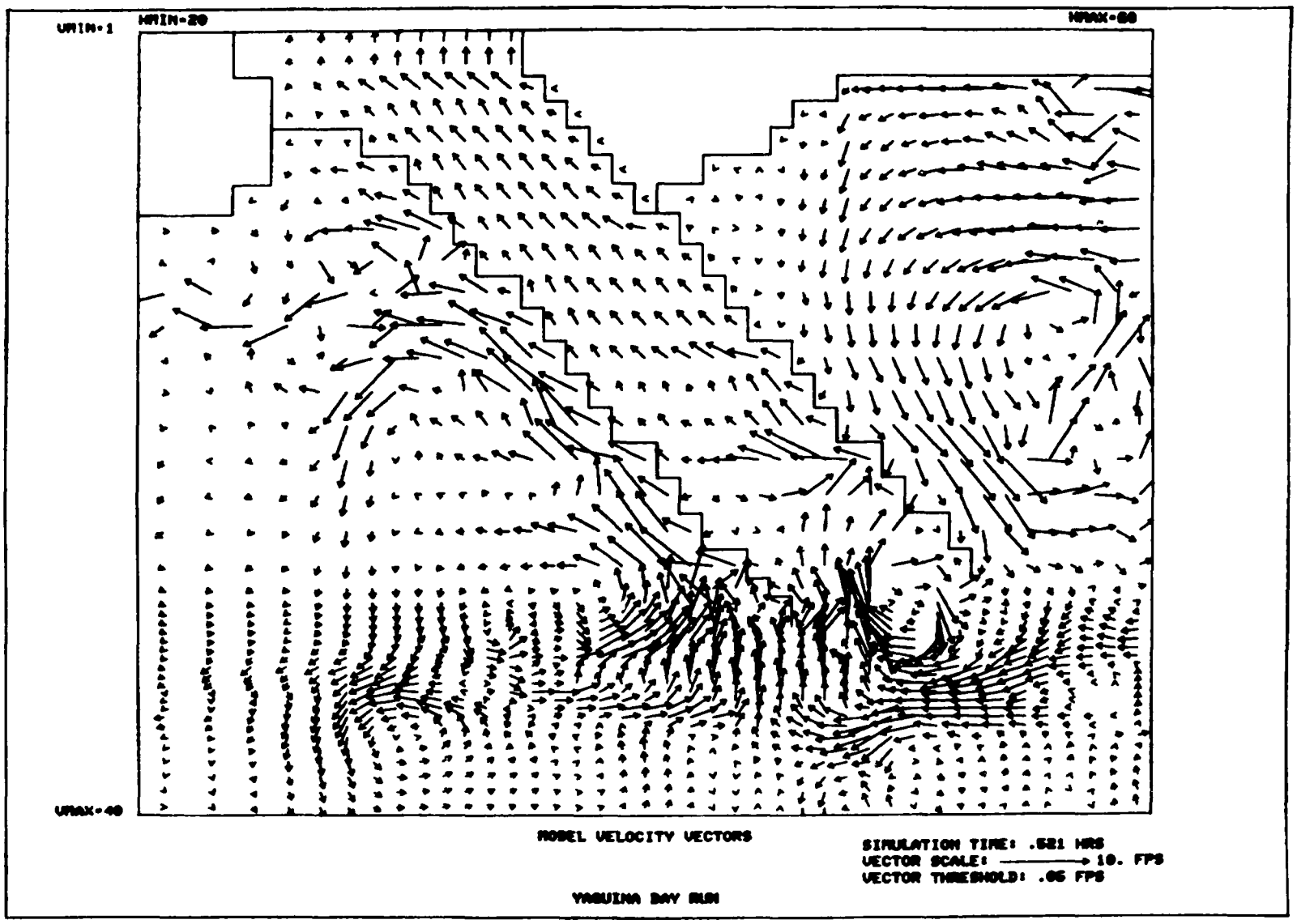

Plate 27. Wave-induced current pattern: H_o = 14 ft, T = 14 sec, θ_o = W

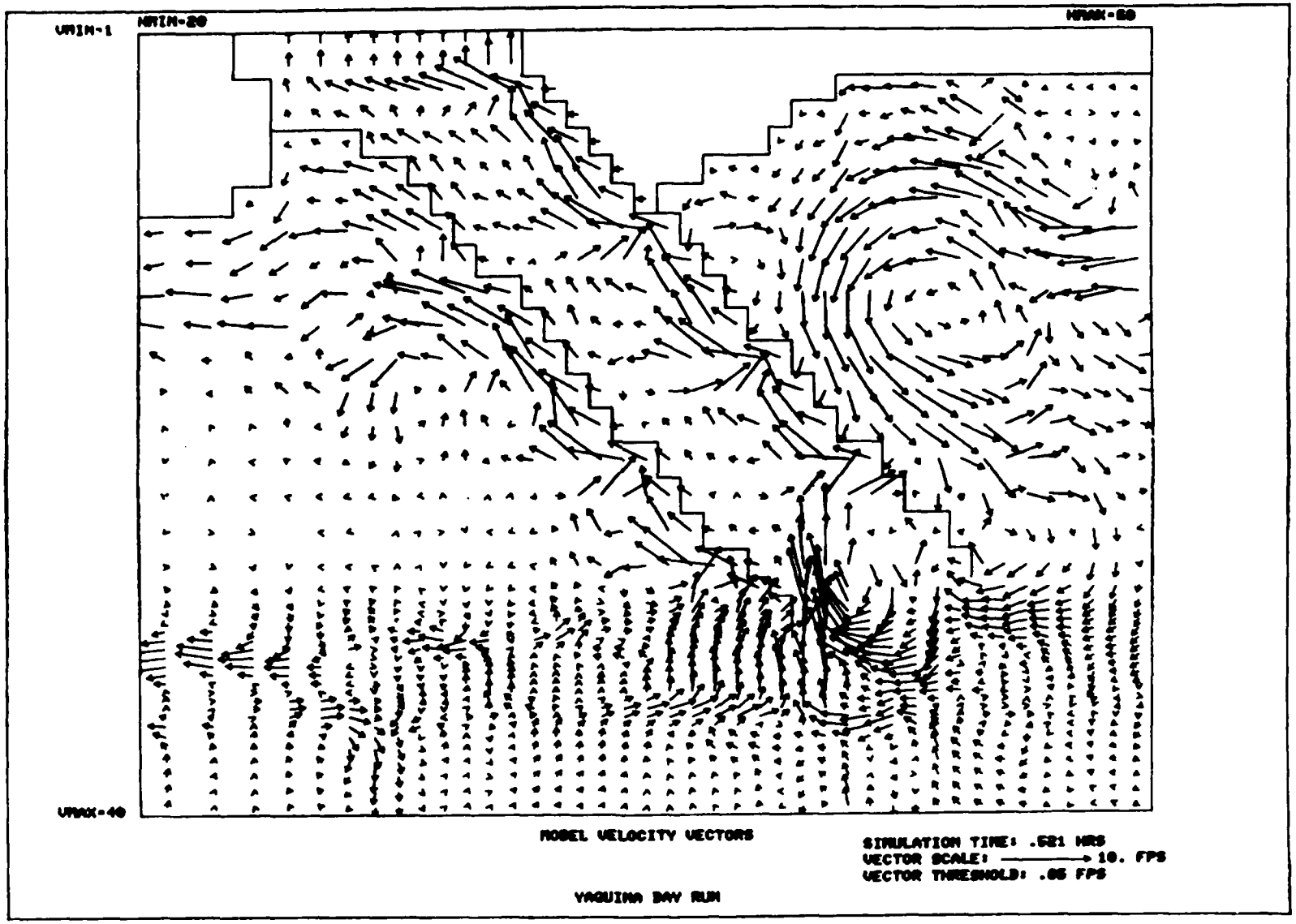

Plate 28. Wave-induced current pattern: H_o = 14 ft, T = 11 sec, θ_o = WSW

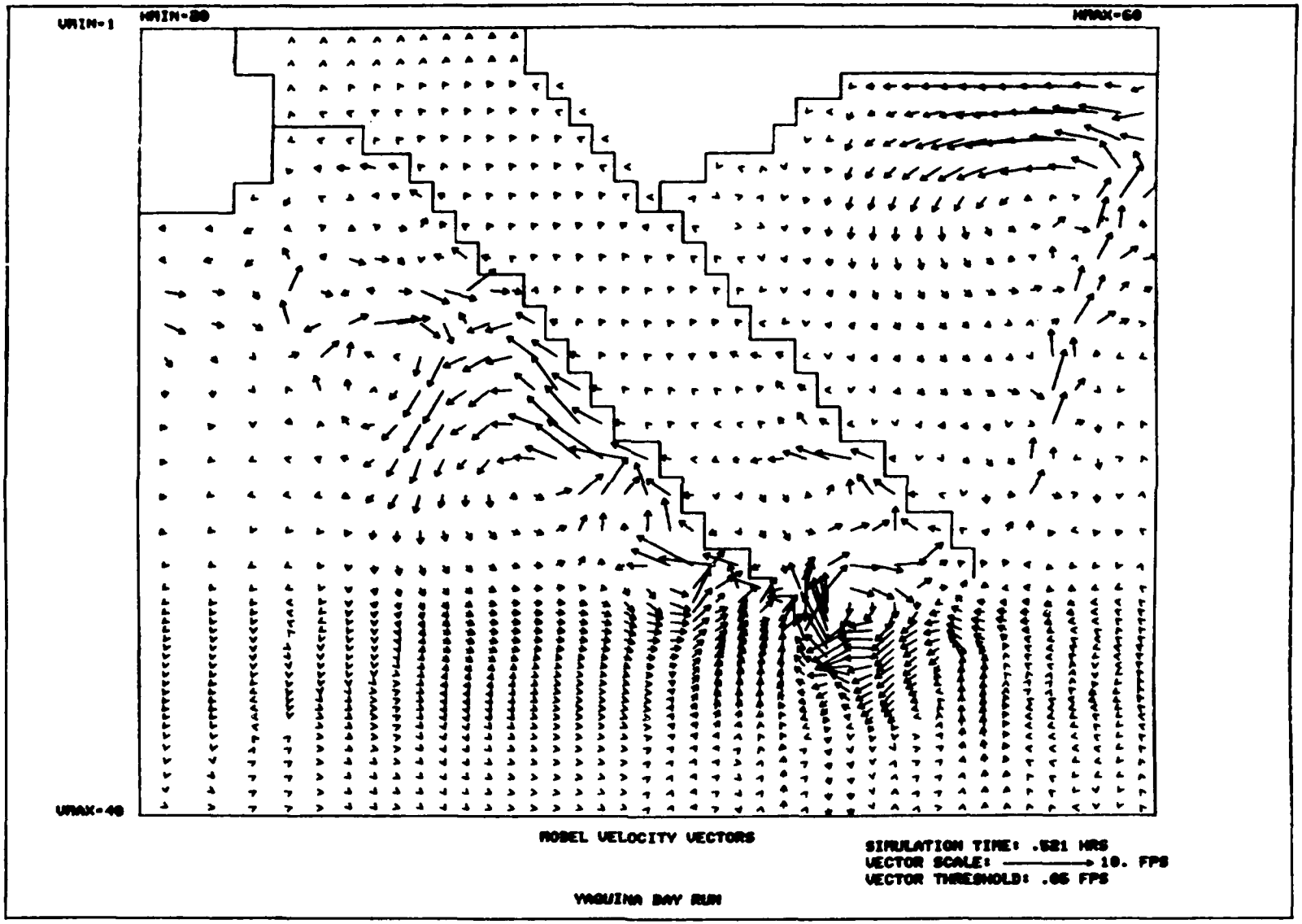

Plate 29. Wave-induced current pattern: H_o = 10 ft, T = 11 sec, θ_o = WNW

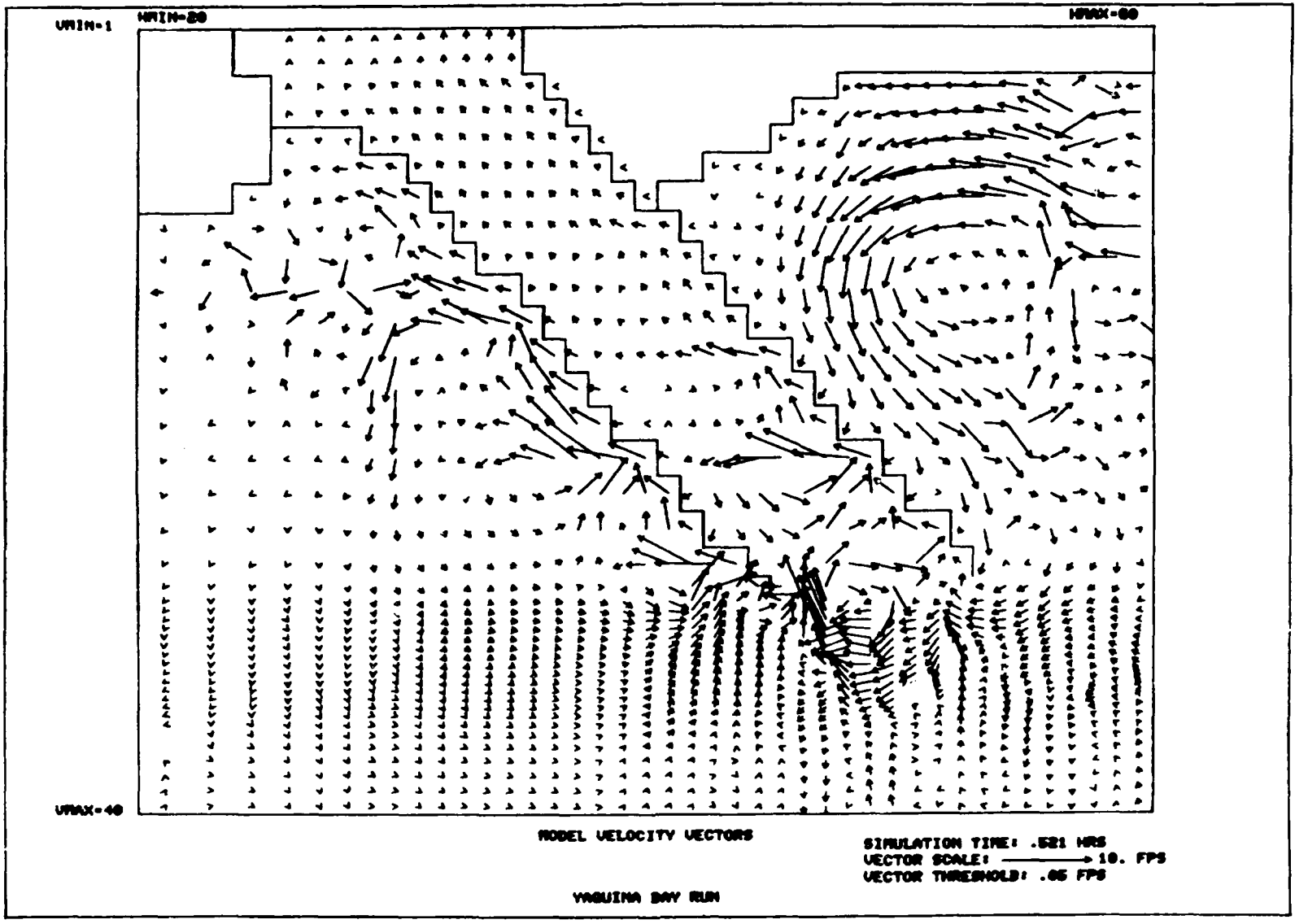

Plate 30. Wave-induced current pattern: H_o = 10 ft, T = 14 sec, θ_o = W

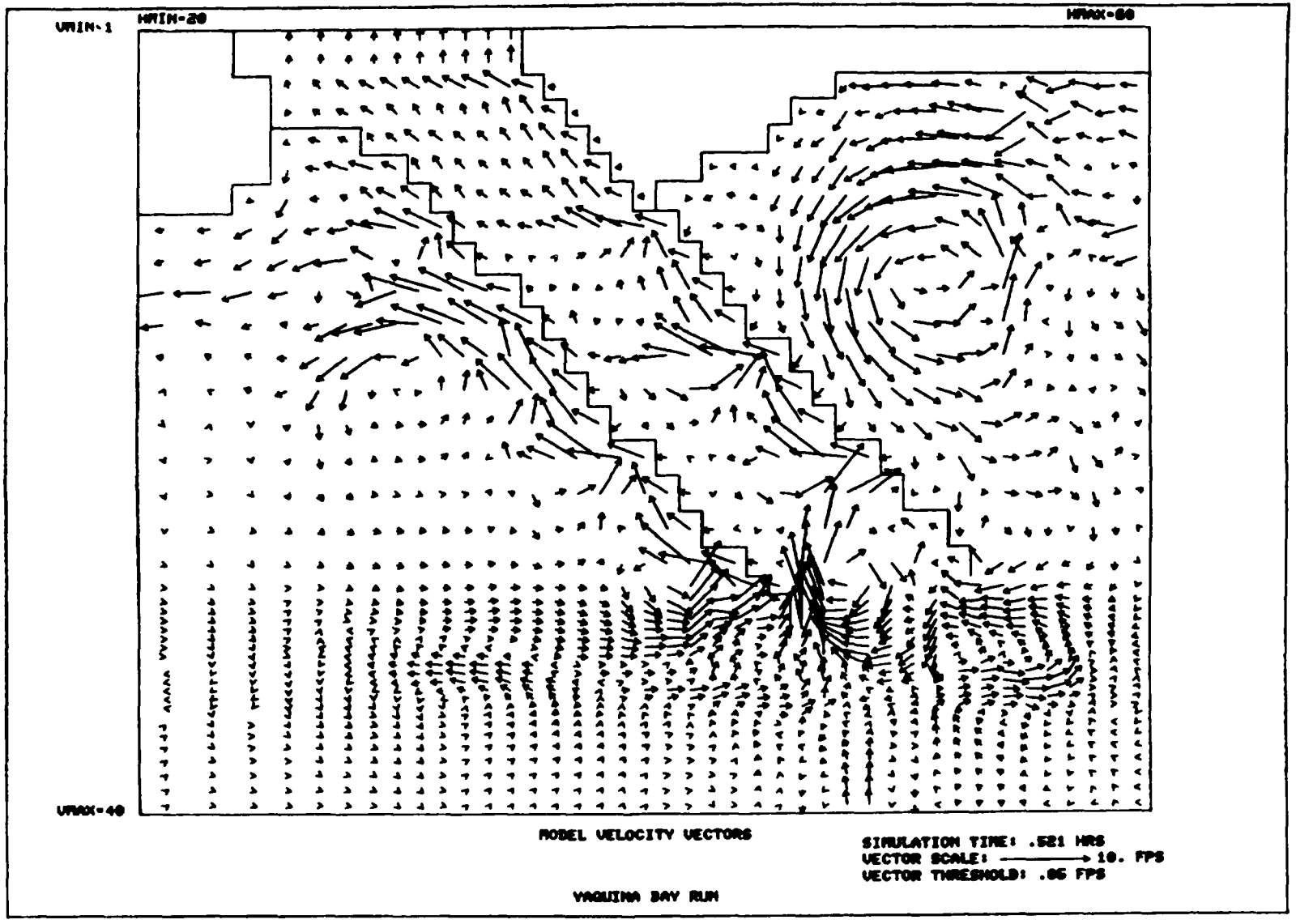

Plate 31. Wave-induced current pattern: H_o = 10 ft, T = 14 sec, θ_o = WSW

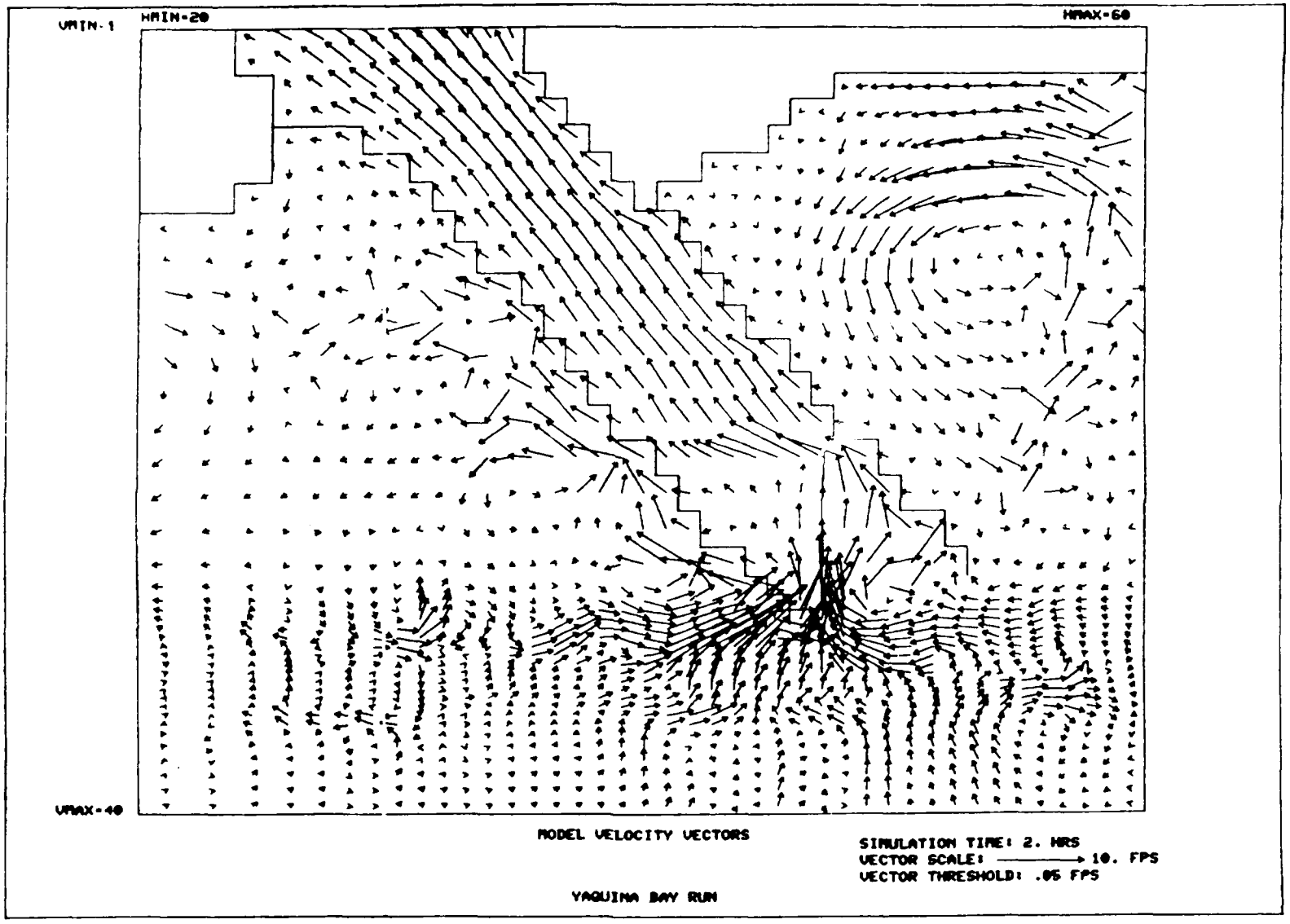

Plate 32A. Superposition of tidal and wave-induced currents at peak flood, H_o = 14 ft, T = 11 sec, θ_o = WNW

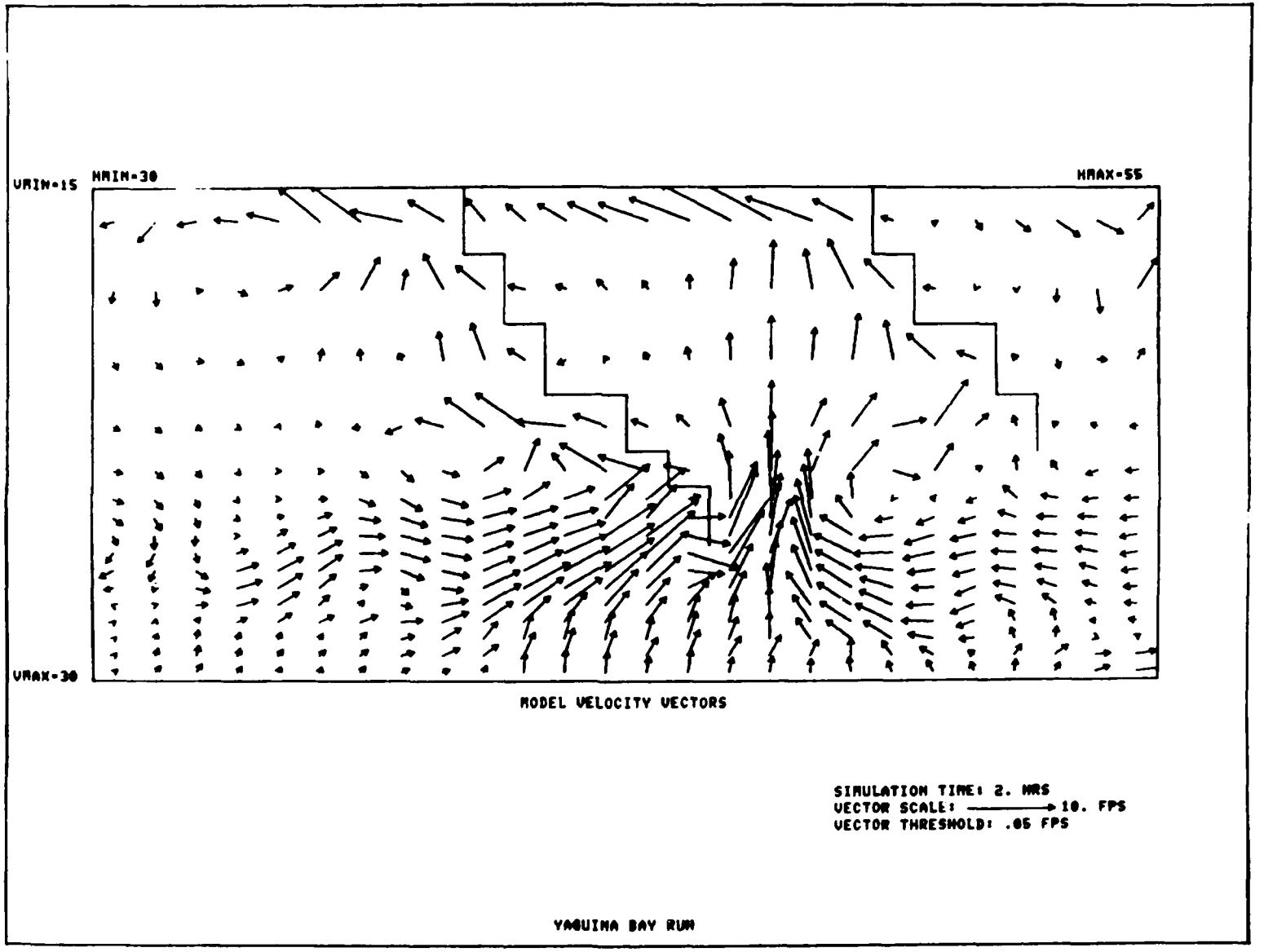

Plate 32B. Inlet entrance: superposition of tidal and wave-induced currents at peak flood, H_o = 14 ft, T = 11 sec, θ_o = WNW

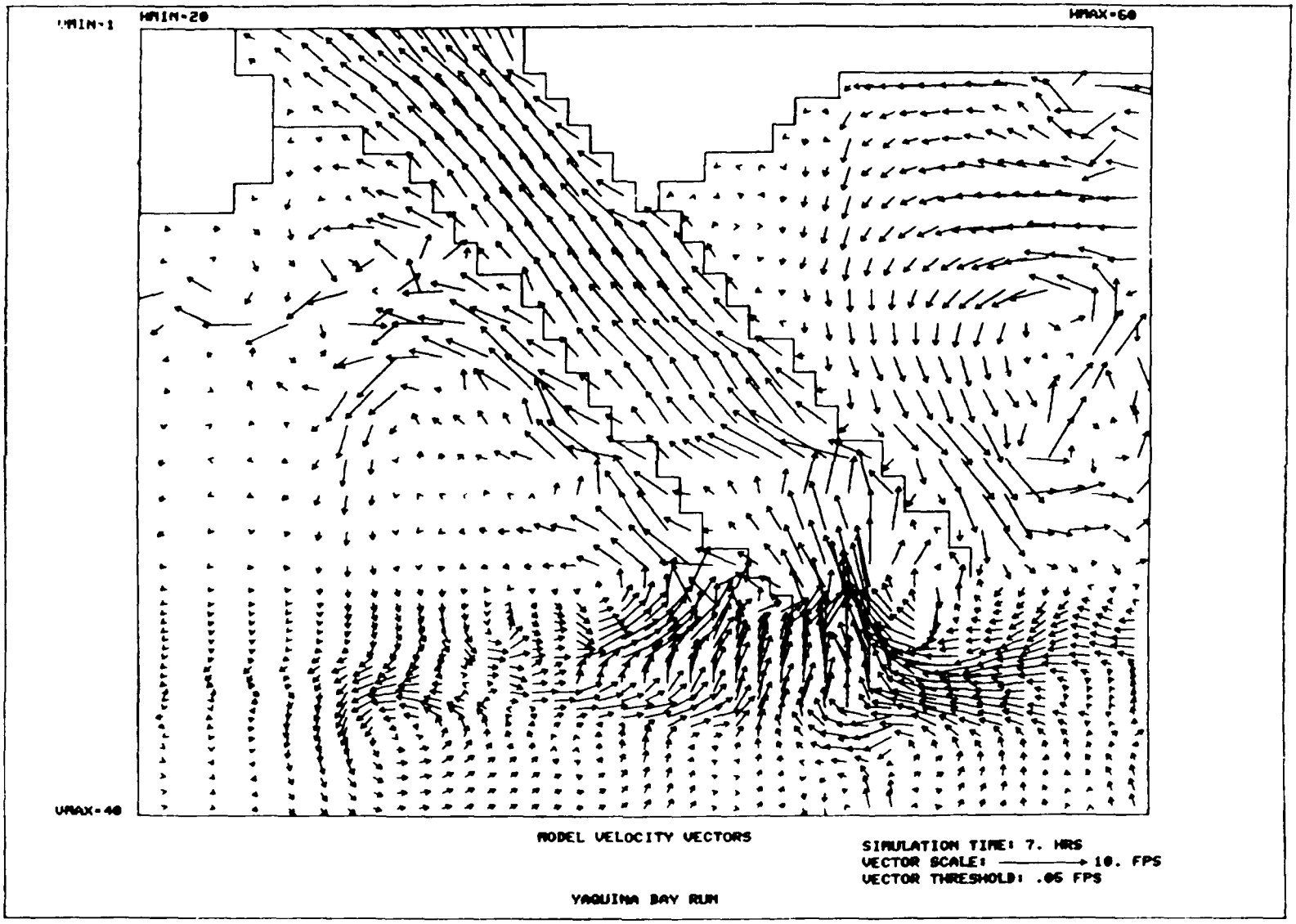

Plate 33A. Superposition of tidal and wave-induced currents at peak flood, H_o = 14 ft, T = 14 sec, θ_o = W

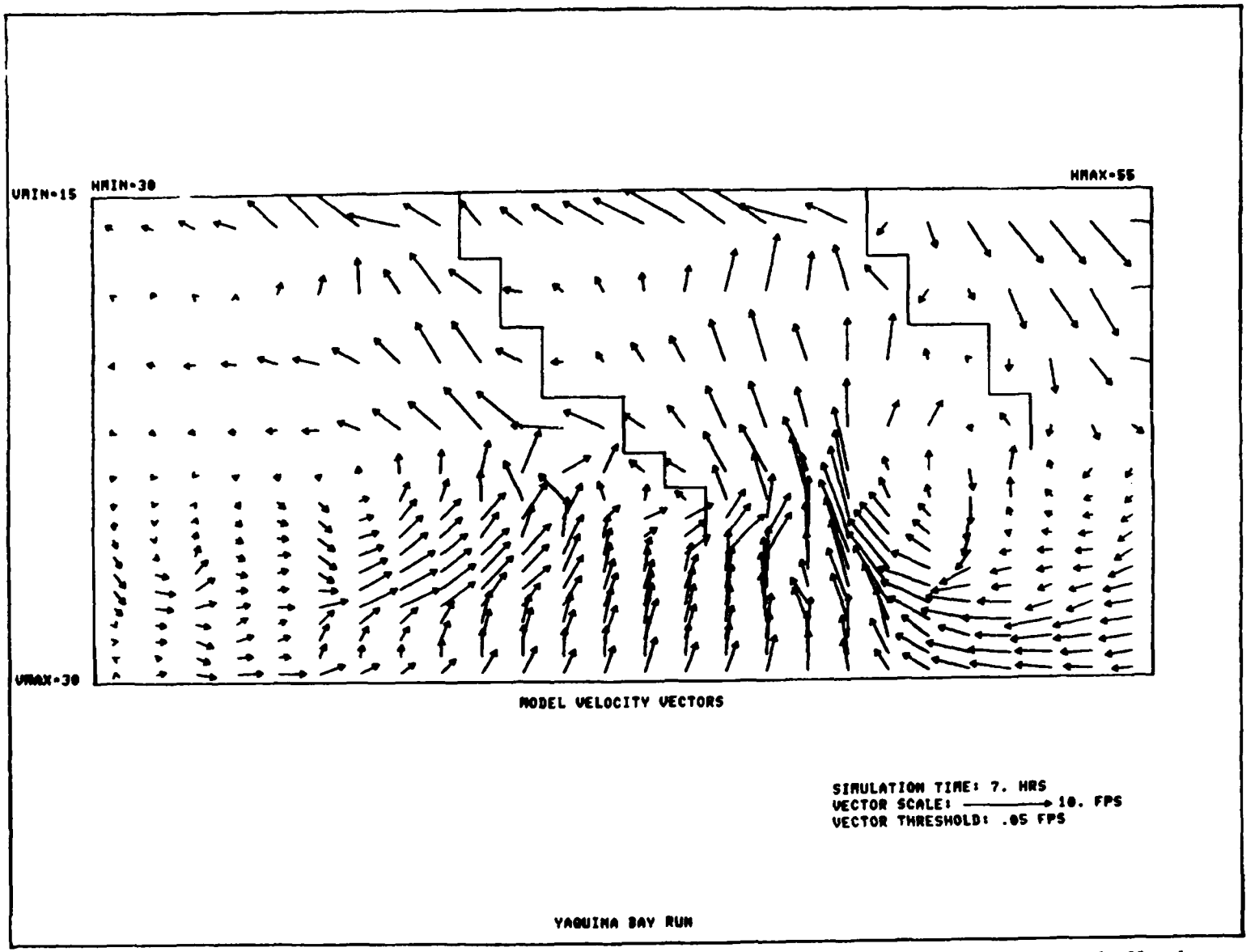

Plate 33B. Inlet entrance: superposition of tidal and wave-induced currents at peak flood, H_o = 14 ft, T = 14 sec, θ_o = W

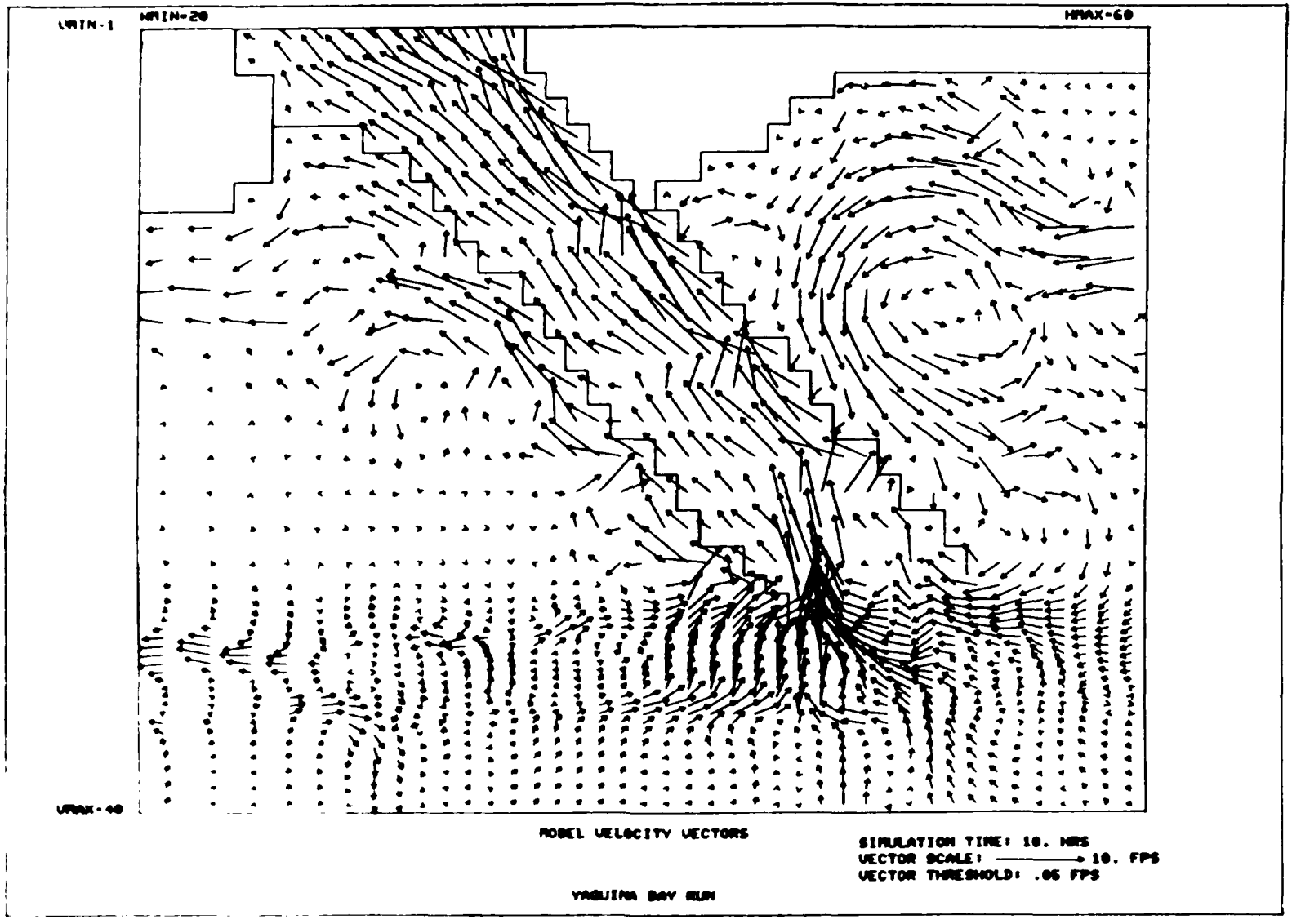

Plate 34A. Superposition of tidal and wave-induced currents at peak flood, H_o = 14 ft, T = 11 sec, θ_o = WSW

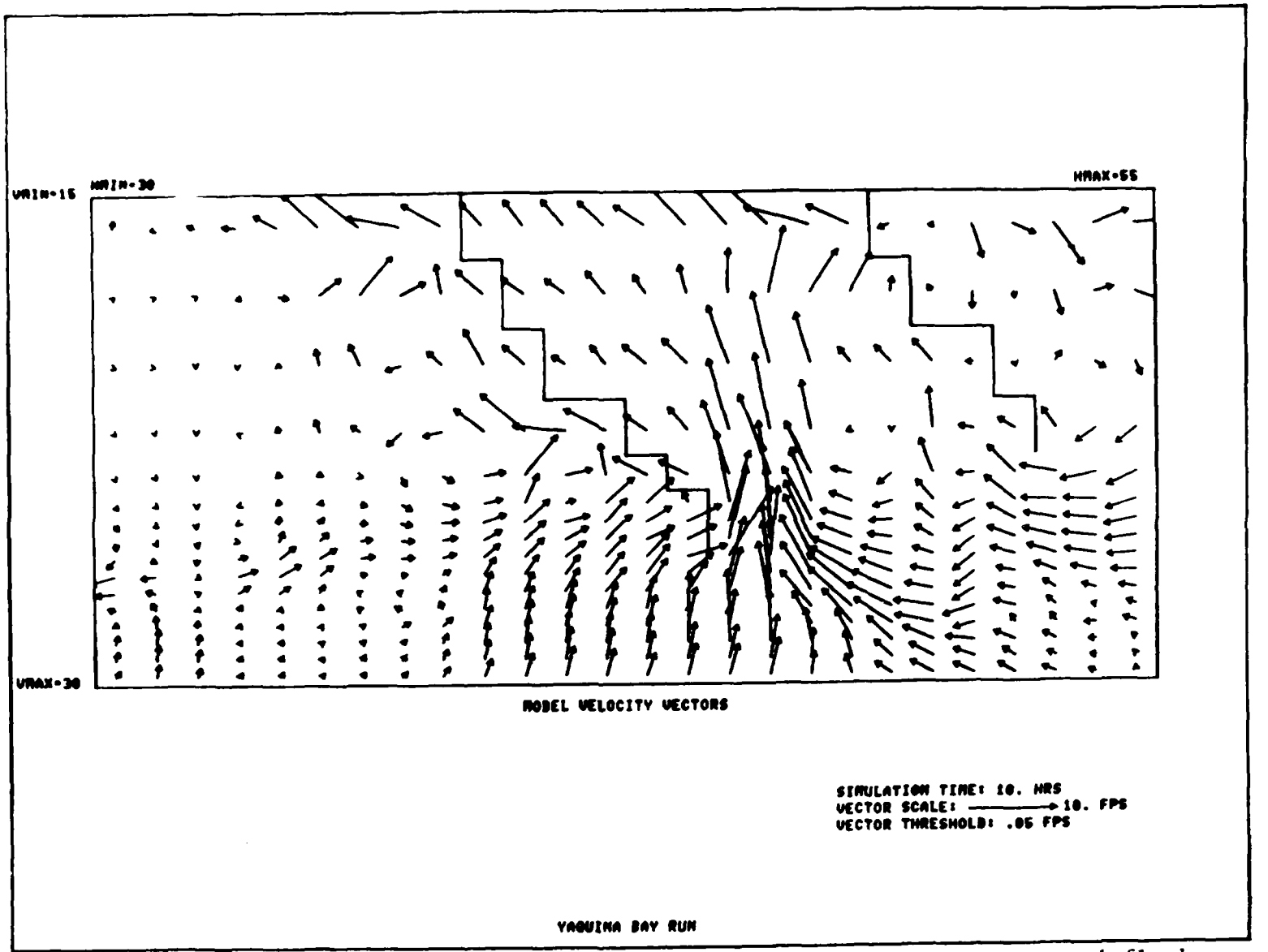

Plate 34B. Inlet entrance: superposition of tidal and wave-induced currents at peak flood, H_o = 14 ft, T = 11 sec, θ_o = WSW

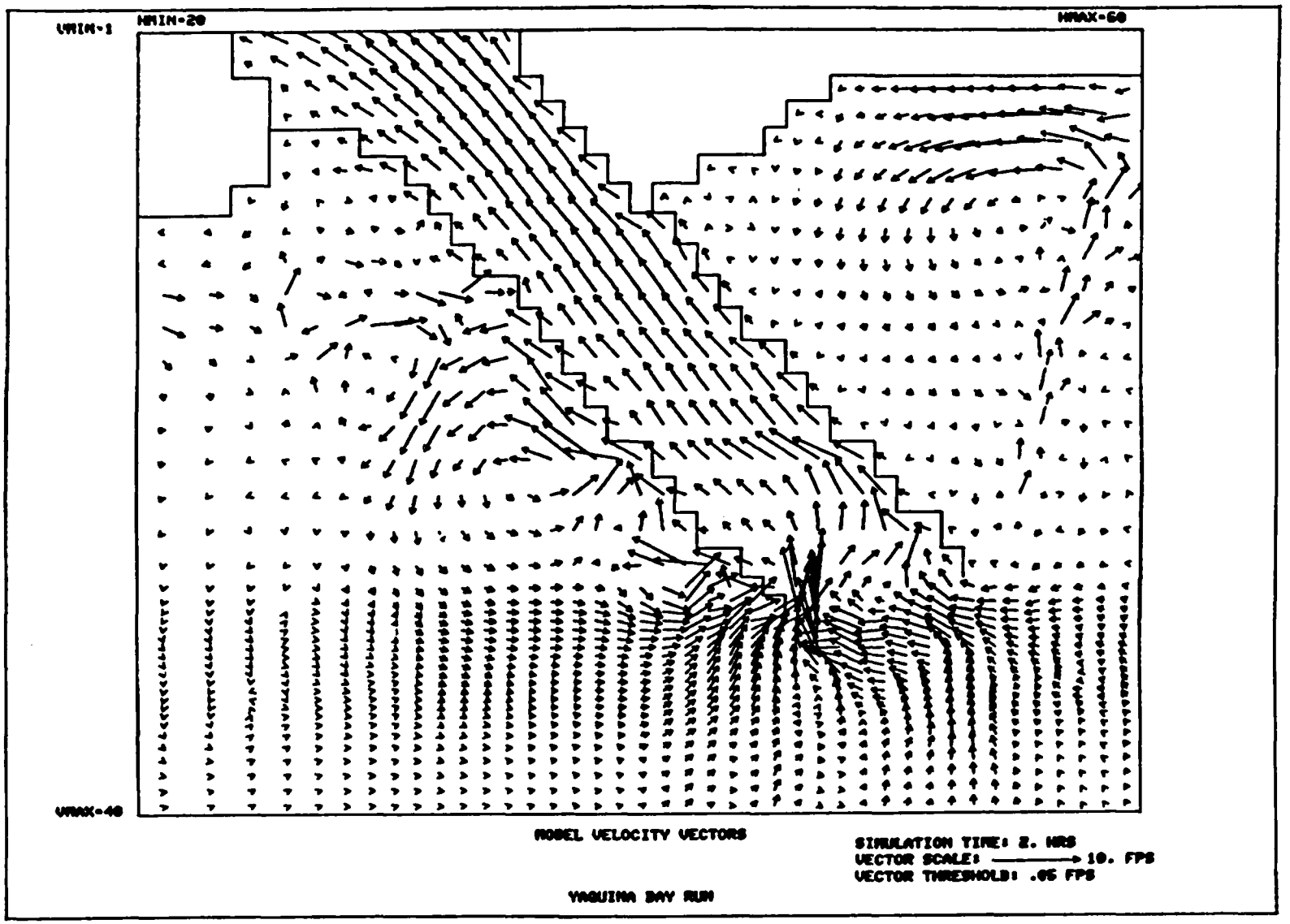

Plate 35. Superposition of tidal and wave-induced currents at peak flood, H_o = 10 ft, T = 11 sec, θ_o = WNW

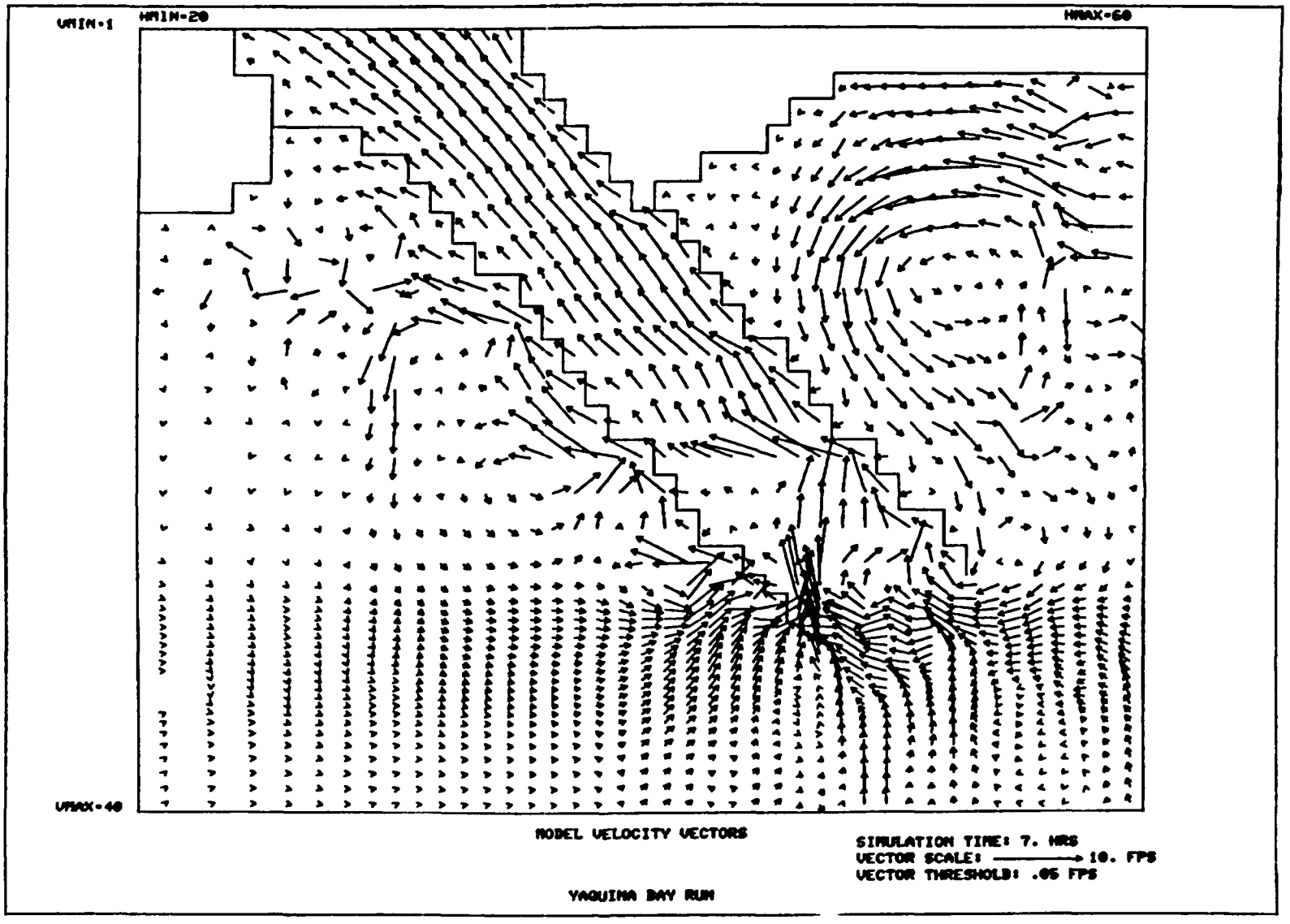

Plate 36. Superposition of tidal and wave-induced currents at peak flood, H_o = 10 ft, T = 14 sec, θ_o = W

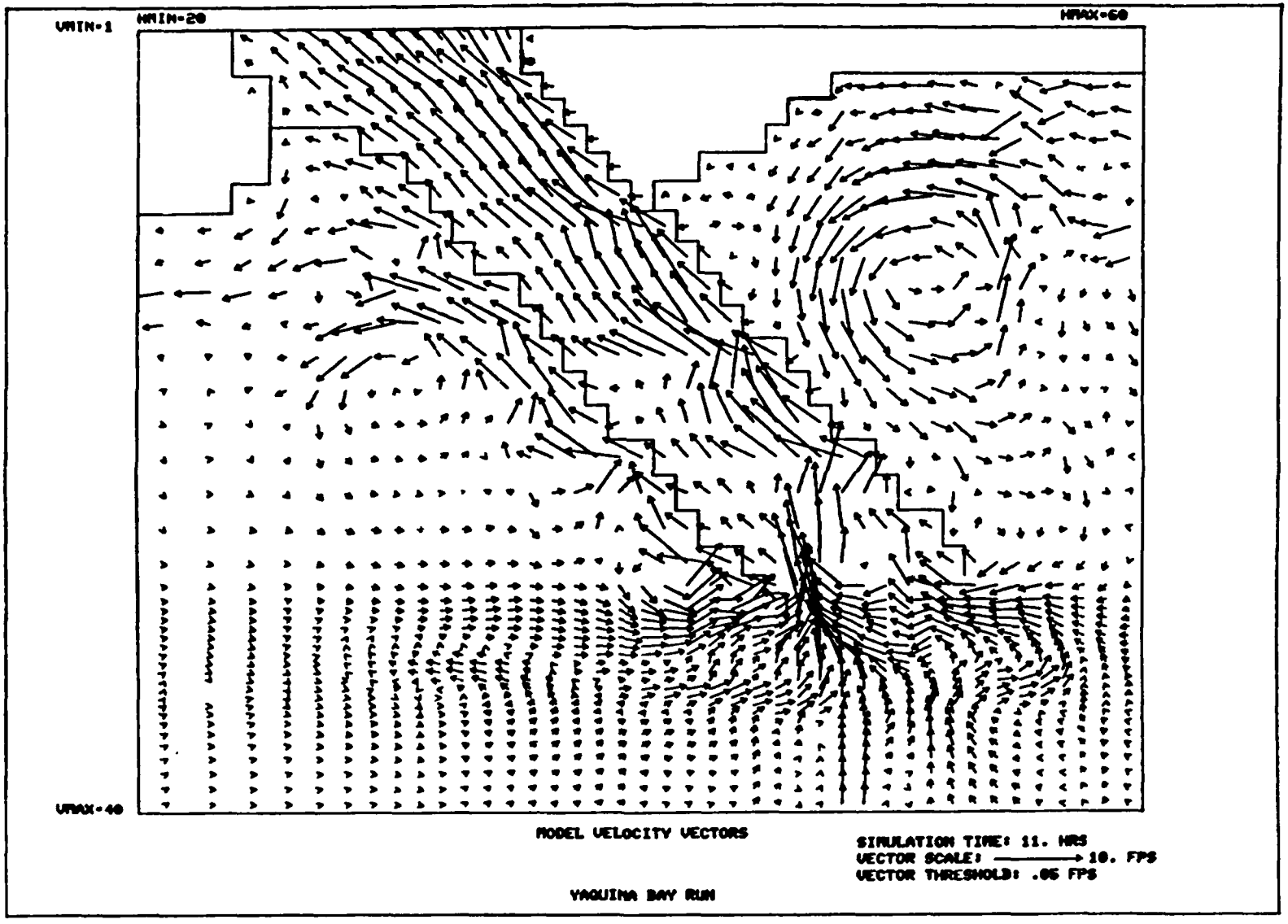

Plate 37. Superposition of tidal and wave-induced currents at peak flood, H_o = 10 ft, T = 11 sec, θ_o = WSW

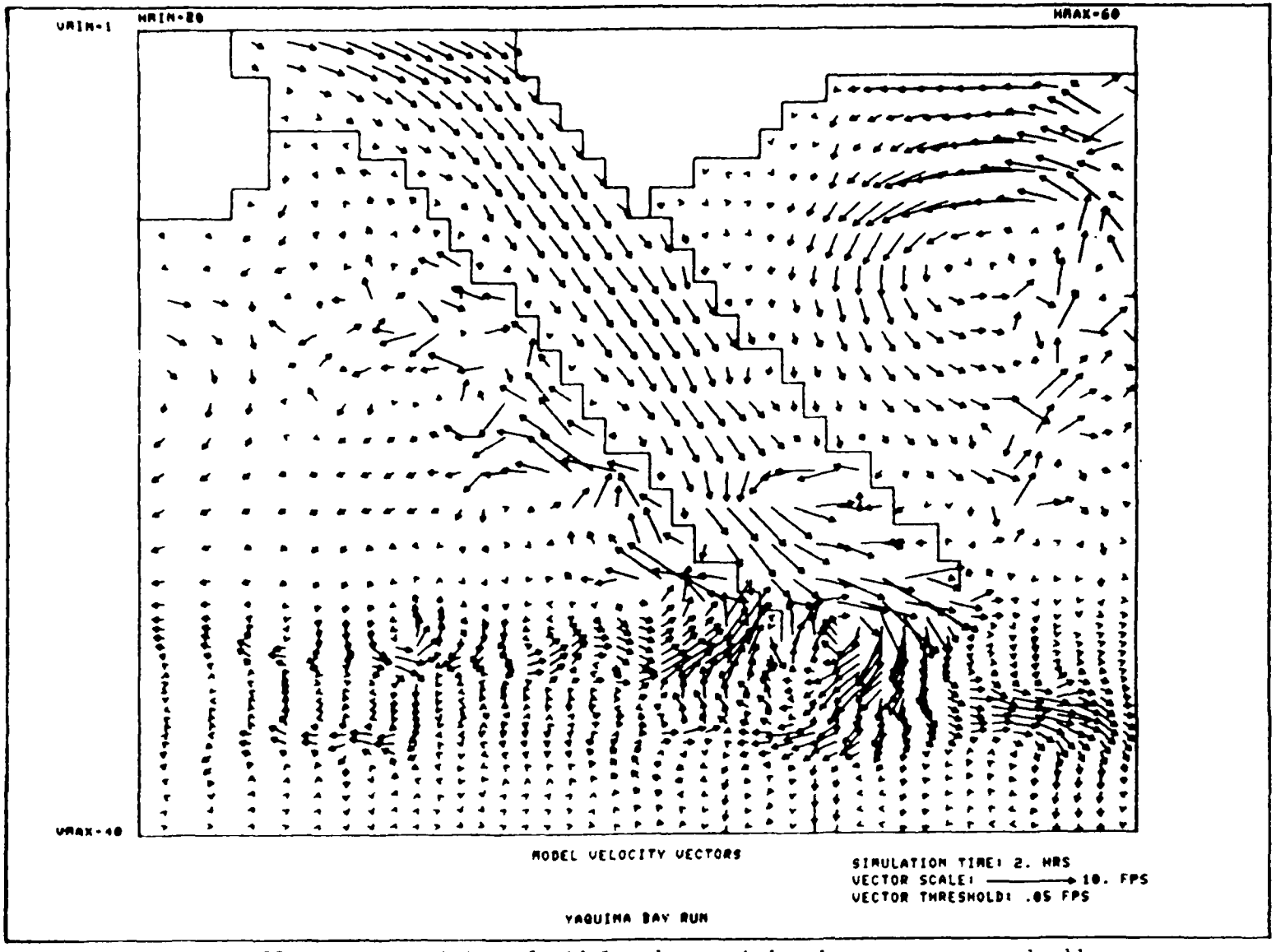

Plate 38A. Superposition of tidal and wave-induced currents at peak ebb, H_o = 14 ft, T = 11 sec, θ_o = WNW

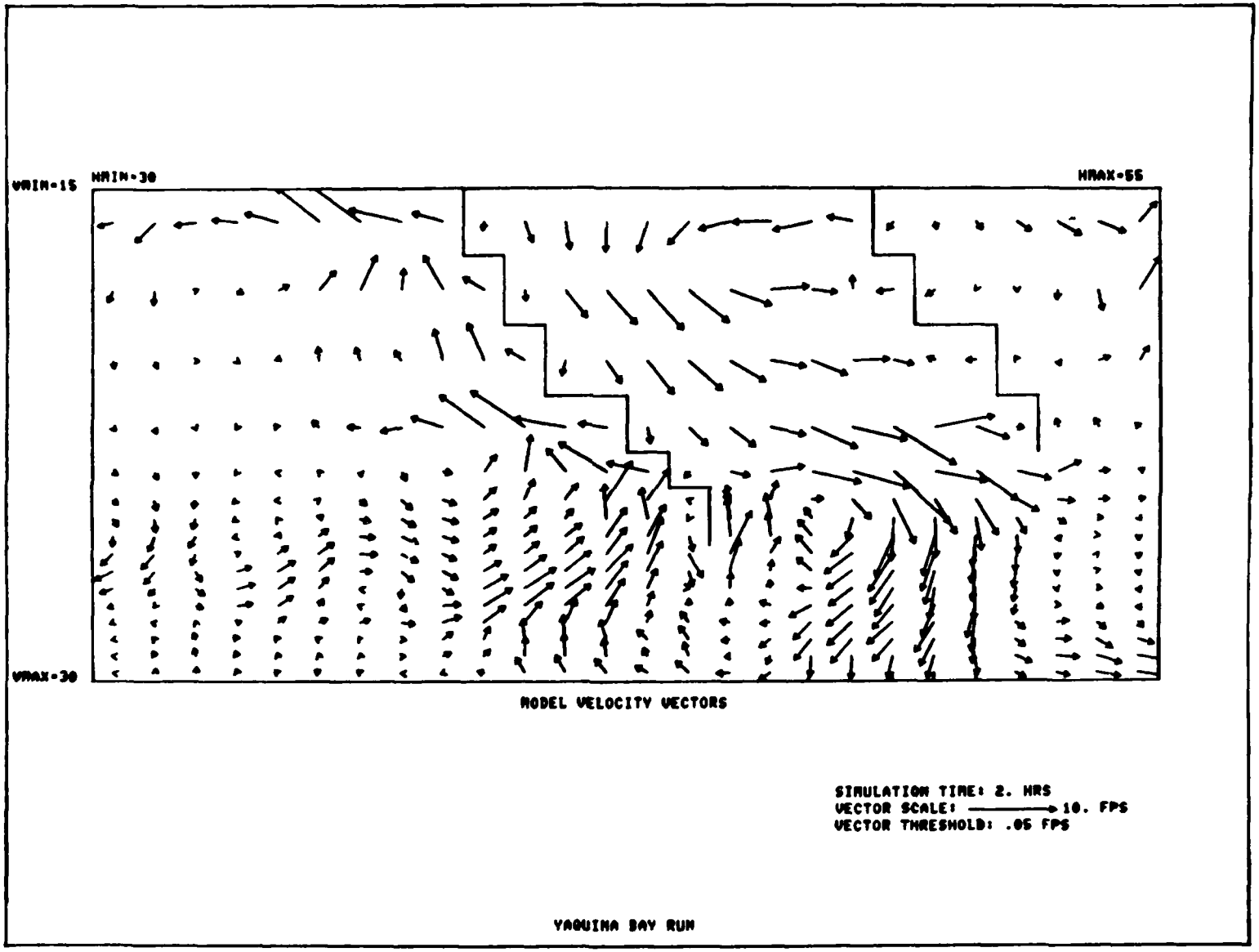

Plate 38B. Inlet entrance: superposition of tidal and wave-induced currents at peak ebb, H_o = 14 ft, T = 11 sec, θ_o = WNW

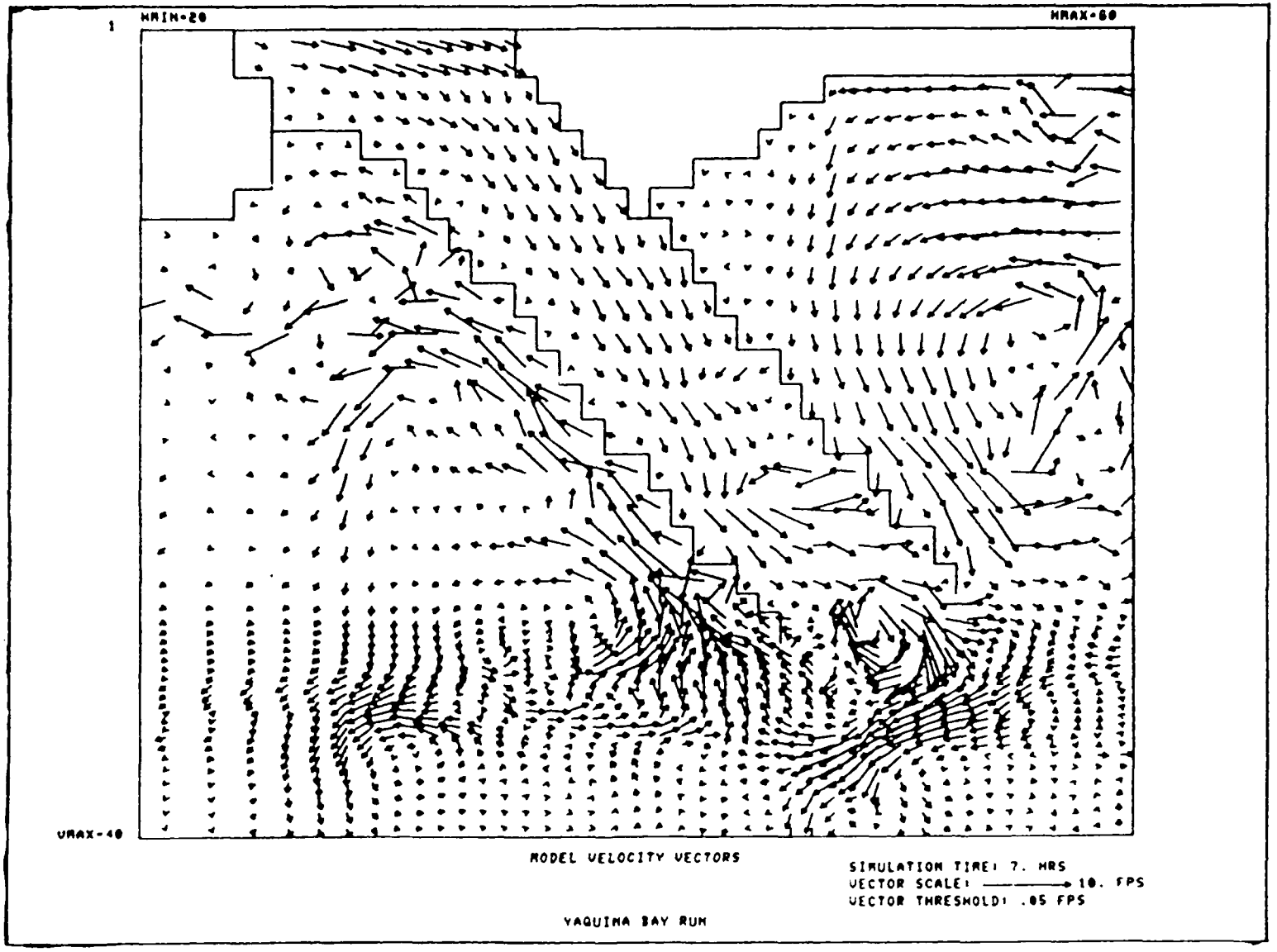

Plate 39A. Superposition of tidal and wave-induced currents at peak ebb, H_o = 14 ft, T = 14 sec, θ_o = W

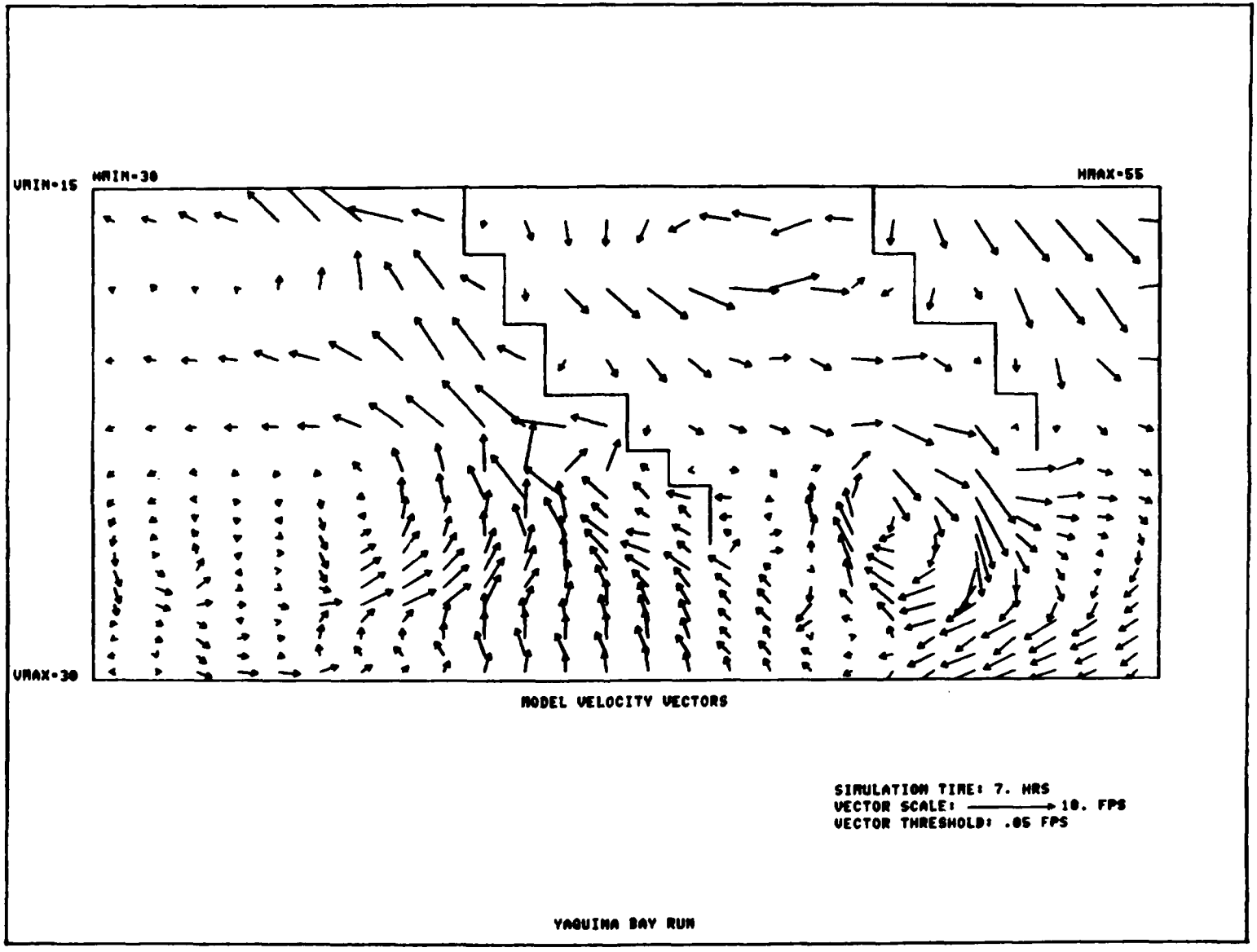

Plate 39B. Inlet entrance: superposition of tidal and wave-induced currents at peak ebb, H_o = 14 ft, T = 14 sec, θ_o = W

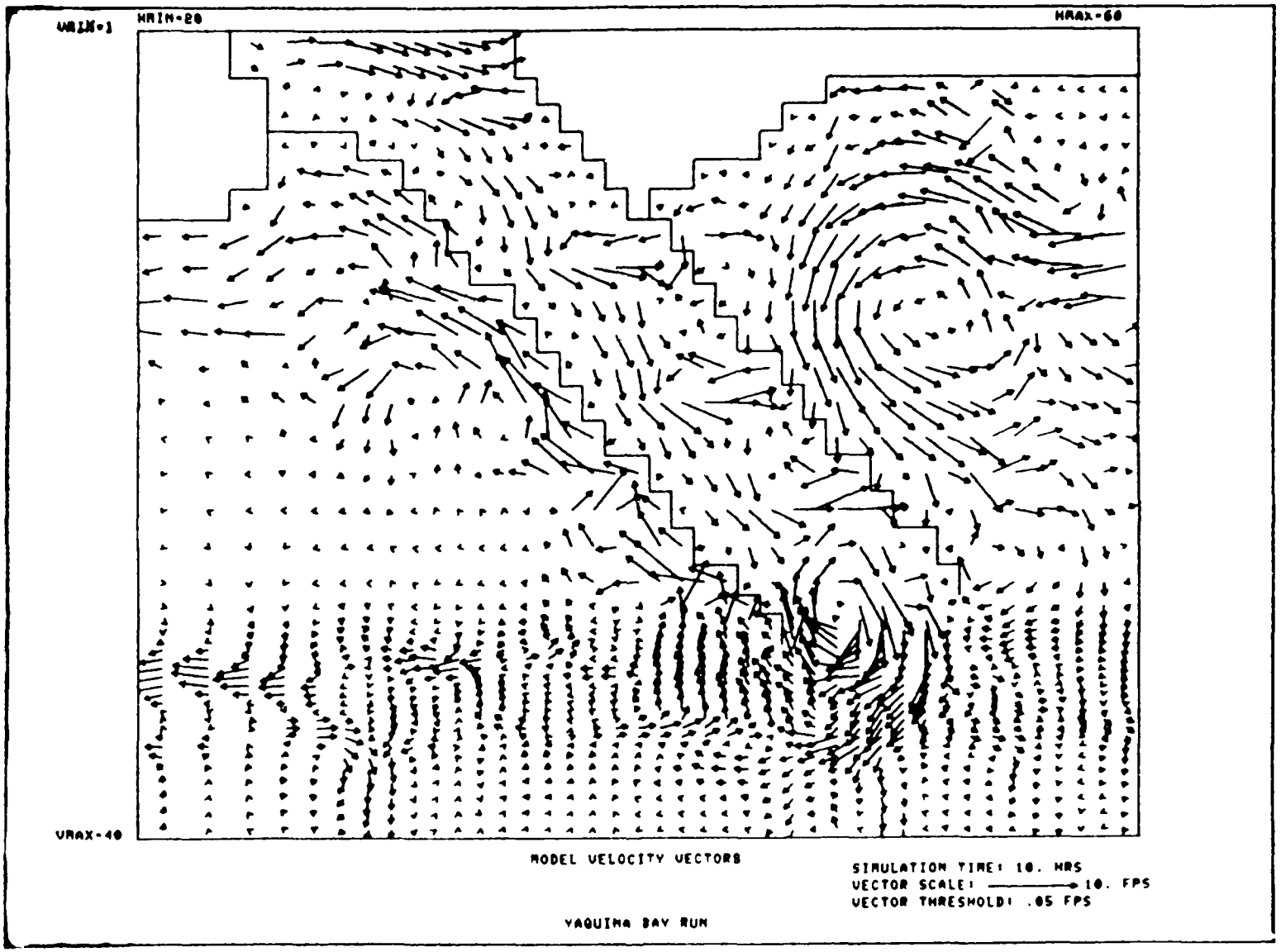

Plate 40A. Superposition of tidal and wave-induced currents at peak ebb, H_o = 14 ft, T = 11 sec, θ_o = WSW

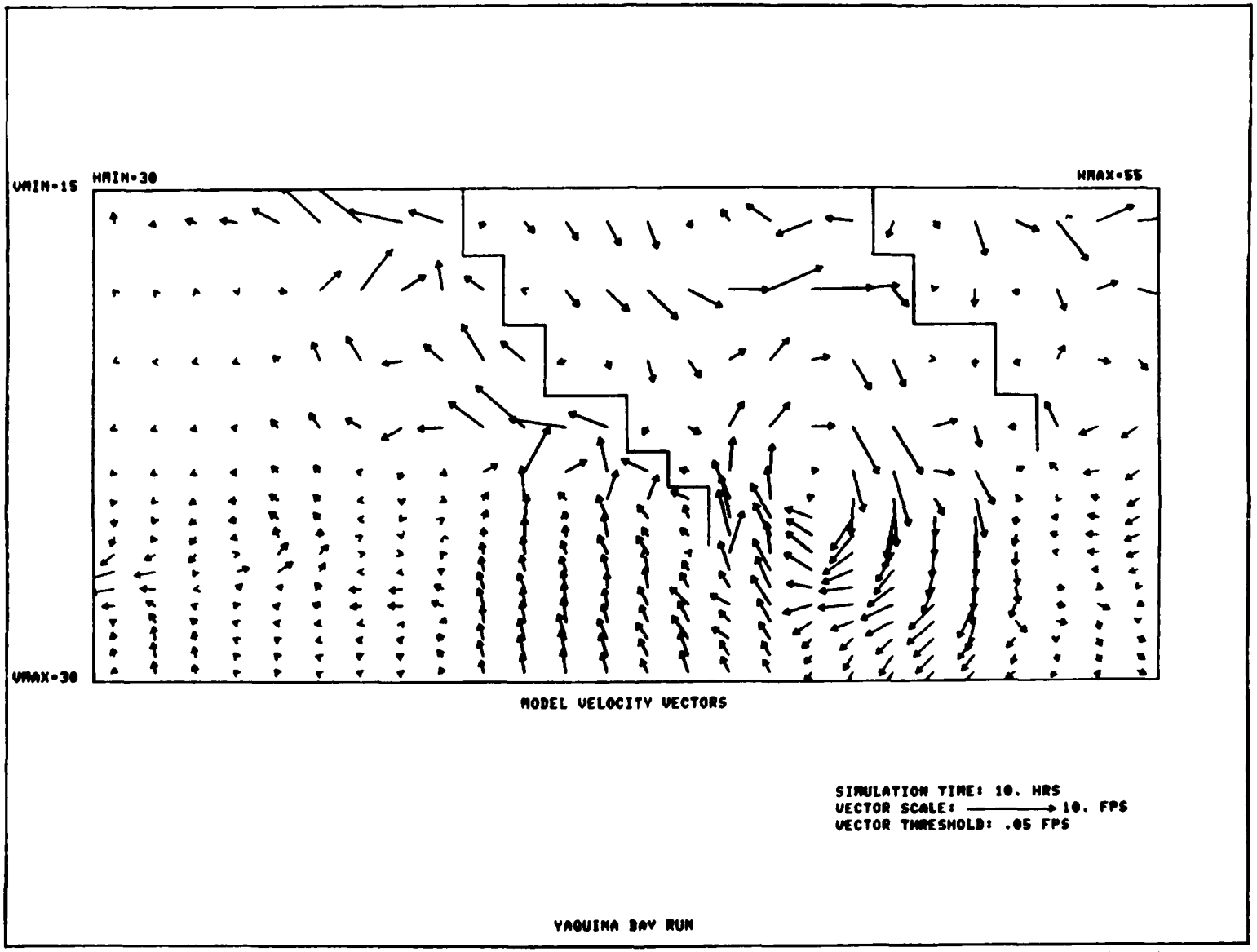

Plate 40B. Inlet entrance: superposition of tidal and wave-induced currents at peak ebb, H_o = 14 ft, T = 11 sec, θ_o = WSW

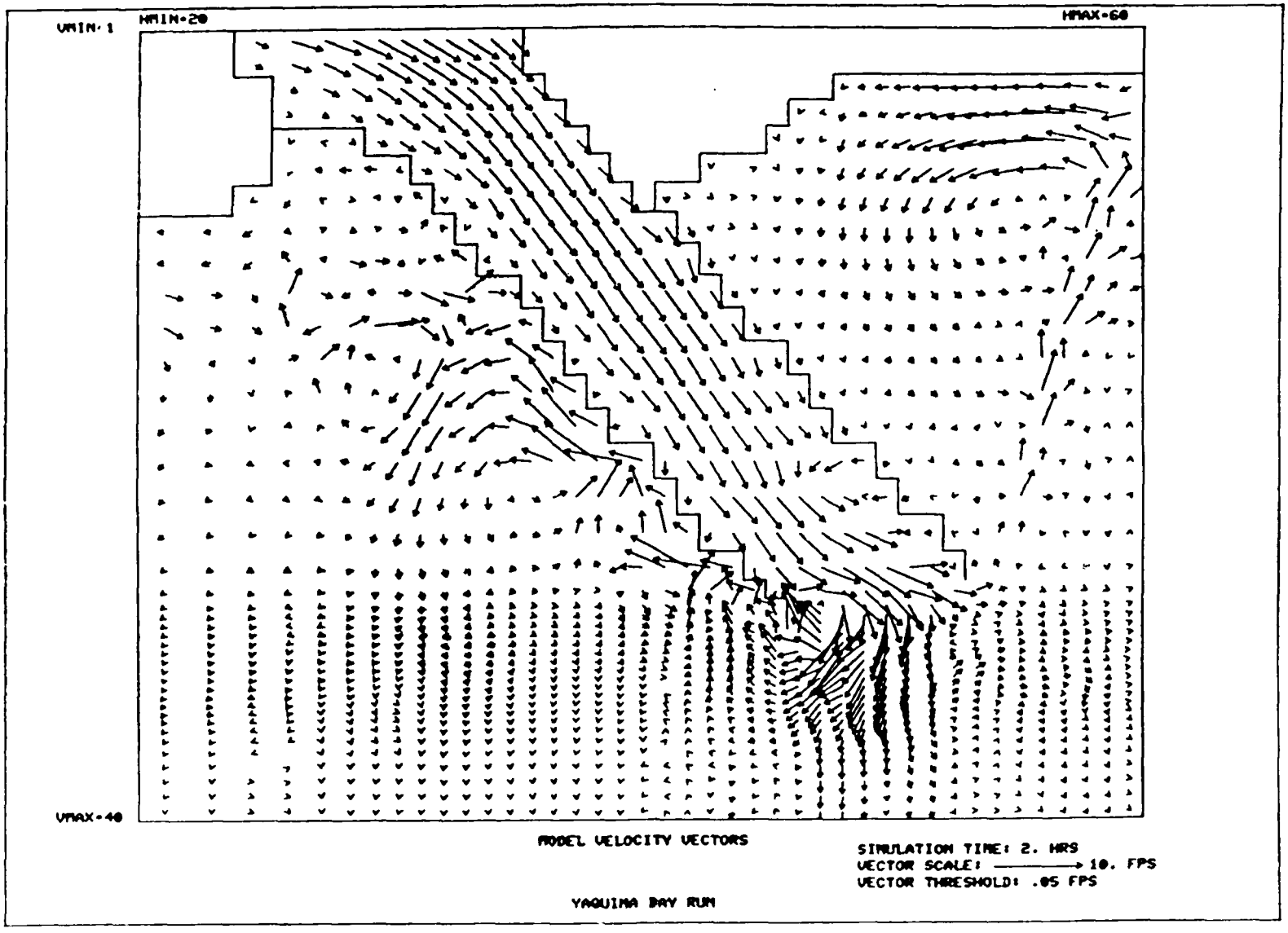

Plate 41. Superposition of tidal and wave-induced currents at peak ebb, H_o = 10 ft, T = 11 sec, θ_o = WNW

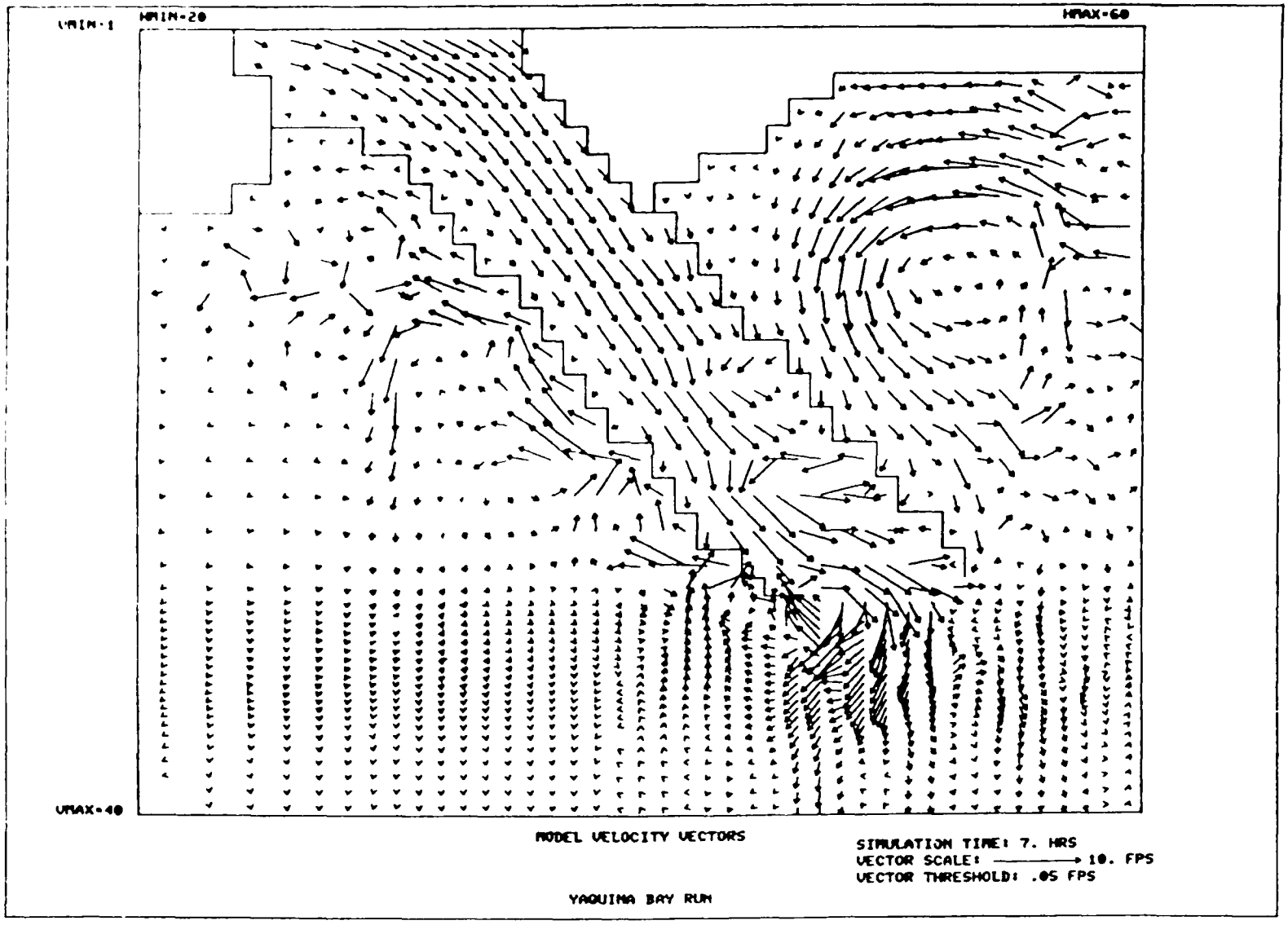

Plate 42. Superposition of tidal and wave-induced currents at peak ebb, H_o = 10 ft, T = 14 sec, θ_o = W

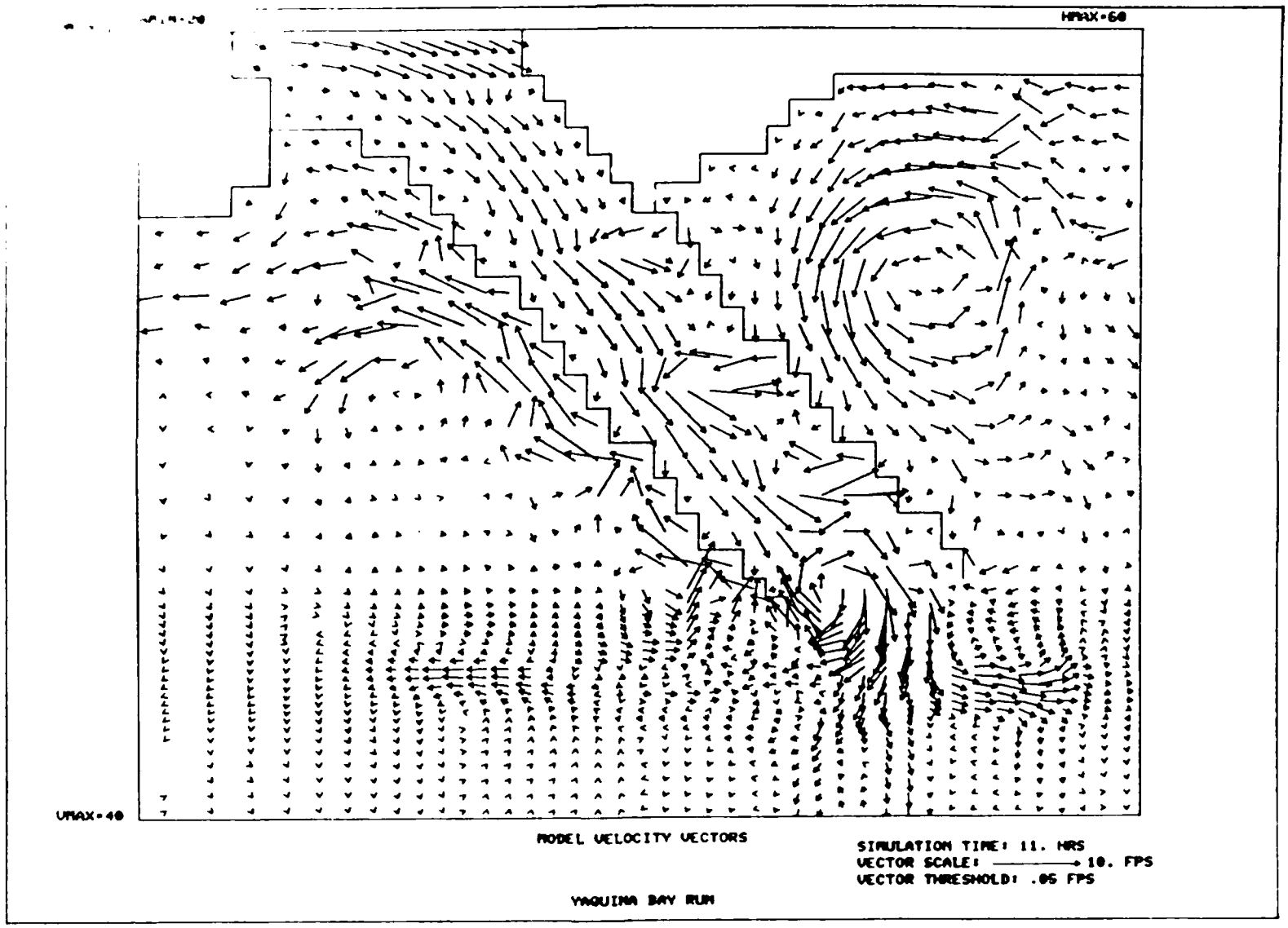

Plate 43. Superposition of tidal and wave-induced currents at peak ebb, H_o = 10 ft, T = 11 sec, θ_o = WSW

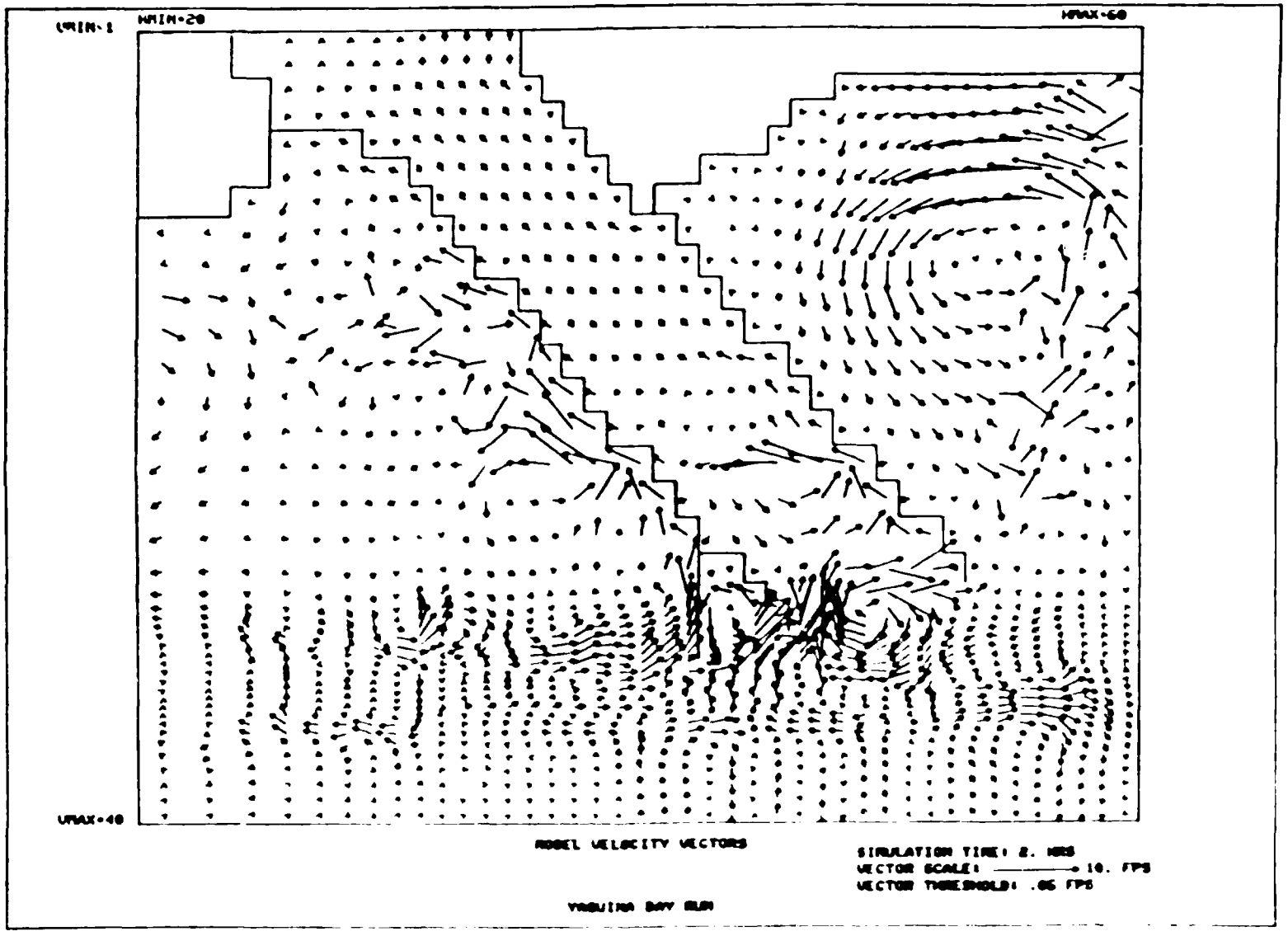
UMIN=1
MMIN=20
MMAX=60
UMAX=40
MODEL VELOCITY VECTORS
SIMULATION TIME: 8. HRS
VECTOR SCALE: 10. FPS
VECTOR THRESHOLD: .05 FPS
VIRGINIA BAY RUN

Plate ...

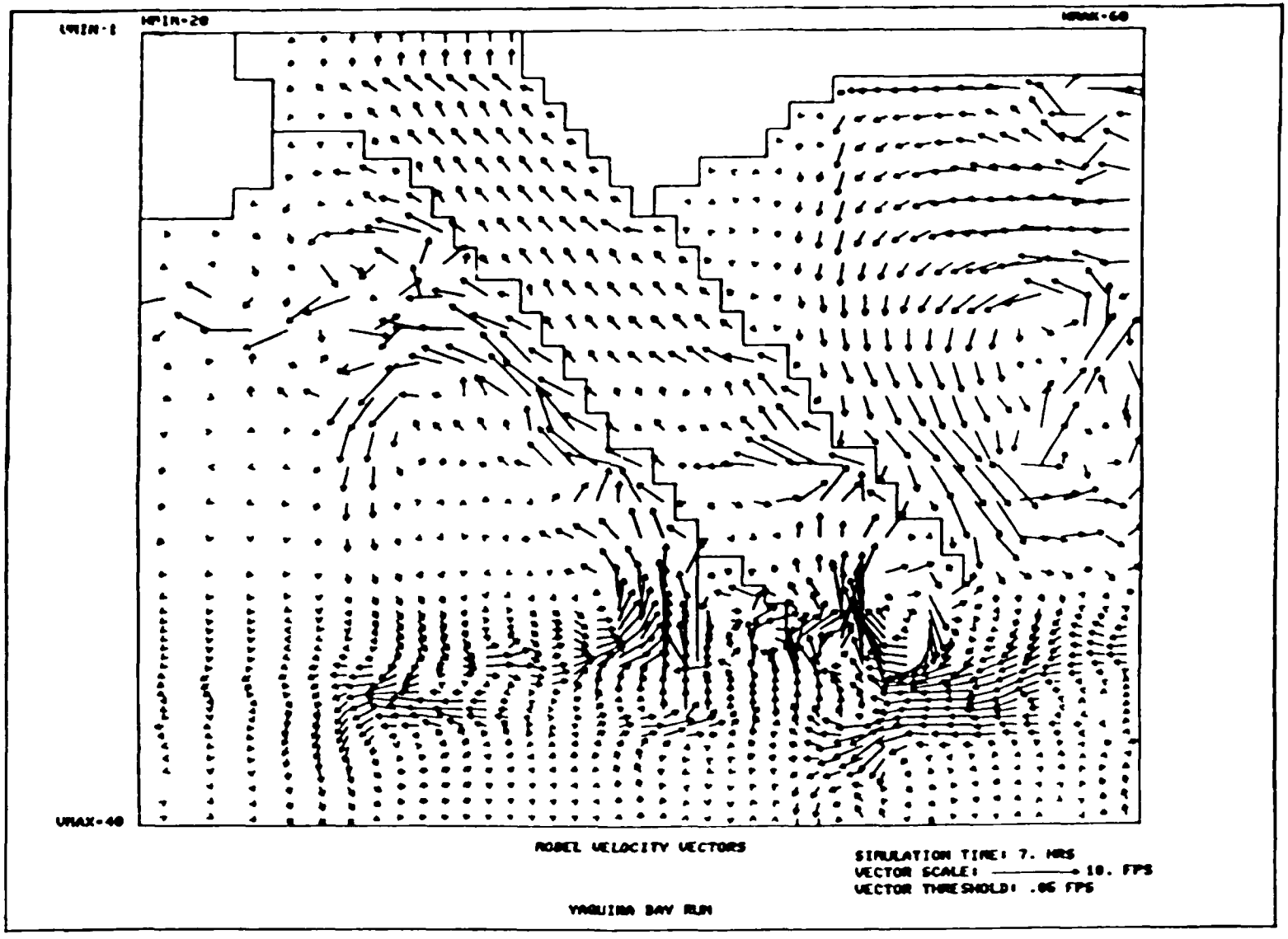

Plate 45. Wave-induced current pattern for alternative b; H_o = 14 ft, T = 14 sec, α_o = W

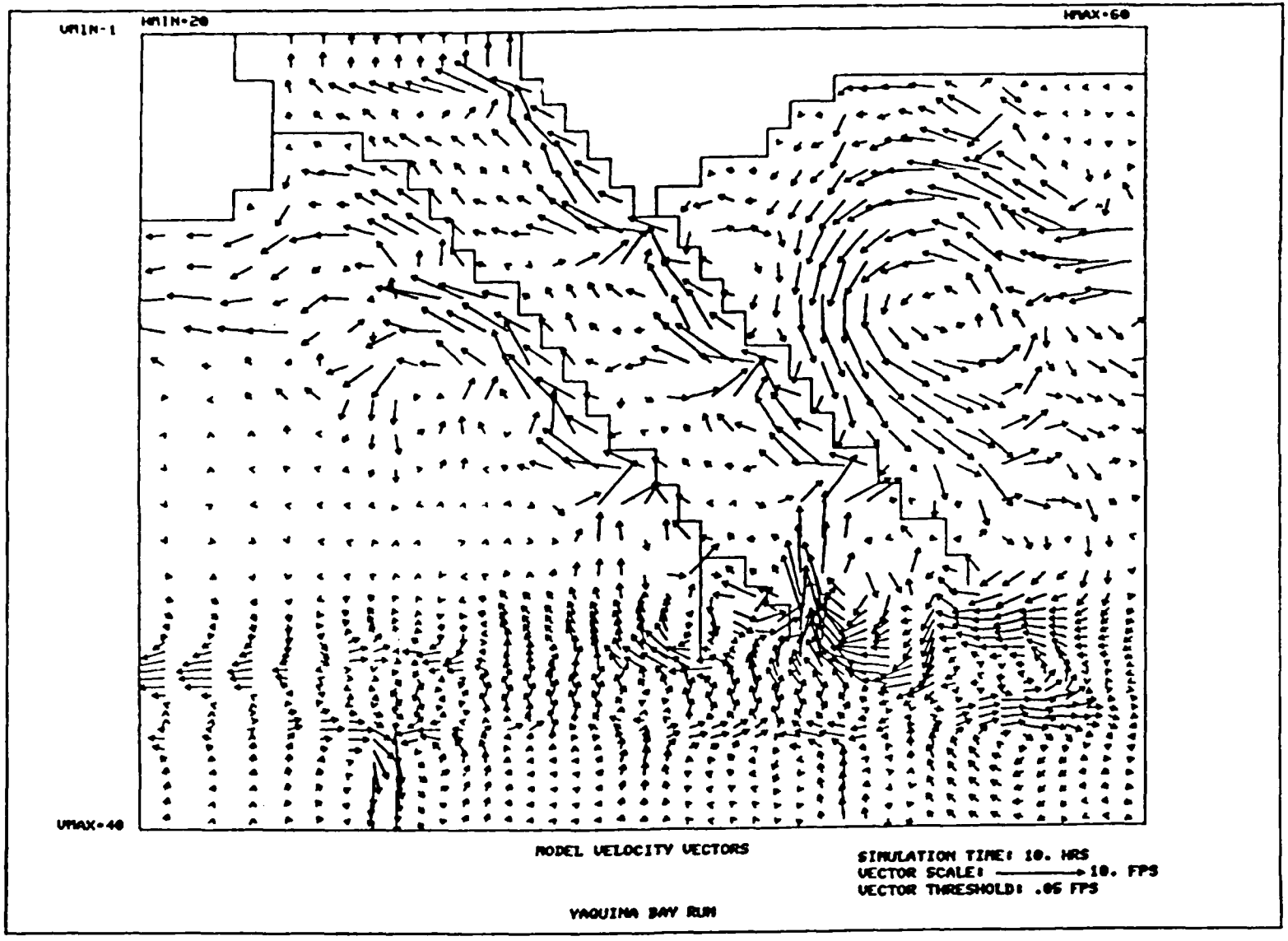

Plate 46. Wave-induced current pattern for alternative b;
H_o = 14 ft, T = 11 sec, θ_o = WSW

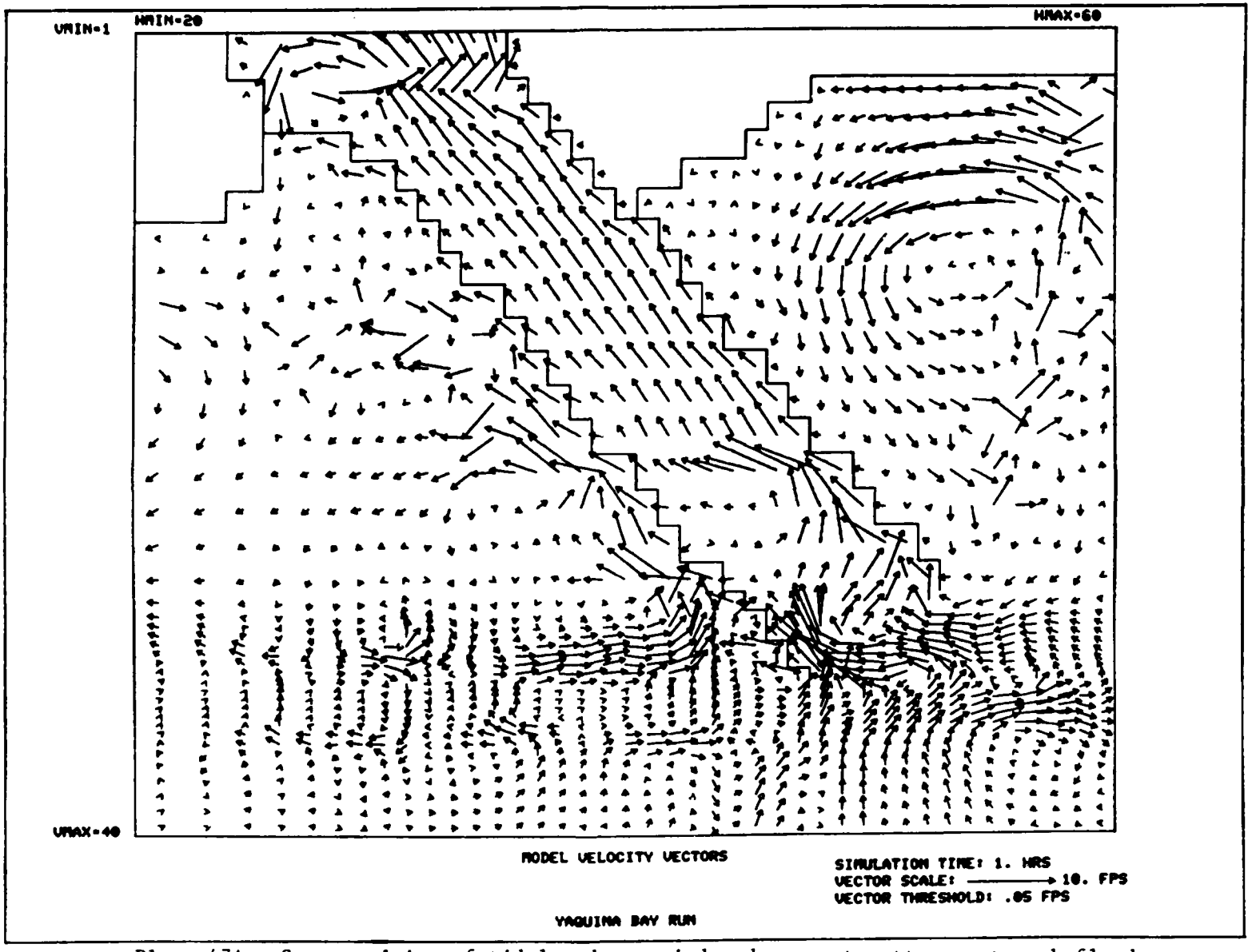

Plate 47A. Superposition of tidal and wave-induced current patterns at peak flood for alternative b; H_o = 14 ft, T = 11 sec, θ_o = WNW

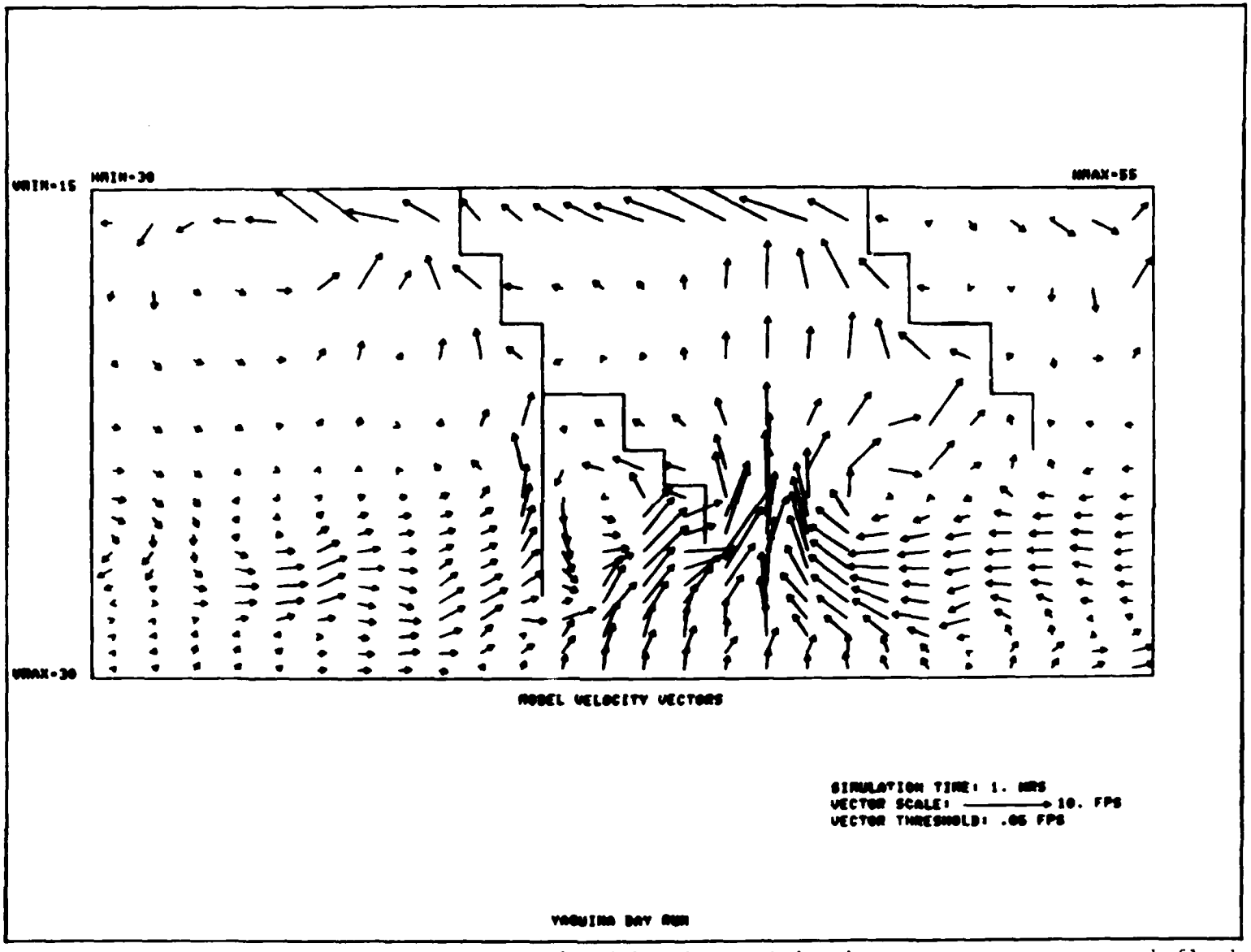

Plate 47B. Inlet entrance: superposition of tidal and wave-induced current patterns at peak flood for alternative b; H_o = 14 ft, T = 11 sec, θ_o = WNW

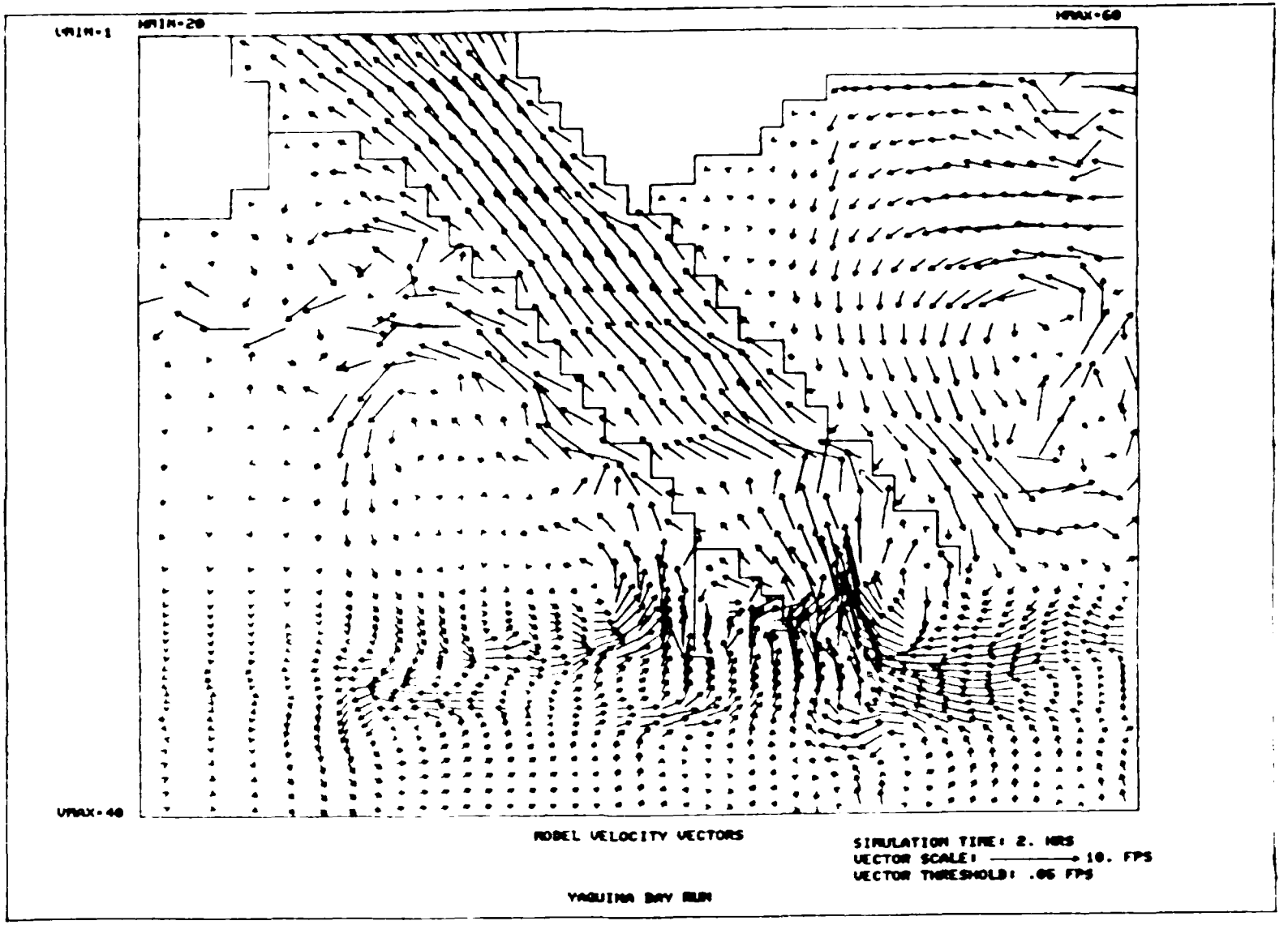

Plate 48A. Superposition of tidal and wave-induced current patterns at peak flood for alternative B: H_o = 14 ft, T = 14 sec, θ_o = 0

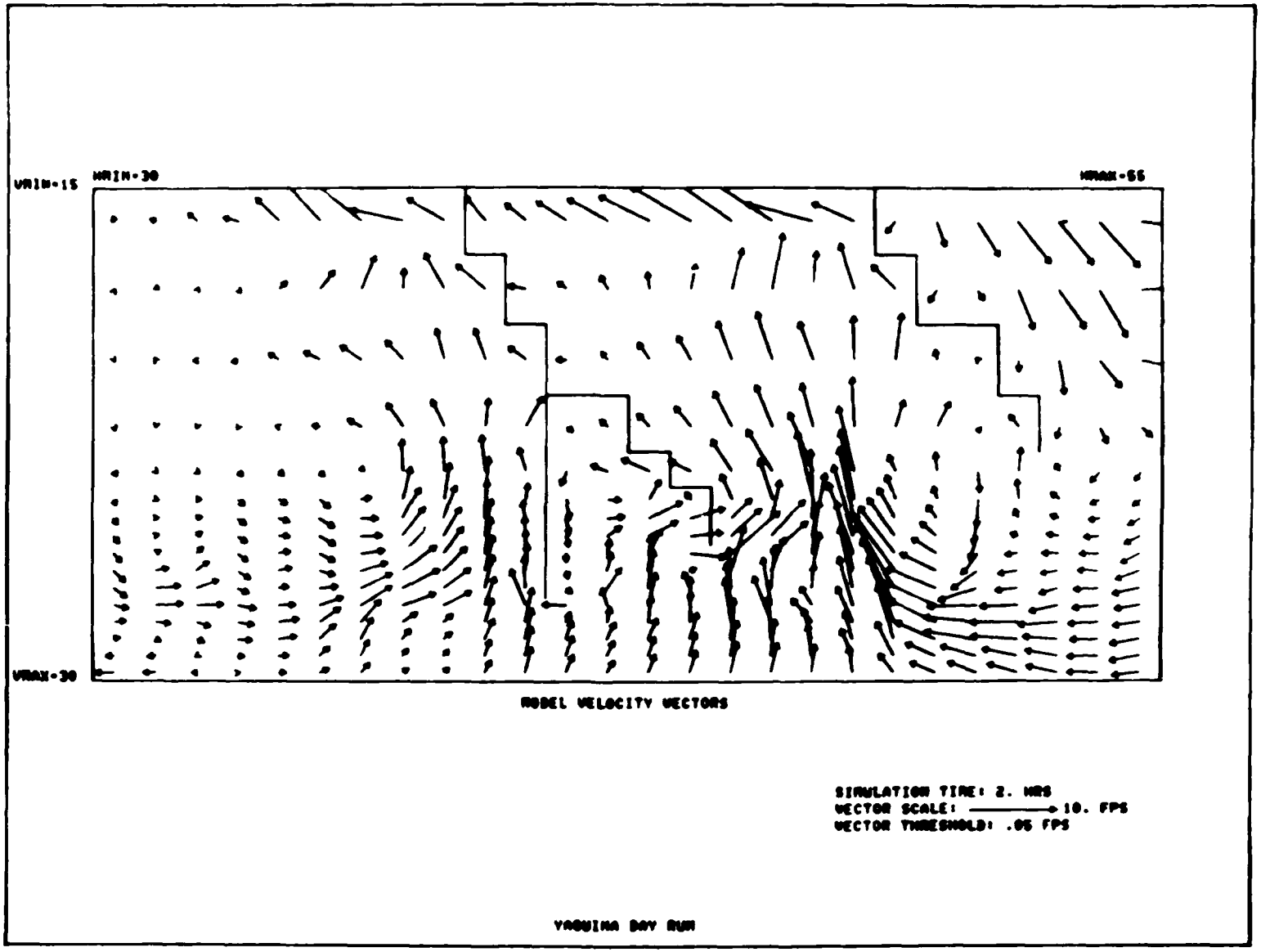

Plate 48B. Inlet entrance: superposition of tidal and wave-induced current patterns at peak flood for alternative b; H_o = 14 ft, T = 14 sec, θ_o = W

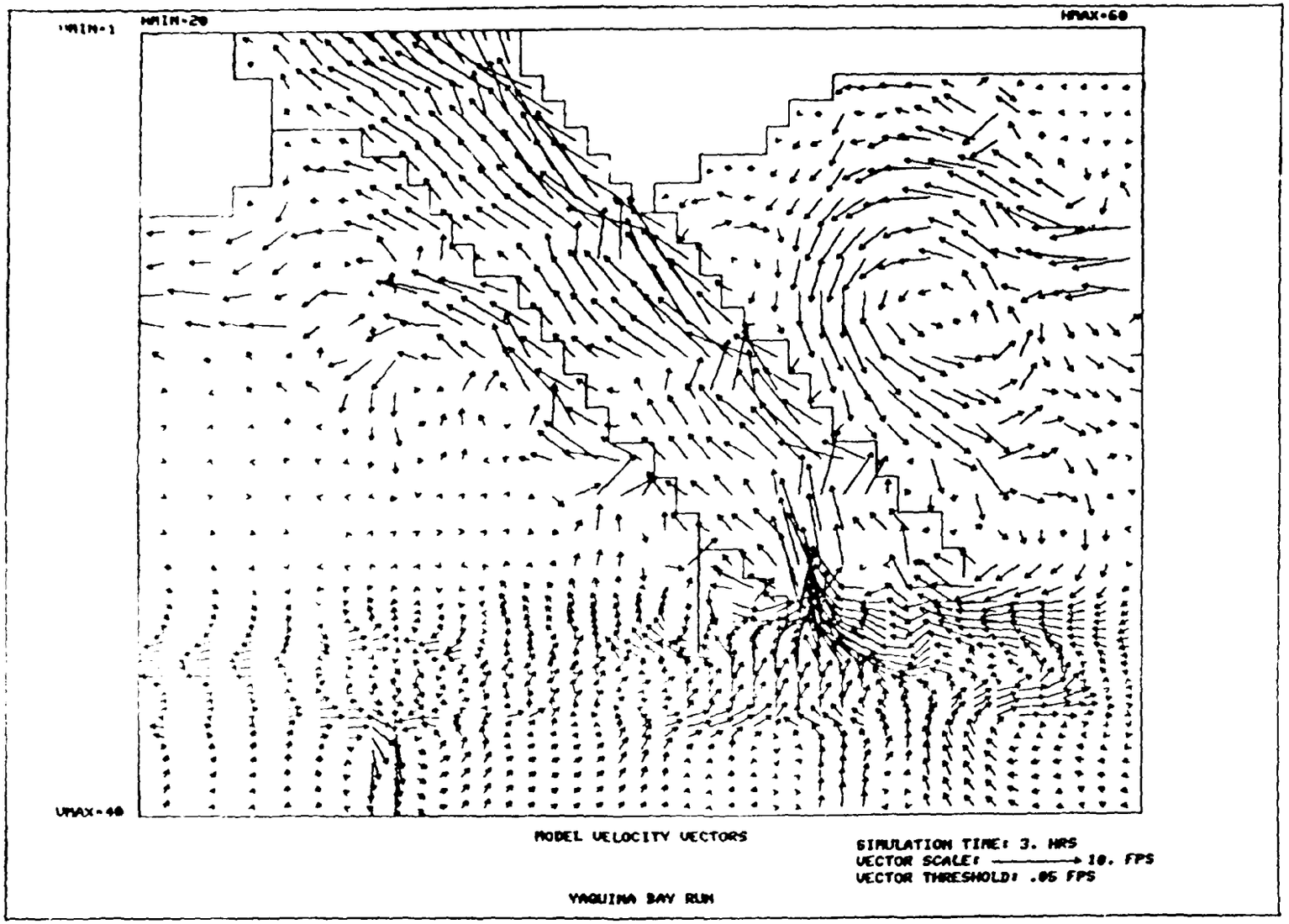

Plate 49A. Superposition of tidal and wave-induced current patterns at peak flood for alternative b; H_o = 14 ft, T = 11 sec, θ_o = WSW

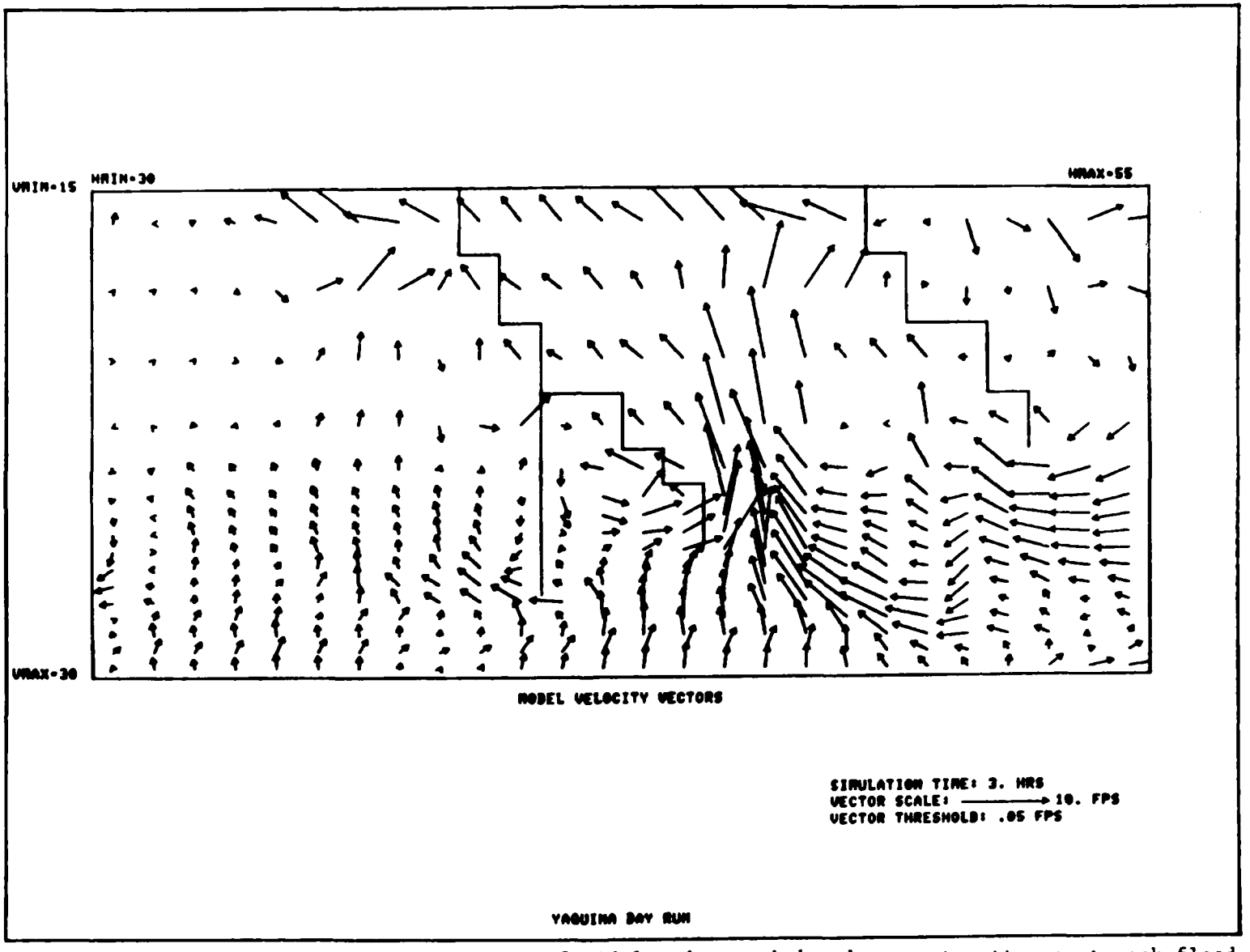

Plate 49B. Inlet entrance: superposition of tidal and wave-induced current patterns at peak flood for alternative b; H_o = 14 ft, T = 11 sec, θ_o = WSW

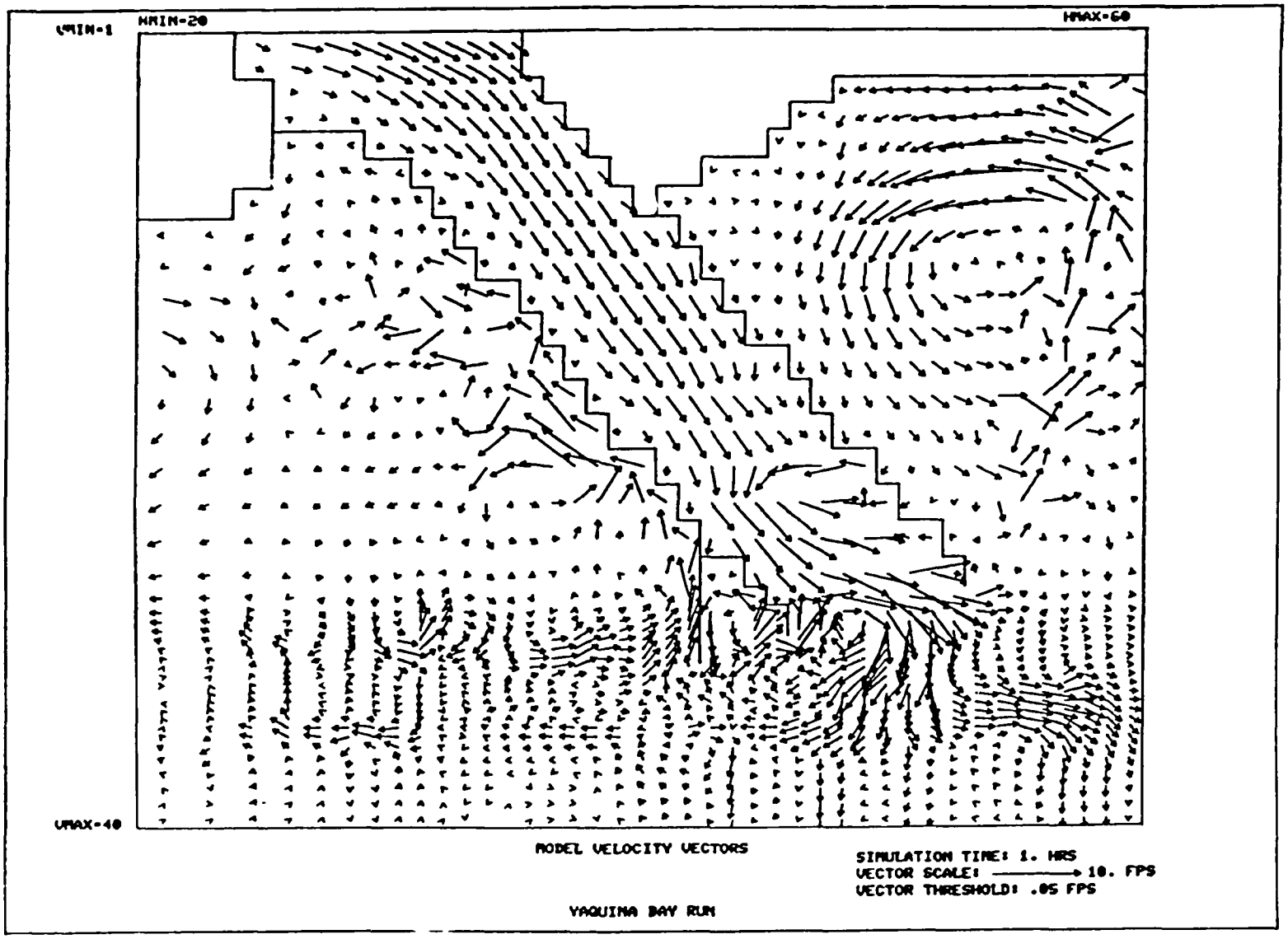

Plate 50A. Superposition of tidal and wave-induced current patterns at peak ebb for alternative b; H_o = 14 ft, T = 11 sec, θ_o = WNW

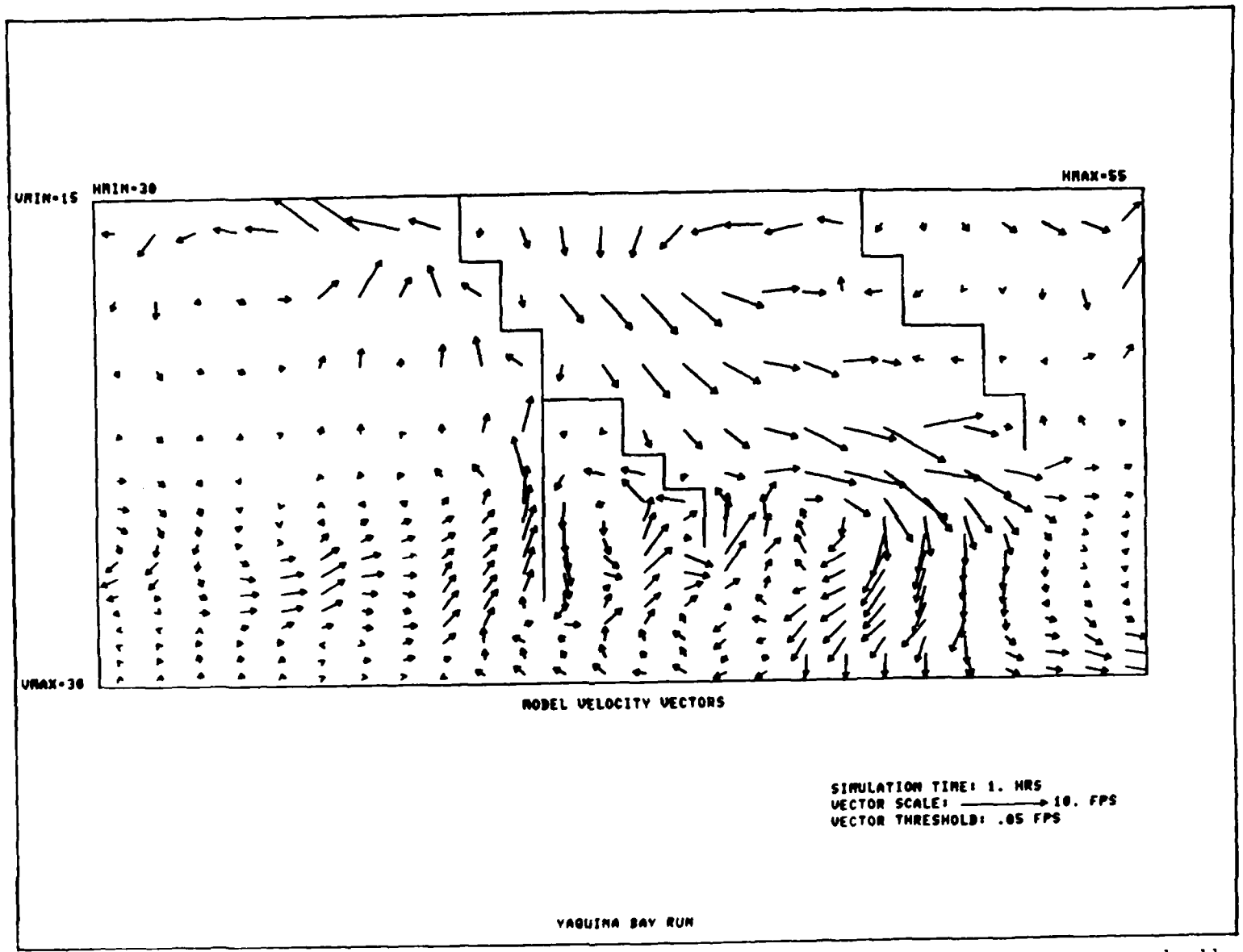

Plate 50B. Inlet entrance: superposition of tidal and wave-induced current patterns at peak ebb for alternative b; H_o = 14 ft, T = 11 sec, θ_o = WNW

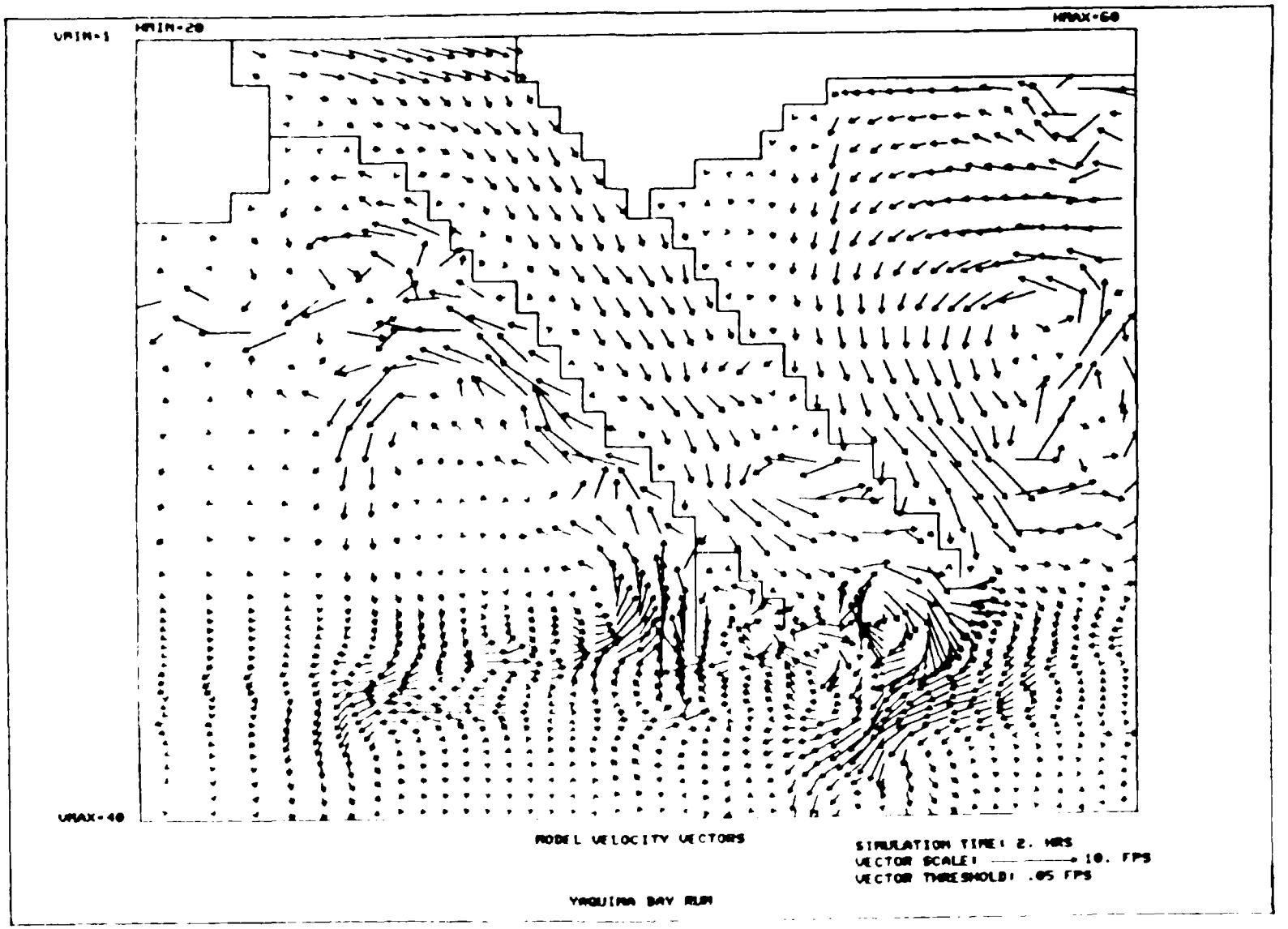

Plate 51A. Superposition of tidal and wave induced current patterns at [illegible] for alternative [illegible]

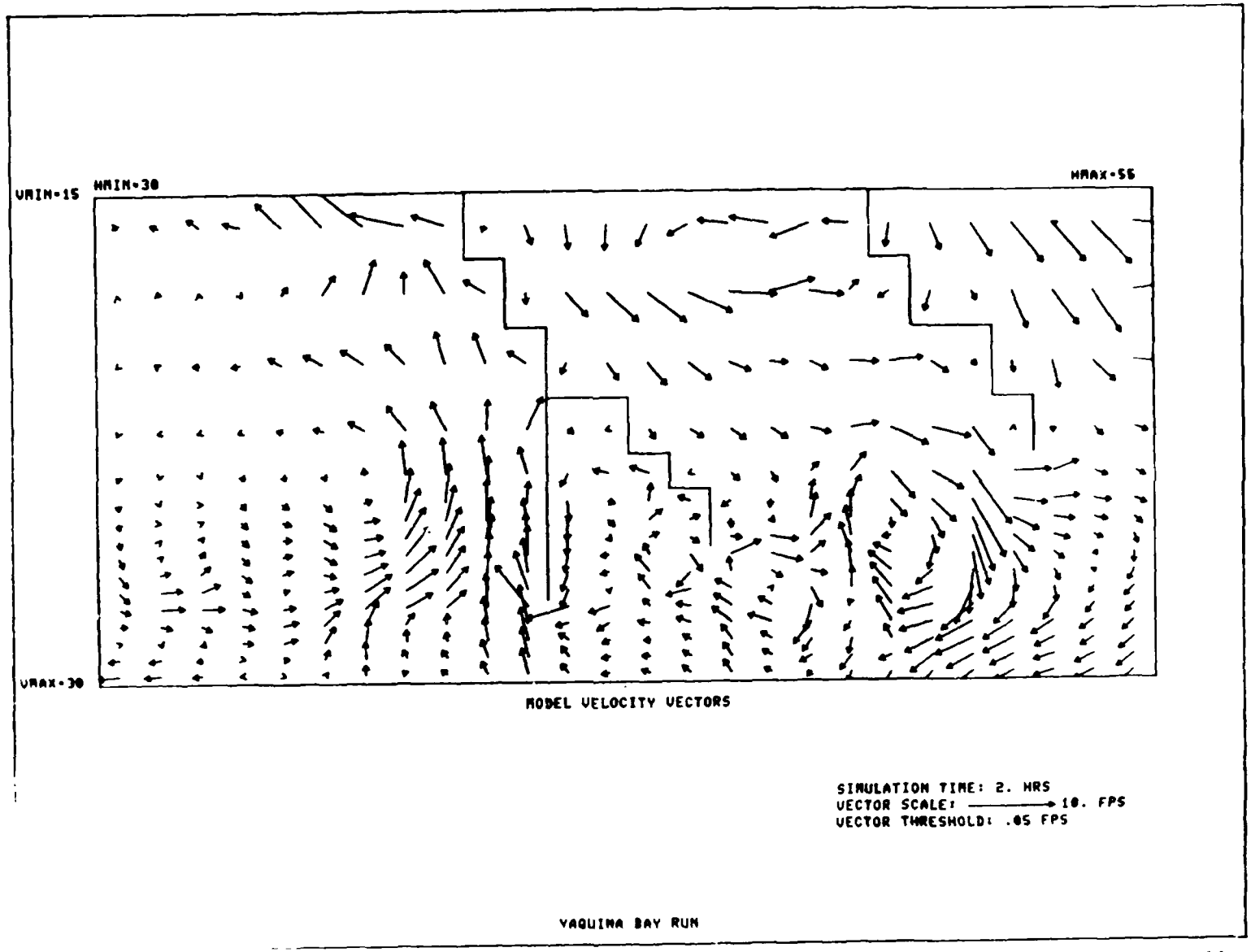

...r entrance: superposition of tidal and wave-induced current patterns at peak ebb for alternative b; H_o = 14 ft, T = 14 sec, θ_o = W

AD-A179 822 YAQUINA BAY OREGON TIDAL AND WAVE-INDUCED CURRENTS NEAR 2/2
THE JETTIED INLET (U) COASTAL ENGINEERING RESEARCH
CENTER VICKSBURG MS M A CIALONE DEC 86 CERC-MP-86-14

UNCLASSIFIED F/G 8/3 NL

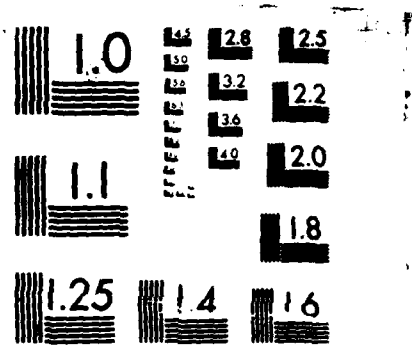

MICROCOPY RESOLUTION TEST CHART
NATIONAL BUREAU OF STANDARDS 1963 A

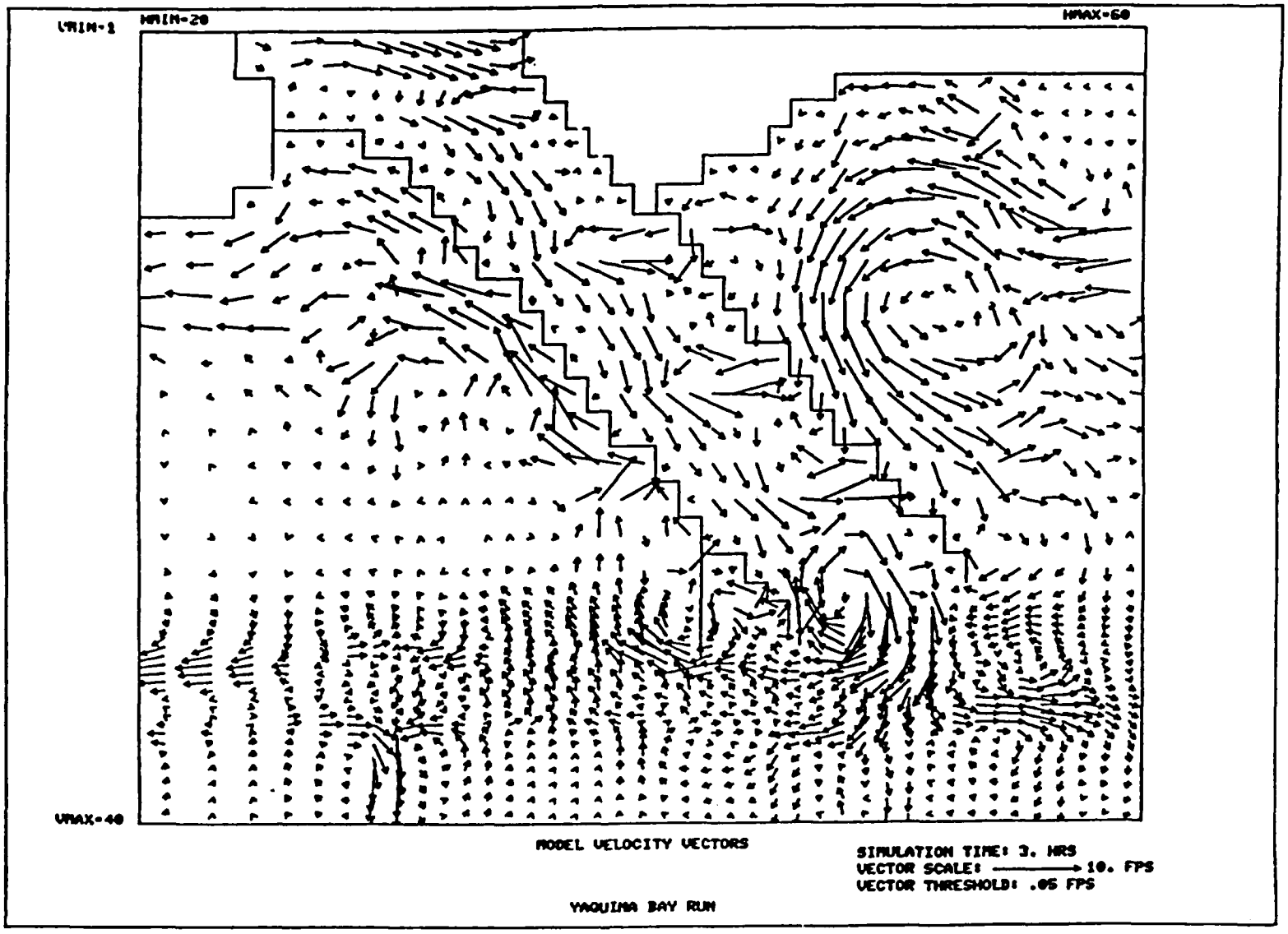

Plate 52A. Superposition of tidal and wave-induced current patterns at peak ebb for alternative b; H_o = 14 ft, T = 11 sec, θ_o = WSW

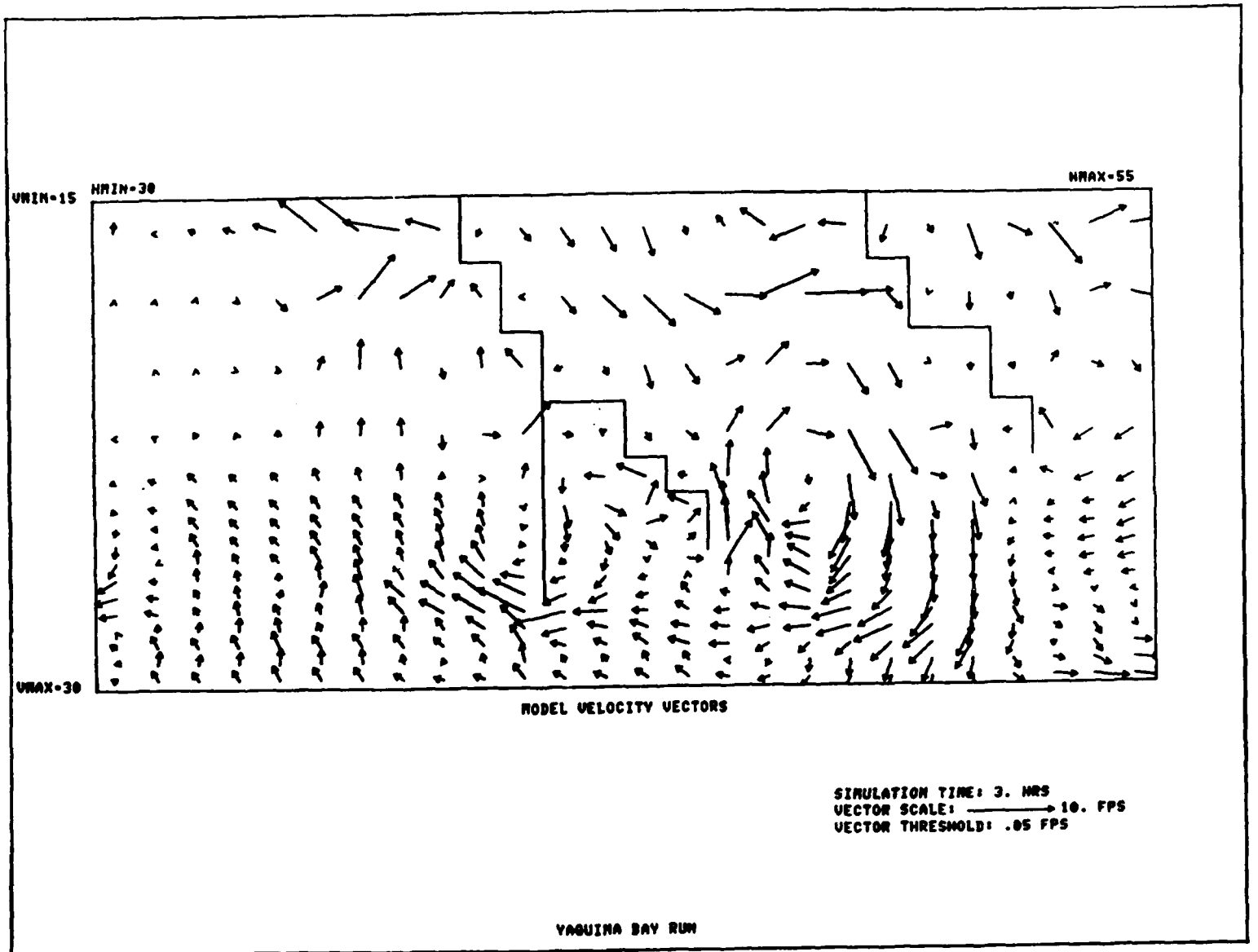

Plate 52B. Inlet entrance: superposition of tidal and wave-induced current patterns at peak ebb for alternative b; H_o = 14 ft, T = 11 sec, θ_o = WSW

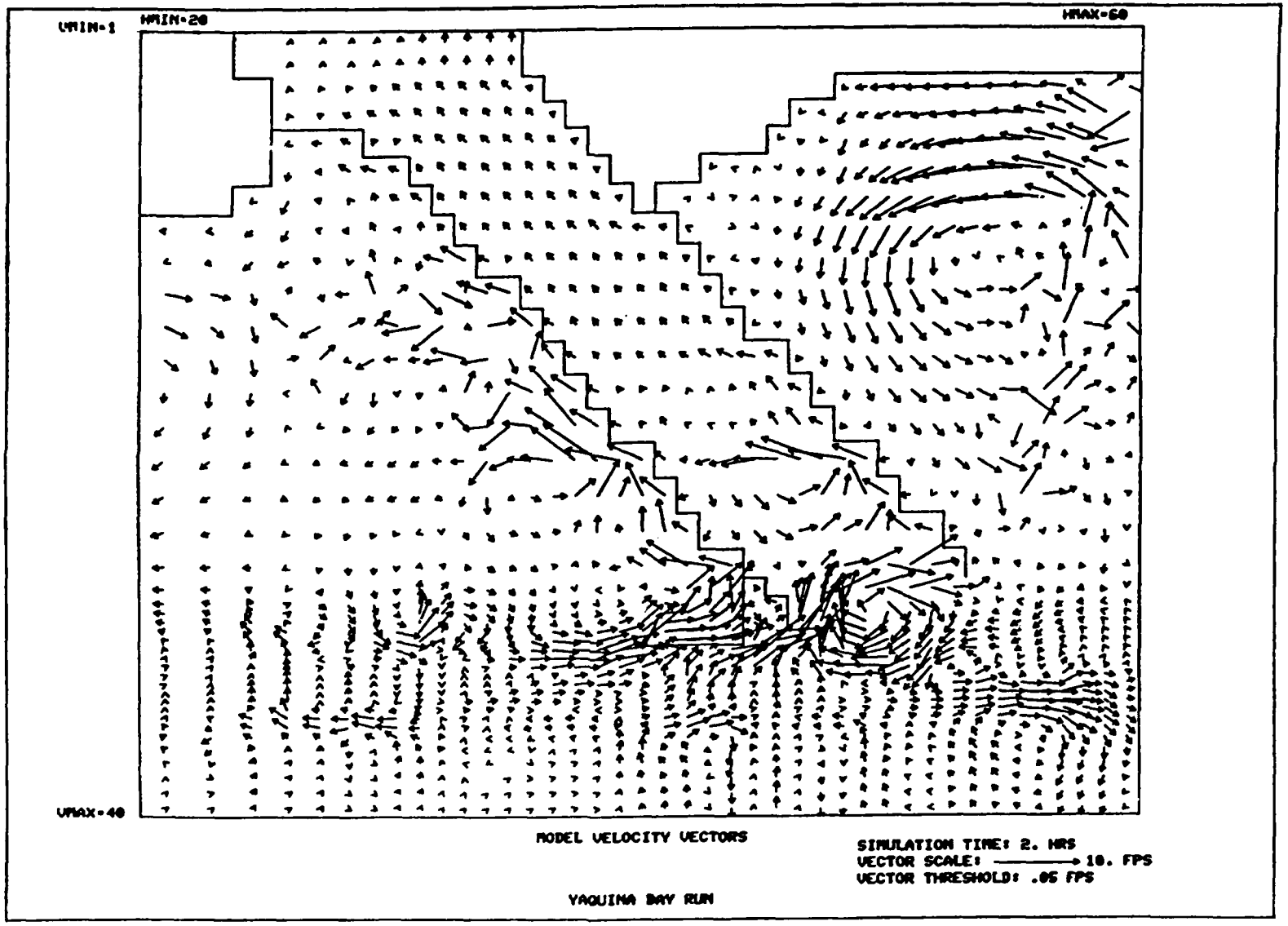

Plate 53. Wave-induced current pattern for alternative e; H_o = 14 ft, T = 11 sec, θ_o = WNW

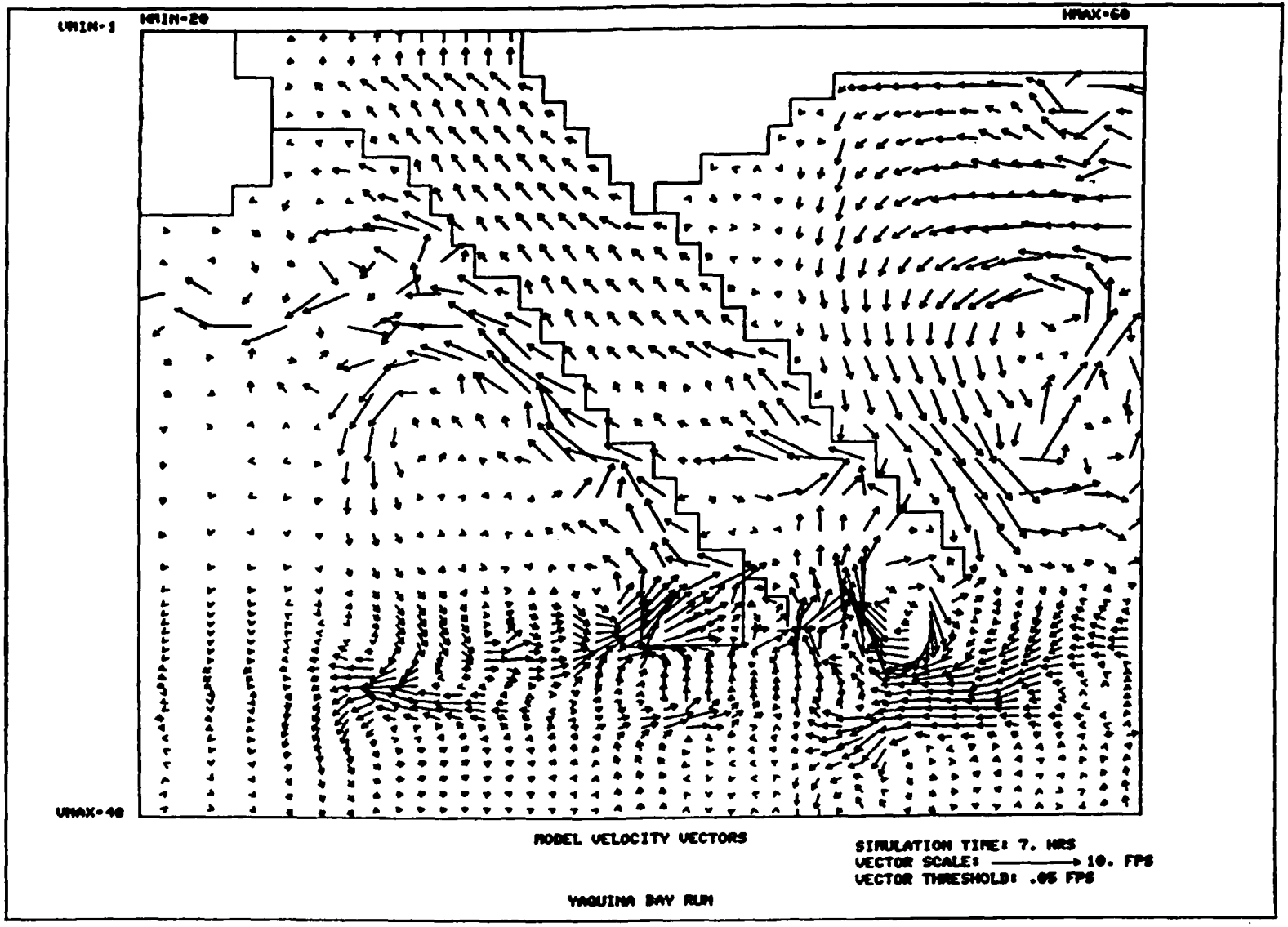

Plate 54. Wave-induced current pattern for alternative e; H_o = 14 ft, T = 14 sec, θ_o = W

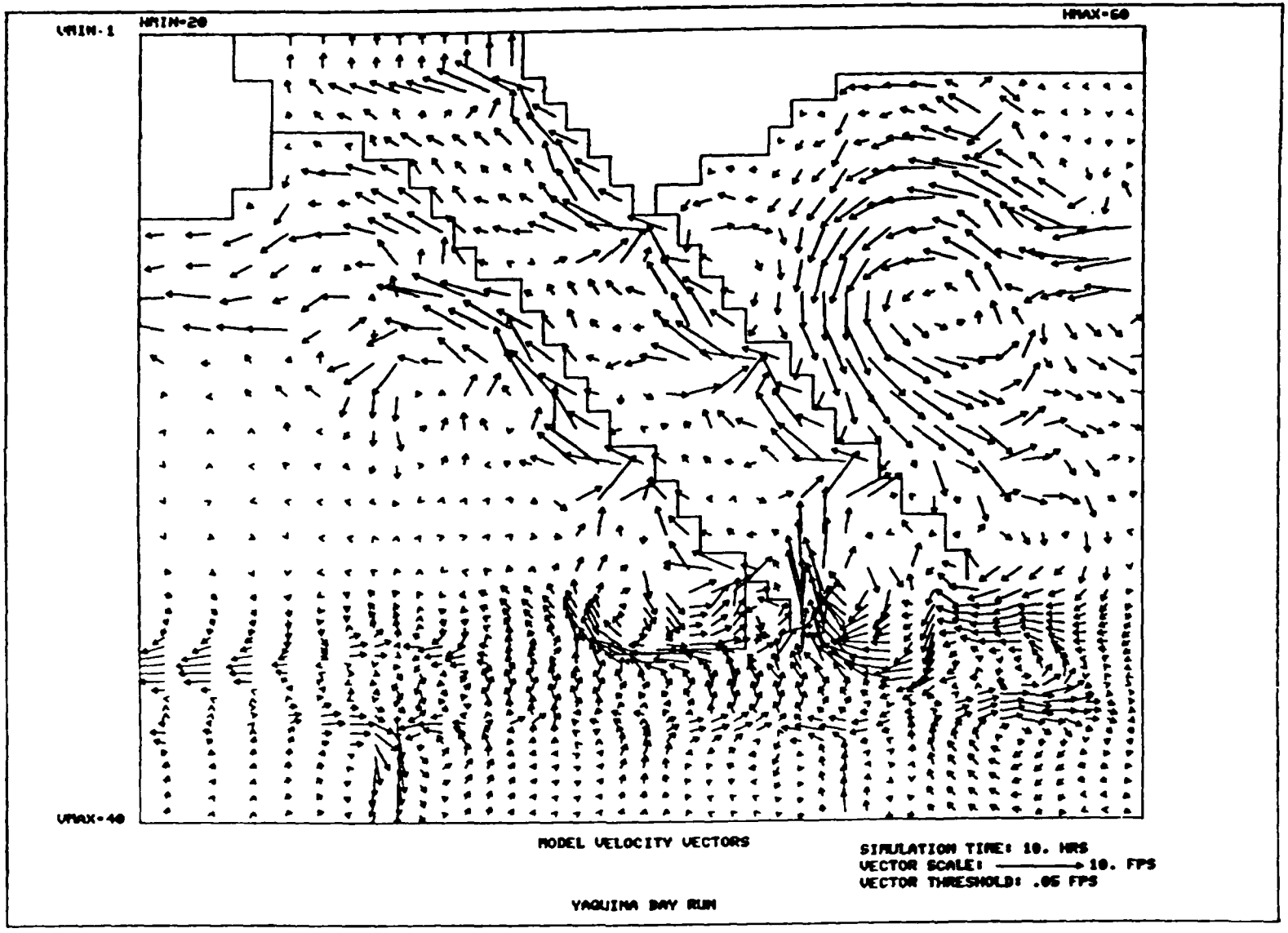

Plate 55. Wave-induced current pattern for alternative e; H_o = 14 ft, T = 11 sec, θ_o = WSW

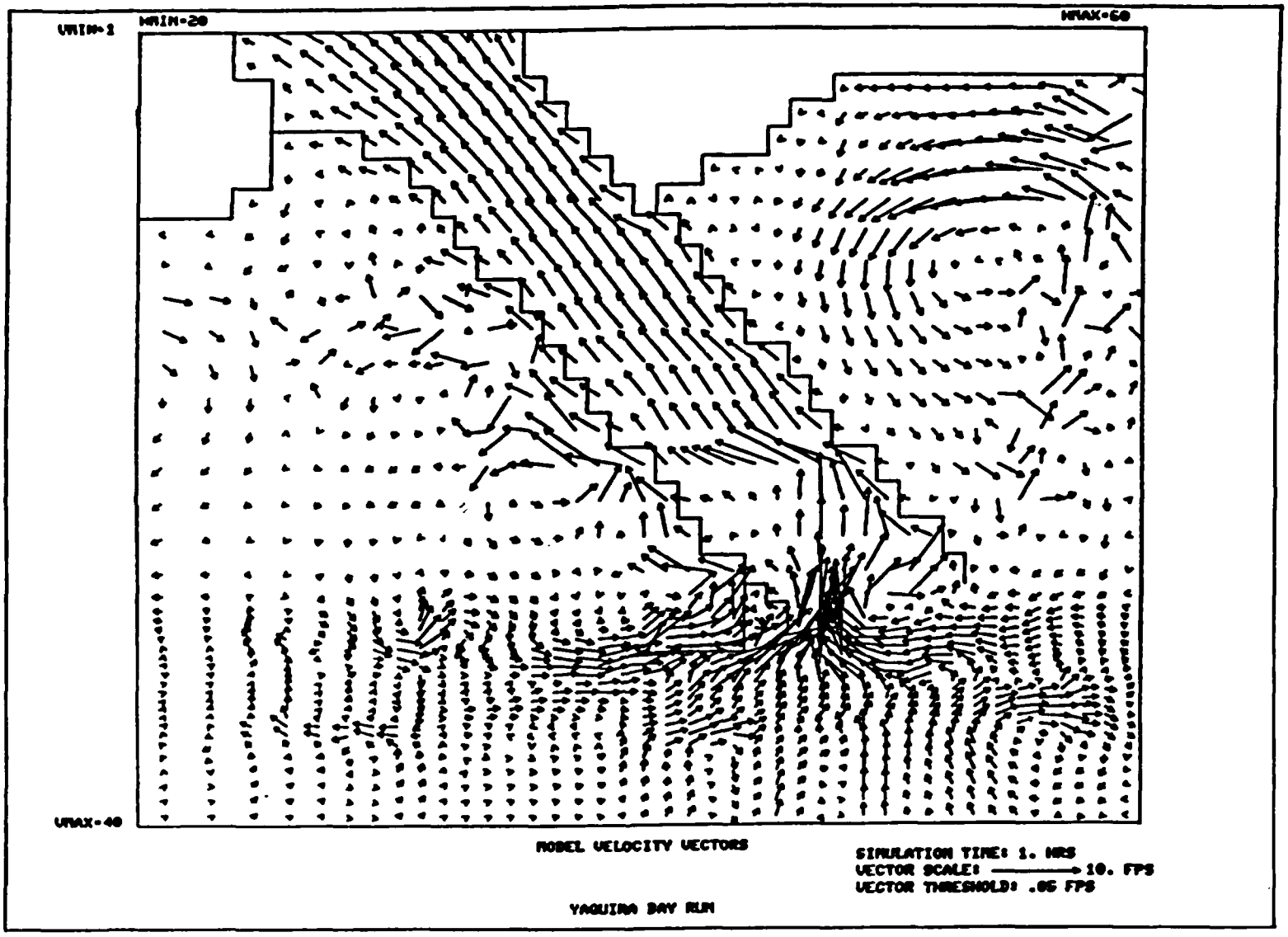

Plate 56. Superposition of tidal and wave-induced currents at peak flood for alternative e; H_o = 14 ft, T = 11 sec, θ_o = WNW

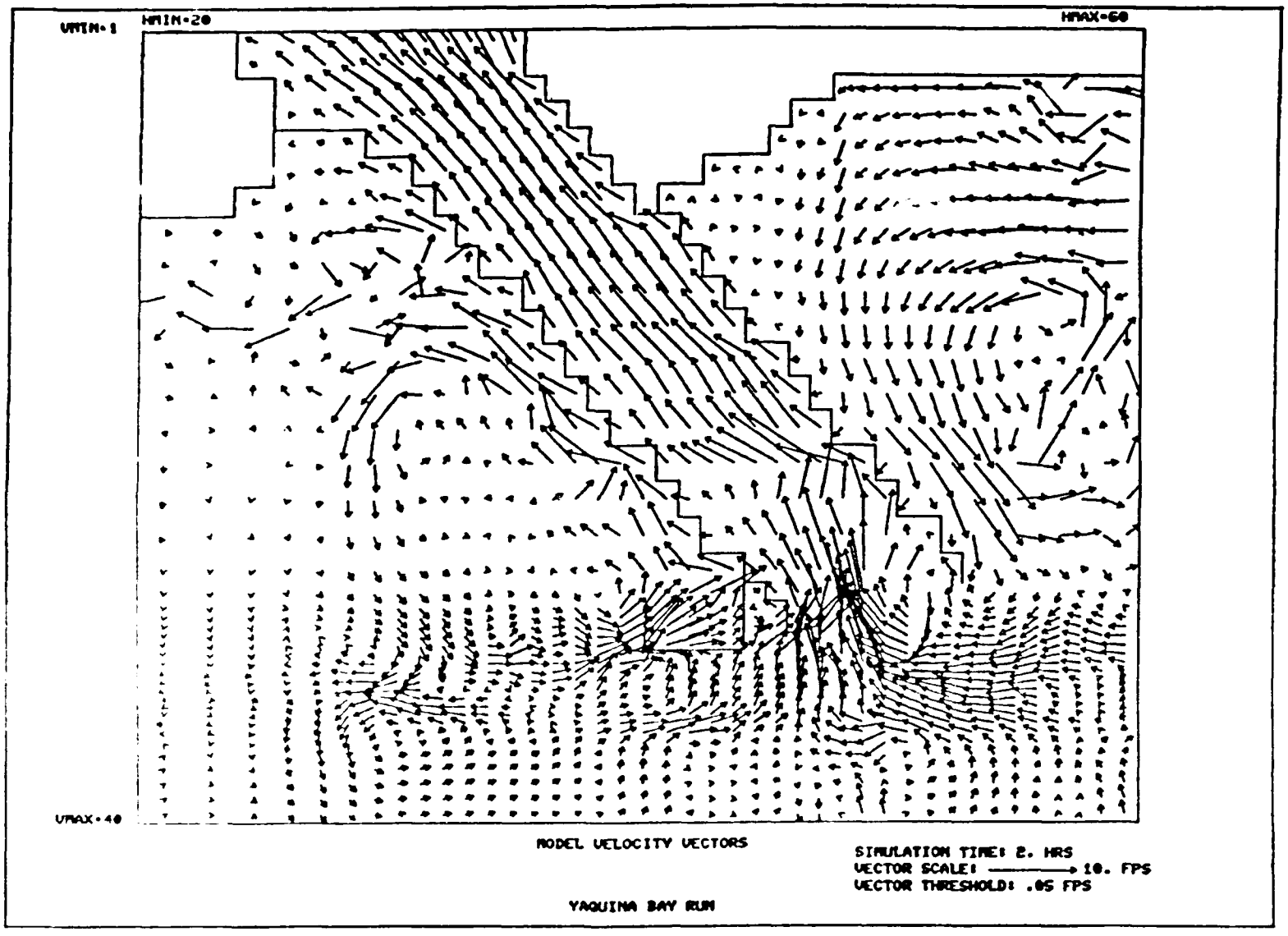

Plate 57. Superposition of tidal and wave-induced currents at peak flood for alternative e; H_o = 14 ft, T = 14 sec, θ_o = W

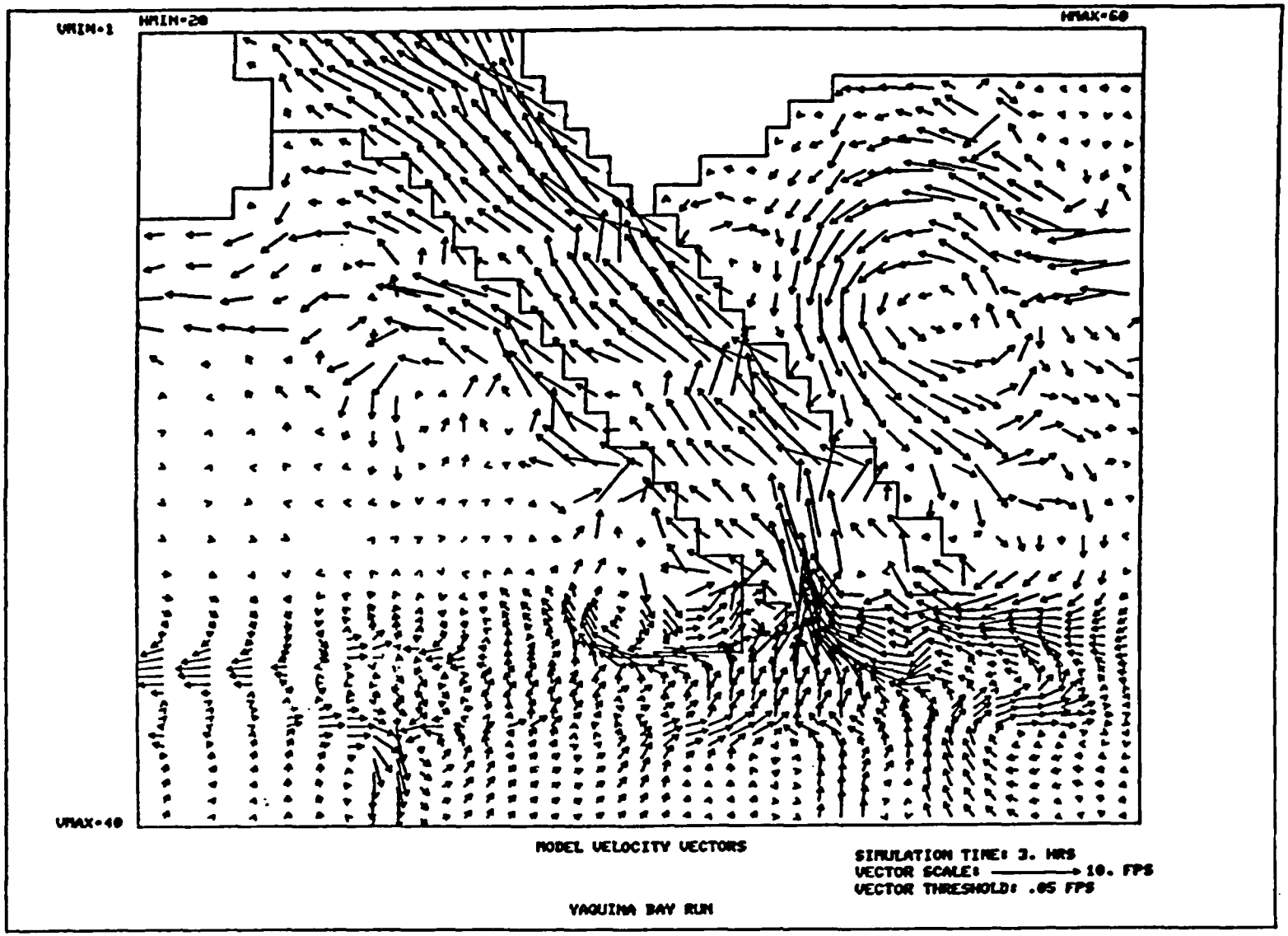

Plate 58. Superposition of tidal and wave-induced currents at peak flood for alternative e; H_o = 14 ft, T = 11 sec, θ_o = WSW

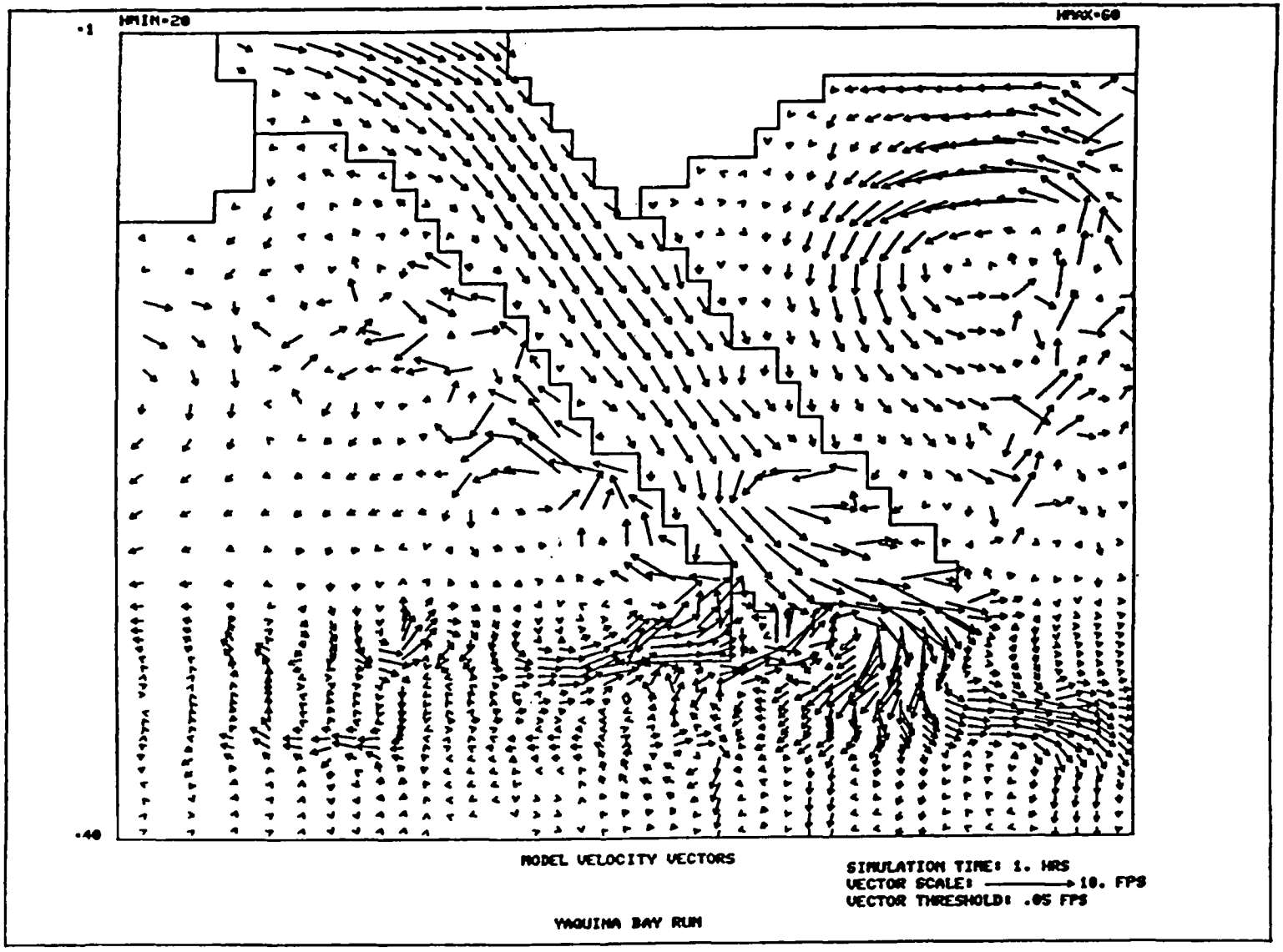

Plate 59. Superposition of tidal and wave-induced currents at peak ebb for alternative e; H_o = 14 ft, T = 11 sec, θ_o = WNW

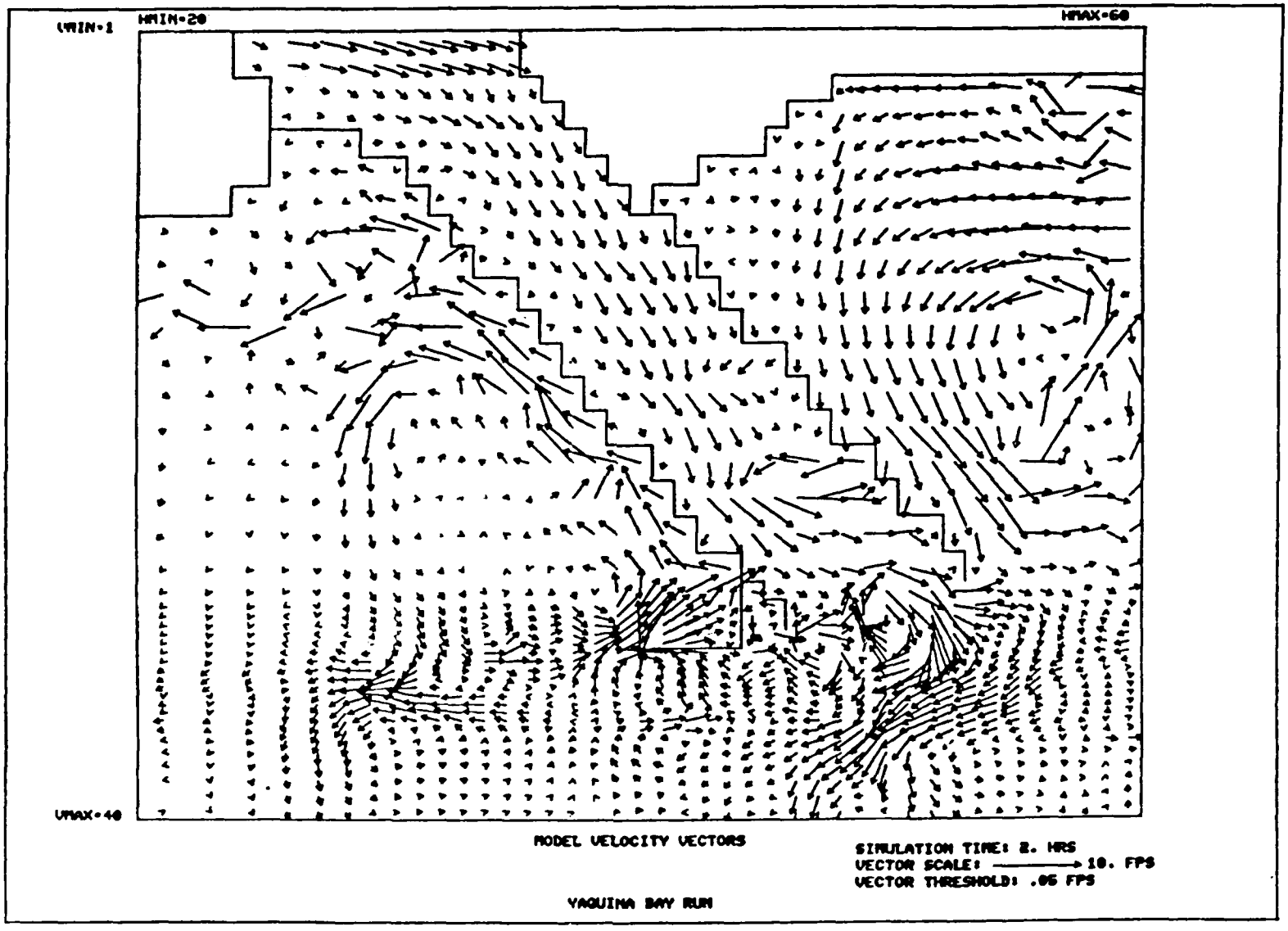

Plate 60. Superposition of tidal and wave-induced currents at peak ebb for alternative e; H_o = 14 ft, T = 14 sec, θ_o = W

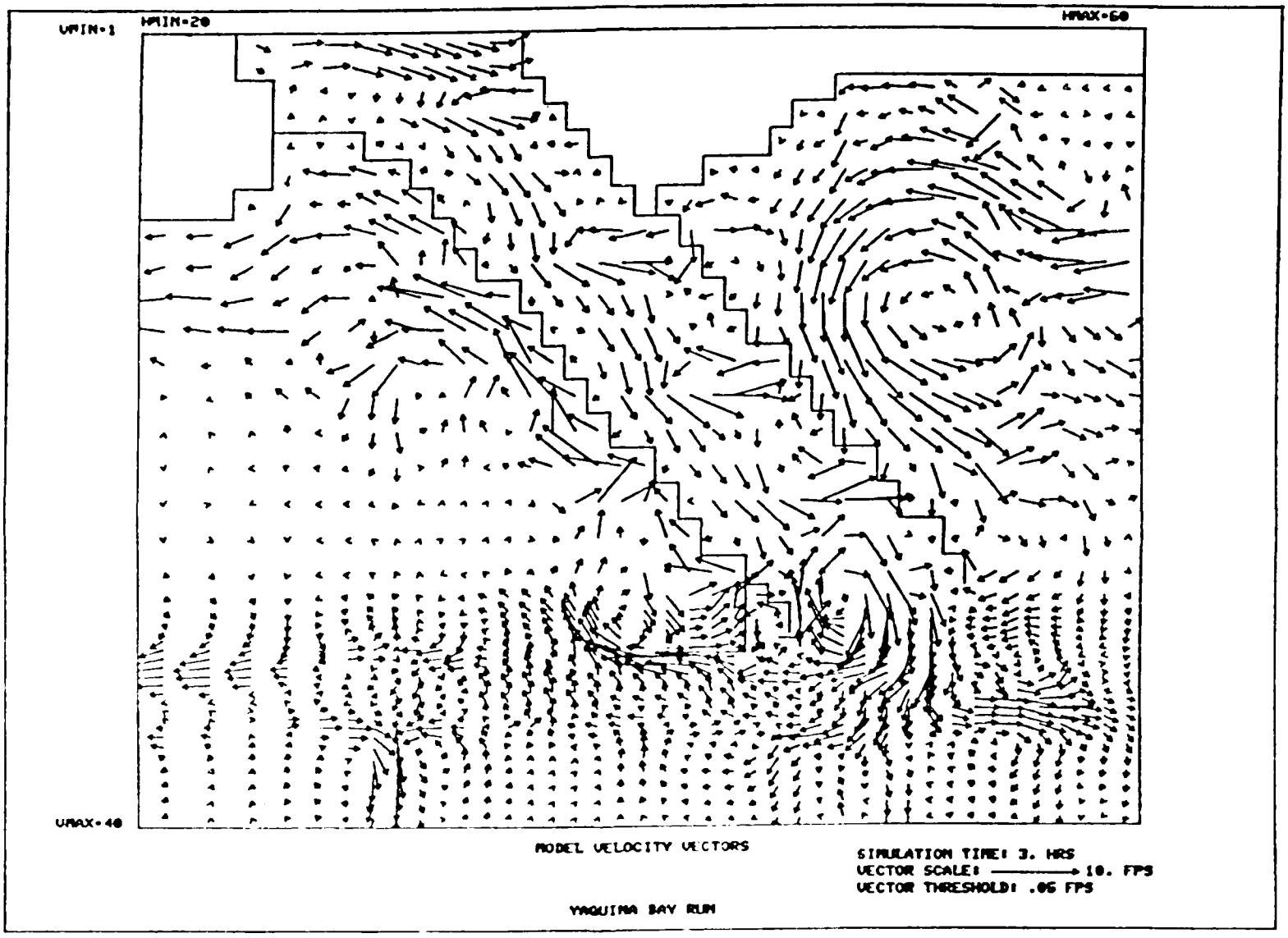

Plate 61. Superposition of tidal and wave-induced currents at peak ebb for alternative e; H_o = 14 ft, T = 11 sec, θ_o = WSW

END

6-87

DTIC